Titre: Title:	Modeling the pull force while pultruding epoxy/glass and polyester/glass composites
Auteur: Author:	Sean Reymond
Date:	1998
Type:	Mémoire ou thèse / Dissertation or Thesis
Référence: Citation:	Reymond, S. (1998). Modeling the pull force while pultruding epoxy/glass and polyester/glass composites [Master's thesis, École Polytechnique de Montréal]. PolyPublie. https://publications.polymtl.ca/6917/

URL de PolyPublie: PolyPublie URL:	https://publications.polymtl.ca/6917/
Directeurs de recherche: Advisors:	Rachid Boukhili
Programme: Program:	Unspecified

UNIVERSITÉ DE MONTRÉAL

MODELING THE PULL FORCE WHILE PULTRUDING EPOXY / GLASS AND POLYESTER / GLASS COMPOSITES

SEAN REYMOND

DÉPARTEMENT DE GÉNIE MÉCANIQUE

ÉCOLE POLYTECHNIQUE DE MONTRÉAL

MÉMOIRE PRÉSENTÉ EN VUE DE L'OBTENTION

DU DIPLÔME DE MAÎTRISE ÈS SCIENCES APPLIQUÉES

(GÉNIE MÉCANIQUE)

DÉCEMBRE 1998

UNIVERSITÉ DE MONTRÉAL

ÉCOLE POLYTECHNIQUE DE MONTRÉAL

Ce mémoire intitulé:

MODELING THE PULL FORCE WHILE

PULTRUDING EPOXY / GLASS AND

POLYESTER / GLASS COMPOSITES

Présenté par: REYMOND Sean

en vue de l'obtention du diplôme de: Maîtrise ès sciences appliquées

a été dûment accepté par le jury d'examen constitué de:

M. FISA Bohuslav, Ph.D., président

M. BOUKHILI Rachid, Ph.D., membre et directeur de recherche

M. MARTIN Eric, B.Ing., membre

Dedication

This work is dedicated to my parents for their support and encouragement throughout my life time.

Acknowledgements

I wish to thank professor Rachid Boukhili for all of his help and guidance throughout this project. I will not forget his insightful manner in resolving problems and determining solutions. Not only did Mr. Boukhili teach research skills but he also taught life skills that I will continue to use for years to come.

I would like to thank Mr. Abdelatif Atarsia for his guidance throughout the project. There was never a problem that Mr. Atarsia couldn't help me with. In addition for his assistance in improving my French.

I would like to thank Mr. Jacques Beausoleil for his assistance in the laboratory. He always helped me when I most needed it.

In addition, I would like to thank all the members of CRASP for their assistance.

Résumé

Ce mémoire est consacré à l'étude de la force de tirage sur un profilé au cours du procédé de pultrusion. De façon à mieux comprendre le développement de la force et son évolution durant la production, il est nécessaire d'étudier les paramètres qui lui sont reliés et leur comportement. Ces paramètres sont le degré de polymérisation de la résine, sa viscosité, son temps de gel, ses changements volumétriques ainsi que la pression développée à l'intérieur de la filière de pultrusion.

Dans l'ordre de ce travail de recherche, on était ramené à utiliser deux résines thermodurcissables soit un polyester isophtalique et une époxy. Ainsi, le degré de polymérisation a été déterminé par la méthode de calorimètre différentielle (DSC). Des essais conventionnels en mode dynamique et isotherme nous ont permis de suivre la réaction de polymérisation sous différents profils de cuisson et, par le fait même, de dévoiler tous les aspects et les paramètres à considérer pour le procédé de pultrusion. En ce qui a trait à la viscosité, les expériences ont été limitées à des essais isothermes sur un viscosimètre à rotation.

Le comportement de la viscosité pour la résine époxy a pu être modélisé au moyen de deux modèles rhéologiques déjà développés dans la littérature. Le premier modèle, basé sur le paramètre temps, prédit bien l'aspect rhéologique de cette résine;

Cependant, il fut rejeté vu les difficultés de son adaptation au procédé de pultrusion. Le second modèle a été retenu pour son habilité à prédire le comportement rhéologique de la résine durant sa cuisson en pultrusion qui est, entre autres, basé sur l'évolution du degré de polymérisation. Pour la résine polyester, le comportement visqueux était influencé par l'effet de masse et la non-uniformité de la résine dans les échantillons testés. Ces phénomènes ont rendu difficile la modélisation de la viscosité de la résine. Finalement, la modélisation du paramètre viscosité, n'a été fait que pour l'époxy.

L'étude de la viscosité nous a permis de remonter au temps de gel qu'on a défini comme étant un temps barrière entre la phase liquide et la phase gel durant la cuisson. Ainsi, deux techniques ont été utilisées à cette fin. Pour la première technique, il était question de déterminer l'instant où la viscosité a tendance à augmenter vers une valeur infinie. La seconde technique, mise au point dans notre laboratoire, fait intervenir le chauffage de la résine sur une plaque préchauffée et tient compte du temps nécessaire à l'apparition de l'état gélatineux. Ainsi, le degré de cuisson au gel a été déduit à partir des essais de calorimètre isotherme et on a constaté qu'il reste constant et indépendant de la température de l'essai. La théorie de Flory a été abordée afin de vérifier les résultats obtenus pour le temps de gel et la comparaison aboutit à une bonne corrélation.

La polymérisation des résines au cours du procédé de pultrusion est connue comme étant accompagnée et influencée par des changements volumiques. De ce fait, il devient indispensable d'étudier ce phénomène de nature physique et de voir, par le fait

même, son influence sur le déroulement de procédé. C'est pourquoi on a abordé, dans un premier temps, le phénomène de l'expansion volumique vu qu'il est le premier à surgir au cours de la polymérisation de la résine. Par la suite, c'était au tour du retrait qui accompagne la fin de la réaction de cuisson. Un dilatomètre a été conçu pour cette cause et était capable de fournir des résultats qu'on a pu modéliser pour déduire ces comportements durant la pultrusion.

Le dernier paramètre nécessaire pour cette étude était la pression développée à l'intérieur d'une filière de pultrusion. Comme ce paramètre n'est pas imposable par un opérateur mais plutôt induit; il est, jusqu'à maintenant, difficile à mesurer vu la complexité du montage nécessaire. Ainsi, on a choisi de la modéliser par des lois déjà existantes.

La dernière étape de cette étude était de quantifier la force de tirage exercée sur le profilé pultrudé. À ce stade, une nouvelle méthode simple, non coûteuse, a été développée aussi bien pour calibrer et mesurer ce paramètre. Il est à noter que la force de tirage est la somme arithmétique de six forces composantes soit celle de collimation. Pour cette étude, il nous était possible de développer une stratégie de façon à déterminer la contribution des forces de collimation et forces visqueuses à la force totale. De plus, une relation linéaire reliant la vitesse de production à la force de tirage fut déduite suite aux essais réalisés sur une pultrudeuse. Cependant, cette relation n'est valable que pour une gamme de vitesse de traction supérieure à 0,5 m/min. Cette valeur de vitesse de

traction est une marge minimale d'opération dans une production en continu, c'est pourquoi la loi linéaire discutée ci-dessus serait d'une grande utilité.

Finalement, l'intérêt majeur qui court derrière l'étude d'un paramètre si important qui est la force de tirage est surtout le contrôle de procédé tout en ayant des fenêtres opératoires au moyen desquelles le pultrudeur pourra résoudre les problèmes qui peuvent surgir au cours du procédé.

Abstract

The objective of the study was to begin a introductory investigation into determining the pull force on a profile during pultrusion. In order to completely understand how the pull force is developed, a fundamental understanding of all the parameters which control it had to be studied. These parameters are the degree of cure, viscosity, gel time, volumetric changes and pressure in or on the resin while inside the pultrusion die.

The research into the degree of cure was modeled for the epoxy resin, and the polyester resin was investigated with a differential scanning calorimeter. The degree of cure was used as the principal parameter to further model the process. The viscosity of the resin inside the die was the second property that had to be modeled. The epoxy resin was modeled using two models found in the literature. The first model was based on time and the second on the degree of cure. The time-based model was capable of modeling the resin very well. However, it was rejected because it did not meet the requirements that were needed to be incorporated with the degree of cure. The polyester resin was attempted to be modeled using two cure-based models. Due to the large *mass effect* associated with the polyester resin, it was not possible to accurately model the resin to the results that were obtained with the rotary viscosimeter.

The gel point was needed as a boundary condition for the viscosity model. In addition, it was very valuable in marking the end of the liquid zone inside the die. The degree of cure at the gel point was determined using two techniques and was also modeled. The first technique to determine the gel time was during the isothermal viscosity tests. The gel time is simply the point where the viscosity tends toward infinity. The second technique that was used to determine the gel time was the hot plate technique. These tests consisted of placing a small quantity of resin on a metallic plate at a controlled temperature. The gel time was defined as the time where the resin begins to build up in front of the stirrer. The gel times obtained are then coupled with the isothermal degree of cure curves to yield the degree of cure at the gel point. The degree of cure at the gel point was also modeled using Flory's classical approach. The experimental and theoretical results were in good agreement. Flory's classical approach was not applied to the polyester resin, because the functionality of the resin could not be determined.

The volumetric changes in the resin was the next parameter that was investigated. To measure the volumetric expansion of the resin during heating and polymerization, a dilatometer was designed and built in the laboratory for this series of tests. The apparatus consisted of a 120 ml quasi-cylindrical container with 40-45 g of resin at the bottom, followed by a layer of silicon oil, then sealed with a pipette inserted into the oil. This apparatus was able to measure the thermal expansion and the cure shrinkage of the resin. From these tests, the coefficients needed to model the volumetric changes where

determined. As with all tests that used large quantities of resin, there is a mass effect for this series of tests.

The pressure profile inside the die was not measured due to the complexity of the task. However, the shape of the pressure profile is predicted from existing models which are presented.

A method to measure the pull force on the profile was developed. It consisted of measuring the energy consumed by the puller motor and the line speed. With these measurements, the pull force was obtained from calibration curves that were obtained by lifting known weights at speeds greater than 0,5 m/min.

The contribution to the total pull force of the collimation and viscous forces was investigated. The collimation forces were measured when dry rovings were pulled through the die. The viscous forces were measured by pulling fibers wet with silicon oil through the die. These forces were then compared to the total pull force to pultrude a polyester / glass profile. It was found that the viscous drag accounted for 5% of the total pull force and the collimation accounted for 50% of the total pull force.

A linear relationship was found between the line speed and the pull force. This result is different from the literature which predicts an exponential increase. Since the

viscous drag accounted for only 5% of the total force, this might explain why the relationship was linear.

The main advantage of knowing the pull force is its use as a monitoring tool. At a given speed the pull force should remain constant. However, if it slowly increases, it is a signal to the operator to take corrective measures.

Condensé en français

La mise en œuvre des matériaux composites par pultrusion suscite de nos jours un intérêt majeur aussi bien du côté de la recherche et développement que du côté industriel, et ceci en vue d'élargir de plus en plus les champs d'application des produits pultrudés. Ces produits sont caractérisés par de bonnes propriétés mécaniques associées à de faibles densités comparés aux matériaux conventionnels. À l'heure actuelle, la maîtrise des paramètres de mise en forme par pultrusion reste toujours un thème en voie de développement afin de minimiser le temps de production et, par conséquent, améliorer le taux de production. C'est ainsi qu'il devient important d'étudier l'ensemble des phénomènes physiques et chimiques ayant lieu au cours du procédé et de connaître, par la suite, leur impact d'un côté sur les paramètres de mise en œuvre et d'un autre côté sur les propriétés du produit fini.

Les difficultés entourant la modélisation du procédé de pultrusion sont dues en majeure partie au nombre restreint de paramètres contrôlables durant la production. Ces paramètres se résument à une vitesse de traction exercée sur le profilé ainsi que le profil de température nécessaire à la cuisson du matériau. Cependant, la modélisation des transformations physiques et chimiques fait appel à d'autres paramètres, notamment le degré et le temps de conversion du polymère, l'évolution de sa viscosité, la pression créée au cours du moulage et la force de tirage requise pour le déplacement du produit d'un bout à l'autre d'une ligne de pultrusion.

Le degré de polymérisation a déjà fait l'objet de plusieurs recherches qu'on retrouve dans la littérature. En prenant ces études comme référence pour notre cas, des expériences de types dynamiques et isothermes ont été réalisées sur un calorimètre. Les essais dynamiques avaient pour objectif la détermination de la quantité de chaleur exothermique que dégage la résine jusqu'à sa cuisson complète. Plusieurs vitesses de chauffe ont été testées, et ce pour étudier la cuisson de la résine quand elle est soumise à différents profils de chauffe ou à des profils non uniformes. Les essais isothermes ont été réalisés, et ce en suivant une technique déjà développée dans la littérature. Cette dernière fait de sorte qu'un essai dynamique doit être réalisé afin de déterminer la quantité de chaleur résiduelle qui reste emmagasinée dans la résine suite à une cuisson isotherme. Il a été aperçu ainsi, que la somme des quantités de chaleur isotherme et résiduelle est pratiquement égale à la quantité de chaleur dégagée au cours de la cuisson dynamique. Suite à ceci, des essais dynamiques reproduisant un profil de température dans une filière de pultrusion ont été réalisés sur le calorimètre afin d'étudier et de suivre la réaction de la résine durant la pultrusion et d'extraire par la suite son degré de polymérisation à la sortie de la filière.

La viscosité était le deuxième paramètre à étudier, et ce en réalisant des essais isothermes sur des échantillons de résines formulées dans un viscosimètre Brookfield. Les résultats obtenus ont pu être prédits par deux modèles rhéologiques dont le premier est basé sur le paramètre temps alors que le second est basé sur le degré de

polymérisation. Le second modèle a été retenu pour la continuité de l'étude vu que le degré de polymérisation a été pris comme paramètre de base pour la modélisation du procédé de pultrusion.

Les essais de viscosité réalisés à basses températures ont montré une bonne concordance avec les prédictions du modèle pris en question. Cependant, au cours des essais à hautes températures, le déclenchement de la réaction de polymérisation après une courte durée à partir du début des essais avait pour effet d'augmenter la température de l'échantillon et, par conséquent, diminuer la concordance avec les prédictions du modèle vu que ce dernier ne prend pas en considération l'échauffement dû à la forte exothermie notamment dans le cas de la résine époxy. Dans ce cas, une approche semi-dynamique a été adoptée afin de faire varier la température de la résine durant la modélisation. Dans le même contexte, les essais sur la résine polyester ont montré une transition liquide-solide assez lente et compte tenu de l'effet de masse, il était difficile de prévoir le comportement de la viscosité par le moyen des modèles déjà utilisés.

Les mesures de la viscosité nous ont permis de remonter au temps de gel qui a été défini comme étant le moment où la viscosité de la résine a tendance à augmenter vers une valeur infinie. Une deuxième technique fut adoptée pour le temps de gel et consistait à suivre l'échauffement de la résine sur une plaque préchauffée et d'agiter jusqu'au moment d'une accumulation de résine gelée sur l'agitateur. La validité de ces résultats nous a permis de déterminer, en accordance avec les essais de calorimétrie, le

degré de conversion au point de gel. Ainsi, pour les résines étudiées, le degré de cuisson au point était de l'ordre de 54 % pour l'époxy alors qu'il était d'environ 5 % pour le polyester. Nous avions mis en doute la validité du résultat pour le polyester, c'est pourquoi on a opté pour un degré de conversion de gel au point où la résine est toujours malléable et déformable. Cette technique nous a révélé que le point de gel est à 27 % de cuisson. Il est à noter que le degré de conversion au gel reste constant et indépendant du profil de température qu'il soit uniforme ou non.

La durée de vie de la résine époxy a été étudiée en considérant l'effet de certains additifs afin de dévoiler l'influence de chacun d'entre eux. Pour la résine époxy, il était trouvé que l'accélérateur a pour effet de diminuer la vie en pot de la résine vu qu'il aide à accélérer la réaction de cuisson comme son nom l'indique. L'agent débullant qu'on rajoute durant le mixage de la formulation a tendance à diminuer la viscosité de la résine et aussi prolonger sa vie en pot. Finalement, l'agent de démoulage produisait des effets non désirables comme augmenter la viscosité et créer une non-homogénéité dans la formulation de résine vu sa tendance à séparer les ingrédients en couches et par ordre de densité. À des températures plus élevées, comme la valeur de la viscosité minimale diminue, il a été remarqué que l'effet de l'accélérateur est surtout pointé sur le temps de gel qui le fait diminuer. Pour remédier à ce phénomène, on a étudié l'effet de l'ajout des charges renforçantes en billes de verre. Ces derniers avaient tendance à augmenter la viscosité et prolonger le temps de gel. Cependant, on a constaté qu'à un instant donné de

la réaction, ces billes de verre immergent vers le fond du contenant de l'échantillon testé, et ce à cause de la différence de densité.

Le paramètre suivant dans cette étude était le changement volumique de la résine durant sa cuisson. Ce changement a été mesuré en terme d'expansion et de retrait volumique, et un montage expérimental a été construit pour cette investigation. La modélisation du changement volumique nous a incité à déterminer expérimentalement certaines constantes reliées à ce changement et aux paramètres de l'essai. Pour ce qui est de l'expansion volumique, il a été bien modélisé et projeté à prédire ce comportement au cours de la pultrusion. Cependant, la modélisation du retrait était perturbée par la non-uniformité de la température dans l'échantillon suite à la réaction de cuisson qui fait de sorte que le centre soit à une température plus élevée et qui diminue en se rapprochant des bords de l'échantillon. Un profil simulé de température a été utilisé dans ce cas pour pouvoir quantifier le retrait de la résine durant la pultrusion.

Les changements volumiques discutés ci-dessus étaient nécessaires à l'étude de la pression développée dans la filière qui reste jusqu'à maintenant le paramètre ambigu dans l'étude du procédé de pultrusion. L'utilisation d'un modèle existant dans la littérature a pu nous faire remarquer que la pression est un paramètre fortement dépendant de la viscosité de la résine en question de son changement volumique. Ainsi, l'étude menée sur le polyester et l'époxy nous a mené à conclure qu'il y a plus de pression développée dans le cas de l'époxy que dans celui du polyester, et c'est pourquoi

nous constatons qu'en pratique la pultrusion de l'époxy nécessite plus d'énergie de production.

La force de tirage sur un profilé au cours de la pultrusion était le paramètre englobant l'ensemble des paramètres étudiés précédemment. Cette force a été d'abord calibrée sur une machine de pultrusion par le moyen de soulèvement d'une masse connue au préalable. En effectuant le même essai à différentes vitesses de soulèvement, on a pu remonter à la puissance consommée par le tracteur pour cette fin. Ainsi, des courbes de calibrations ont été établies pour une gamme de vitesses de tirage allant de 0,5 à 1,5 m/min. Par la suite, on a étudié l'évolution de certaines composantes de la force de tirage, soit la force de collimation et la force visqueuse. La force de collimation était mesurée en tirant des fibres non imprégnées à travers la filière, alors que la force visqueuse a été simulée par une traction sur des fibres imprégnées par de l'huile de silicone. L'amplitude de ces forces a été comparée à la valeur de la force exercée sur un profilé polyester verre au cours de sa production. À ce stade, il a été trouvé que la contribution de composantes étudiées n'étaient que de 5 % pour la force visqueuse et de 50 % pour la force de collimation.

Aux cours des essais de production en pultrusion, les résultats sur la force de tirage ont montré une tendance linéaire en force de la vitesse de pultrusion, alors que dans la littérature, on parle d'une relation de type exponentiel. Cette relation est d'une grande utilité dans le cas où il faut prévoir la force nécessaire pour tirer un profilé de

section donné et éviter les troubles de production qui représentent des pertes de temps souvent énormes et non désirables. C'est ainsi qu'une fenêtre opératoire peut être mise au point afin de pouvoir maintenir une production adéquate et continue.

La continuité de ce travail peut s'établir sur plusieurs façades dont les plus importantes seraient, d'une part, l'établissement d'une base de données pour plusieurs types de résines et d'étudier en particulier et en profondeur le développement de la pression dans la filière. Il serait aussi important de développer un modèle pour la force de tirage en tenant compte des différents paramètres qui ont fait l'objet de la présente étude.

Table of Contents

List of figures

List of tables

Nomenclature

a	Viscosity exponent
a_v	Thermal expansion coefficient
A	Viscosity constant
b_t	Viscosity constant, time model
b_c	Viscosity constant, cure model
B	Viscosity constant
c	Shrinkage constant
C	Viscosity constant
Cr	Compression ratio
C_i	WLF constants
D_f	Fiber diameter
D	Viscosity constant
E	Viscous activation energy
E_η	Arrhenius activation energy
E_{ik}	Kinetic activation energy
E_k	Kinetic analog of E_η
f	Functionality of the branching unit
f_v	Fractional free volume
k_n	Rate constants for the autocatytic-1 model
k	Viscosity rate constant
k_∞	Kinetic analog of η_∞
K	Blake-Kozeny constant
K_b	Compressibility of the resin
Δl	Linear thermal expansion
l	Initial length
L_T	Taper length

m	Order of reaction
n	Order of reaction
$\overline{M}$	Molecular mass
$\overline{M}_c$	Critical molecular mass
$\overline{M}_{wo}$	Initial weight average molecular mass
P_s	Surface pressure
Q_o	Total heat of reaction
Q_{iso}	Heat released from isothermal tests
Q_R	Residual heat from dynamic tests
R	Universal gas constant
r	Radical concentration
r_f	Final radical concentration
S	Viscosity constant
S_f	Final polymerization shrinkage
t	Time
t*	Gel time
T	Absolute temperature
T_o	Reference temperature
$\overline{T}$	Average temperature
V	Speed of the system
V_f	Free volume
V_o	Initial volume
V_T	Total volume occupied
ΔV	Change in volume
$\Delta V'$	Activation volume
V'	Volume in the transient state
V_R	Volume in the reactant state
$\overline{\chi}$	Average degree of cure

α_L	Thermal expansion coefficient
α	Degree of cure
α^*	Degree of cure at the gel point
α_s	Surface degree of cure
β	Compressibility constant
β_m	Volumetric thermal expansion of the monomer
β_p	Volumetric thermal expansion of the polymer
ϕ	System porosity
γ	Volumetric shrinkage of the resin due to the chemical reaction
η	Viscosity
η_{io}	Initial viscosity
η_∞	Viscosity at a specific temperature
λ	Ratio of reactive groups
ν	Volume of the composite
ν_f	Fiber volume
θ	Viscosity constant
θ^*	Ultimate concentration of filler
ζ	Dimensionless length

Introduction

The pultrusion process is a rapidly growing area of research that has the potential of continuing to increase for many years to come. The sudden growth in this domain is driven by the increased awareness of the beneficial properties of pultruded structures. Pultrusion is one of the fastest ways to manufacture composites, thus making it inexpensive to produce large quantities of material. When compared to vacuum or compression molding where the parts are produced one at a time, pultrusion is a continuous process which can by automated. It is the combination of both of these properties that allows pultrusion to produce large quantities at a low cost. In addition to the low cost, the pultrusion process can produce very complex profiles that are increasingly larger and at increasingly faster speeds.

The materials used for pultrusion can be categorised into two groups: resin and fiber. Within the resin category there are again two major sub-divisions, thermosets and thermoplastics. There are many types of both of these materials, but only a few are used extensively in pultrusion applications. The fibers that reinforce the composite are found in numerous forms. The most common configurations are rovings, mats and veils. The rovings are fibers oriented longitudinally along the profile. Mats are composed of either randomly oriented fibers that are intertwined together or woven fibers that typically run at a set angle to each other. Veils are a top layer that covers rougher reinforcement to

produce a smooth surface finish. The typical pultrusion process for thermosets can be seen in figure 1-1. On the left-hand side, a rack holds many spools of rovings, mats and veils. These are then fed into a bath that will impregnate the fibers with the resin. The fibers are then led into the pre-formers that align the fibers into the desired shape before entering the die. While the fibers are pulled through the heated die, the resin cures before reaching the exit of the die. Upon exiting the die, the composite is then air cooled before entering the pulling apparatus that controls the speed of the whole process. As the composite exits the puller, it is cut to the desired length [1].

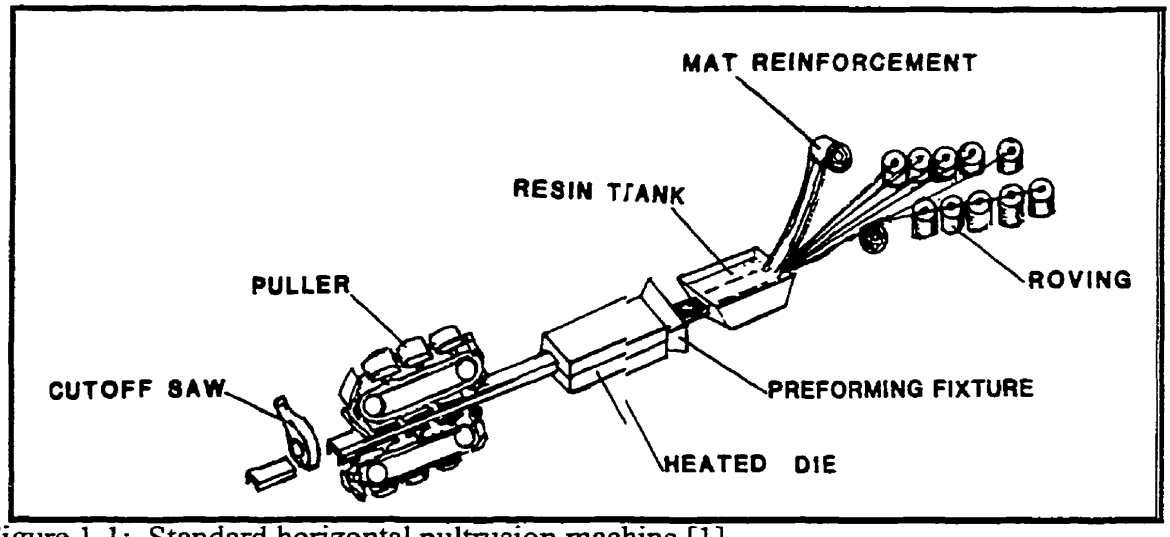

Figure 1-1: Standard horizontal pultrusion machine [1].

The modeling of the pultrusion process is a difficult task. The principal reason for this difficulty is that the only process parameters that can be controlled by the operator are the speed of the system and the temperature settings on the die. Since these are the only parameters that the operator can control, a fundamental understanding of

the phenomenons that occur within the die must be known. Because the die is a closed and transient environment, all of the factors which contribute to the material's evolution, must be investigated one at a time and at a fundamental level.

In this research, six aspects of the pultrusion process have been investigated. The first aspect studied was the cure kinetics of the resin. The isothermal and dynamic cure profiles were determined for various temperatures and heating rates. The second area that was investigated was the changes in viscosity of the resin. The study of the viscosity incorporated the thermal and curing effects. Following the viscosity experiments, the gel times of the resin were determined for a wide range of temperatures. The gel point marks the transition of the resin from a liquid to a gel. The next aspect that was investigated was the pressure development in the pultrusion die. The pressure profile has been calculated for the entire length of the die. The final aspect that was investigated in this work was the pull force required to pull the profile through the die. To accomplish this task, all of the preceding factors were incorporated to determine the pull force.

Chapter 1 Literature Review

1.1 Epoxy / Glass and polyester / glass composites

1.1.1 The matrix of the composite

Polyester resin is the backbone of the composite industry and it accounts for over 90 % of all the resins used in composites. Epoxy is the most common thermosetting resin when high mechanical properties are needed. The main function of the resin within the composite is to give the structure its shape, to protect the load bearing fibers and to transfer the loads to the fibers. Some of the typical properties of epoxy and polyester can be seen in table 1-1 and 1-2, respectively. Some of the advantages and disadvantages of the epoxy's and polyester's more predominant attributes can be seen in the table 1-3 and 1-4, respectively. The type of resin system that is used in pultrusion is the autocatalytic type. An autocatalytic system is a resin that is completely catalysed, but has a low reactivity at low temperatures. As the temperature increases, the heat activates the catalyst and begins the polymerization process. Therefore, it is the temperature profile in the die that controls the rate of reaction.

1.1.2 Glass fibers used in the composite

Glass fibers are the most common type of fiber used in pultrusion. Typically, the

bulk of the fibers are found as rovings which are continuous, and in mats where the fibers can be either continuous or discontinuous. Some typical properties of glass fiber

Table 1-1 Typical properties of cast epoxy resin (at 23°C) [2].

Specific gravity	1,2-1,3
Tensile strength, MPa	55-130
Tensile modulus, GPa	2,75-4,10
Poisson's ratio	0,2-0,33
Coefficient of thermal expansion, 10^{-6} m/m per °C	50-80
Cure shrinkage, %	1-5

Table 1-2: Typical properties of polyester resin [2].

Specific gravity	1,1-1,4
Tensile strength, MPa	34,5-103,5
Tensile modulus, GPa	2,1-3,4
Elongation, %	1-5
Cure shrinkage, %	5-12

Table 1-3: Advantages and disadvantages of epoxy resin [3].

Advantages	**Disadvantages**
Wide range of mechanical properties	High cost
Low cure shrinkage	Long polymerization time
Corrosion resistance	Limited resistance against certain chemicals
Highly dimensional stability up to 150-200°C	Release agents are needed
High surface adhesion	High moisture absorption

Table 1-4: Advantages and disadvantages of polyester resin [2].

Advantages	**Disadvantages**
Low viscosity	High cure shrinkage
Fast cure time	Lower mechanical properties
Low cost	Styrene emission

Table 1-5 Typical properties of glass fiber [2].

Typical diameter	10-25 μm
Specific gravity	2,5
Tensile modulus	72 Gpa
Tensile strength	3,45 GPa
Strain to failure	4,8 %
Coefficient of thermal expansion	5 x 10^{-6} /°C
Poisson's ratio	0,2

Table 1-6 Advantages and disadvantages of glass fiber [2].

Advantages	**Disadvantages**
Low cost	Low tensile modulus
High tensile strength	Relatively high specific gravity
High chemical resistance	Sensitive to abrasion
Excellent insulating properties	Low fatigue resistance

can be seen in table 1-5. Some of the advantages and disadvantages of glass fiber's more predominant attributes can be seen in the table 1-6. It is the fibers that give a composite all of its tensile strength and rigidity. Because of the fiber's high strain to failure, which is in the elastic region, the glass fibers can absorb a tremendous amount of energy before failure.

1.2 Cure kinetics of the resin

Since the fibers that are used in pultrusion are inert, it is uniquely the resin's characteristics that must be controlled during processing. Therefore, the first parameter that is used in modeling the behaviour of a thermosetting resin is the cure kinetics. The cure kinetics are often used as a preliminary step in modeling a resin since its theory and instrumentation are relatively advanced.

1.2.1 Techniques to analyse the cure kinetics

While analysing and modeling the cure kinetics of the resin, there are four main techniques that can be used. They are differential scanning calorimetry (DSC), Fourier transform infrared spectroscopy (FTIR), dielectric measurements and rheokinetic measurement. The DSC technique is the most commonly used for determining the kinetic parameters of curing thermosets.

The DSC technique is based upon the following condition,

$$\frac{1}{Q_o}\frac{dQ}{dt} = \frac{d\alpha}{dt} \qquad 1\text{-}1$$

where Q_o is the total heat of reaction, t is time and α is the degree of cure. The heat of reaction is the heat that is released by the resin during the polymerization process. The

degree of cure is a normalized value that measures the amount of reaction that has taken place. When the degree of cure attains one, the reaction is 100% complete. There are two categories of DSC techniques, isothermal and dynamic. The advantage that dynamic DSC measurements have, is that they are very useful in determining kinetic data for commercial resins.

When a sample is subjected to an isothermal test, the total heat of the reaction is determined with the following equation,

$$Q_o = Q_{iso} + Q_R \qquad 1\text{-}2$$

where Q_{iso} is the heat released from the isothermal test, Q_R is the heat released from the dynamic temperature scan and Q_o is the total heat of reaction that is found in equation 1-1. Therefore incorporating 1-2 into 1-1, the degree of cure can then be calculated [4].

Fourier transform infrared spectroscopy uses the changes in the spectral peak heights of functional groups to monitor the kinetics of a thermoset resin. The main advantage that FTIR has is that it can provide compositional changes while the resin is curing [4,5].

Dielectric measurements exploit the polarisation of the polymer molecules. While conducting the measurements, an alternating voltage is applied across the sample and the resistance is proportional to the extent of cure in the sample. There are three types of dielectric measuring systems, parallel plate, comb electrodes and micro-

electrometers. A dielectric measuring system should be selected by evaluating its advantages and disadvantages for the specific application [4].

1.2.2 Cure Kinetic Modelling

There are two types of kinetic models available, empirical and mechanistic. The empirical models are simple and used mainly for industrial applications. Mechanistic models are more complex than empirical models but mechanistic models aren't restricted by compositional changes. The model that has been used by many researchers for thermosetting resins is the autocatalytic-1 that is shown below, [6]

$$\frac{d\alpha}{dt} = \left(k_1 + k_2\alpha^m\right)(1-\alpha)^n \qquad 1\text{-}3$$

$$k_1 = k_0 \exp\left(E_{1k}/RT\right) \qquad 1\text{-}4$$

$$k_2 = k_0 \exp\left(E_{2k}/RT\right) \qquad 1\text{-}5$$

where k_1 & k_2 are rate constants, n & m are the reaction orders (n+m=2), E_{ik} is the kinetic activation energy, R is the universal gas constant, and T is the absolute temperature .

1.3 Behaviour of the resin's viscosity

There are many instruments that are used to measure the viscosity of the resin but there are only three main categories. The most popular category is the rheometers that measure the dynamic properties of the resin, such as the parallel plate, cone and plate, and eccentric disc. These instruments are the most popular because they can do isothermal and dynamic runs as well as determining the complex viscosity of the resin. The next category is the torque viscometers that measure the viscosity as a function of the spindle speed. This type of instrument can perform tests at various shear rates but is only capable of isothermal measurements. The last type of instrument to measure viscosity is that of capillary rheometers. These instruments are mainly used for obtaining high shear rates [4].

An important process parameter in pultrusion is the viscosity of the resin. The viscosity effects the fiber wetting and the drag forces within the die. Once the behaviour of the viscosity is known, the optimum viscosity and the temperature can be determined. The curing of the resin is an exothermic reaction and this internal heat source can yield undesirable effects in the final product. Therefore, the die temperature must be set to compensate for the heat that is released internally [6]. If the temperature profile of the die is not set correctly, the material can overheat, decompose, cause blocking and damage the material. Once the temperature profile is optimised, the pull force will be minimised, and the product quality will be at its highest. As the reaction proceeds, the

structural changes that take place are associated with an increase in the glass transition temperature.

A method developed by Hinrichs is called the Engineering Cure Transformation Diagram. This diagram, seen in figure 1-2, consists of a temperature versus reaction time plot with iso-viscosity curves. This provides the engineer with the allowable temperature window in which to operate while maintaining a specific viscosity range [7].

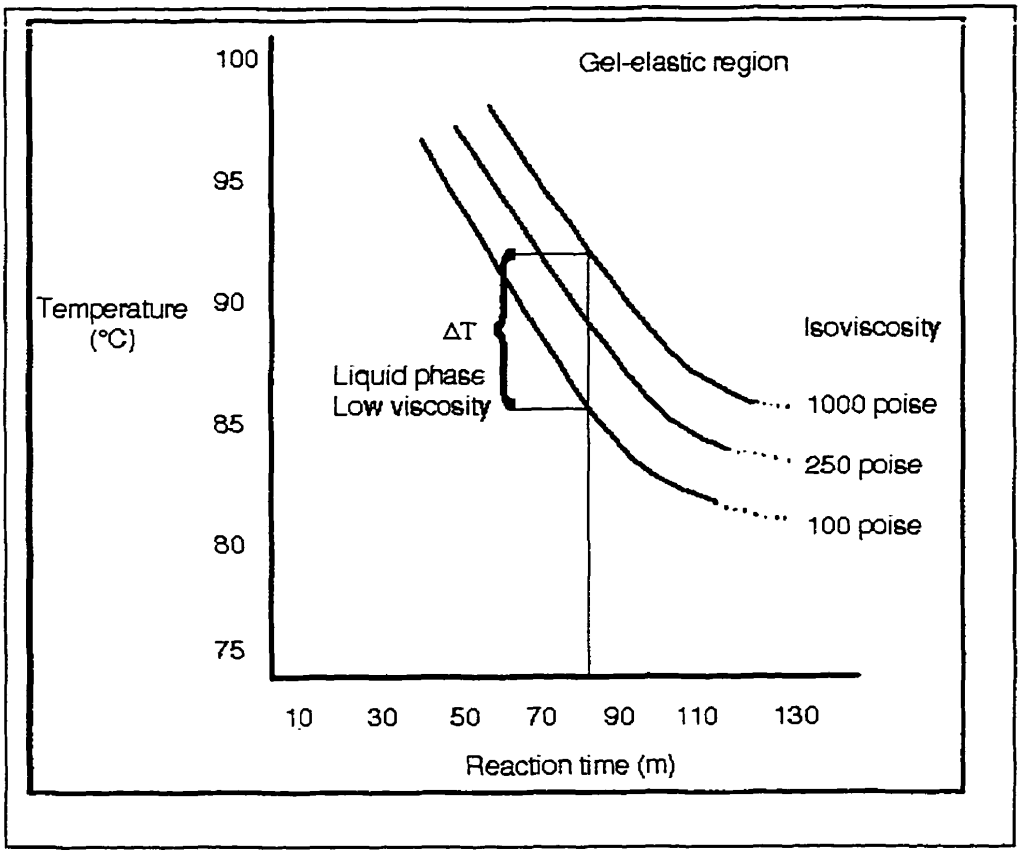

Figure 1-2: Iso-viscosity engineering diagram [7].

1.3.1 Factors which affect viscosity

The chemoviscosity of thermoset resins is affected by many factors such as shear rate, pressure, temperature, degree of cure and filler properties. To study these variables, the tests are usually broken up into three sections, cure effects, shear rate effects, and filler effects. While monitoring the cure effects, the temperature and time are the most important factors.

Two of the main factors which affect the viscosity are the temperature and the degree of cure. The temperature of the resin determines the degree of mobility of the reacting components, thus the greater the temperature, the greater the mobility. The second factor that controls the viscosity is the curing that takes place. As the reaction proceeds, the molecules become larger and larger, which results in the formation of macromolecules. Once a sufficient amount of macromolecules have formed, gelation will take place, and immediately after, the macromolecules will combine to form one large molecule [8].

As seen in figure 1-3, there are three viscosity stages that take place while a thermoset is curing at a constant heating rate. In stage 1, the viscosity decreases because the thermal effects are greater than the curing effects. Stage 2 is the point at which the thermal effects balance the curing effects, thus reaching a minimum viscosity. In stage 3, the curing effects are greater than the thermal effects.

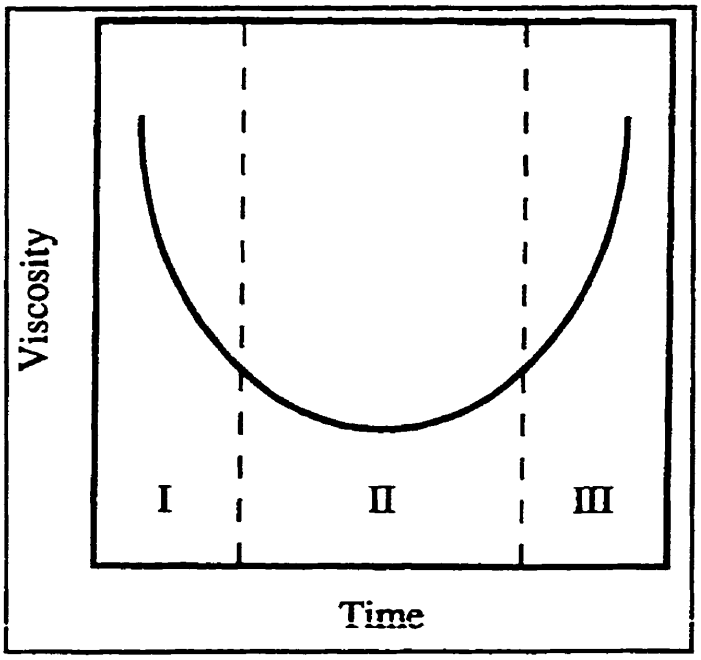

Figure 1-3: Viscosity of polyester during processing at a constant heating rate [4].

The shear rate is also important in determining the chemoviscosity. During the polymerization process there are two different situations that can take place. The viscosity can either increase exponentially losing its ability to shear flow or secondly, it can increase eventually reaching a plateau where it retains its ability to shear flow [9]. While studying the shear rate effects, shear rate and temperature are the most important factors to investigate. It has been shown that polyester and polyurethane exhibit Newtonian behaviour, while epoxy and phenolics show slight shear thinning. The power law, Carreau, Ellis, WLF, Cross, Bueche-Harding models have been used, but the power law has been used the most predominantly [4].

1.3.2 Effect of ingredients on the viscosity

Within the mixture of a epoxy resin system there are many different ingredients. There are the base resin, hardener, accelerator, filler, internal and external mold release agents, de-gassing agents, pigments, UV inhibitors and other additives that are used depending upon the application. In general, the base resin, hardener and accelerator are the ingredients that can affect the viscosity of the system.

1.3.2.1 Effect of the concentration of hardener on the viscosity

Varying the concentration of the hardener has an instant effect on the epoxy system. Typically, the ratio of resin to hardener is stoichiometrically balanced. If this balance is changed there will be a surplus of one ingredient and a shortage of the other. This imbalance will prevent the system from reaching a full cure. A surplus of one ingredient will remain dispersed within the cured resin. The excess acts as a plastifying agent which lowers the modulus and increases the toughness [10]. The effect that the hardener has on the viscosity of the system is dependent on its own viscosity. If its viscosity is greater than the resin viscosity, it will cause an increase in viscosity. If the stoichometric ratio is very far from being balanced, the level of polymerization will be lower. Thus, there is the possibility that the resin will never surpass a gelatinous state.

1.3.2.2 Effect of the concentration of accelerator on the viscosity

The accelerator is one of the factors that controls the rate of the reaction. As the concentration of accelerator increases, the rate of the reaction also increases. Initially, it has no effect on the viscosity since its concentration is very low. The manner in which the viscosity is affected is the speed at which the gel point is attained. Therefore, the accelerator can cause a very fast transition from liquid to solid.

1.3.2.3 Effect of the concentration of glass filler on the viscosity

The effect of filler on viscosity has not been studied extensively, however, it is of great importance while modeling filled thermosets. The filler effects are studied in the same manner as either the shear rate or the cure effects, with the exception that filler properties are also introduced into the problem. It has been found that filler concentration, particle shape, surface interactions, orientation and particle diameter can affect the reaction kinetics, exaggerate the shear thinning and the overall viscosity. While compiling the cure, shear rate and filler effects on the thermoset resin, a complete model can be generated. It has also been found that a model can be developed simply by incorporating the effect of the filler to either the cure or shear rate models [4].

1.3.2.4 Effect of additives on the viscosity

The additives typically have no effect on the viscosity of the system. The main reason for this is that their concentrations are very low (in the order of 0.2 -1.0 %). Therefore they do not make a significant contribution to the bulk of the mixture. However, there is one exception to this rule which are the de-gassing agents. These products are used to reduce the trapped air bubbles in the mixture. This is accomplished by reducing the viscosity and surface tension to facilitate the bubble's motion toward the surface [11].

1.3.3 Effect of temperature on the resin viscosity

Temperature is the parameter that controls the speed of the polymerization and the initial viscosity. The initial viscosity, η_o, is described by

$$\eta_o = Ae^{\left(\frac{E}{RT}\right)} \qquad 1\text{-}6$$

where A is a constant, E is the viscous activation energy, R is the gas constant and T is the absolute temperature. Therefore, seen in equation 1-6, the temperature is the only factor that affects the initial viscosity assuming a zero shear rate.

1.3.3.1 Pot life of the resin

The pot life of the resin is defined as the time that the resin can sit in the bath at room temperature before its viscosity doubles [12]. The pot life is not a parameter within the die but more of method to determine the initial conditions of the resin going into the die. As the bath viscosity increases, both the fiber wetting and the time to gel decrease. However, for practical purposes, the difficulties in fiber wetting will develop before any type of cure problems thus limiting the viscosity of the resin in the bath at a certain value [12].

1.3.3.2 Effect of high temperature on the viscosity

Inside the pultrusion die, temperatures up to 220°C can be found for epoxy / glass composites. This sudden rise in temperature causes the viscosity of the resin to drop to extremely low values and then increase in a very short time. The material can actually transform from a liquid to a solid in less than one minute. The high temperature causes the resin viscosity to drop but it will also cause a more rapid transition to the solid state. This rapid transition is caused by the rapid polymerization that is described in the kinetic theory found above [13].

1.3.4 Modeling the viscosity of the resin

The types of models that exist for modeling the viscosity are; empirical, probability-based and molecular, gelation, Arrhenius and models that are based on free volume analyses. As the viscosity of the liquid changes so does the molecular size, thus, the degree of conversion. The following relationship is the principal empirical model that has been used to date,

$$Ln\eta(t) = Ln\eta_{\infty} + \Delta E_{\eta}/RT + tk_{\infty}\exp(\Delta E_K/RT) \qquad 1\text{-}7$$

where $\eta(t)$ is a function of time at a specific temperature, η_{∞} is the calculated viscosity at a specific temperature, E_{η} is the Arrhenius viscous activation energy, R is the universal gas constant, T is the absolute temperature, t is time, k_{∞} is the kinetic analogue of η_{∞}, and E_k is the kinetic analogue of E_{η} . The main drawback with this model is that it offers no control over the chemical conversion versus time and it assumes that the viscosity in the early stages follows a Newtonian behaviour [7]. Further improvements of the model have lead to

$$Ln\eta(T,t) = Ln\eta_{\infty} + {\Delta E_{\eta}}/{RT} + \int_0^t k_{\infty}\exp\left({\Delta E_k}/{Rf(t)}\right)dt \qquad 1\text{-}8$$

The main drawbacks with this approach are that Ln η_{∞} usually becomes non-linear as the reaction proceeds and equation 1-8 develops six parameters, rather than four, thus making it more complex. Also, this approach is not based on polymerization kinetics

and, therefore, is very specific for each resin since it is not related to resin chemistry [7,14].

Measuring the viscosity is the most widely used technique to investigate the initial stages of curing. Because of this, there have been many empirical exponential formulas that have been developed to predict the viscosity.

$$\eta = \eta_o \exp(\theta t) \qquad 1\text{-}9$$

where η is the viscosity, η_o is the initial viscosity, and θ is a constant. The problem with the preceding formula is that it does not acknowledge the gel point. The viscosity can never reach infinity. The viscosity can also be calculated using equations that are based on molecular mass as shown below.

$$\eta = C\overline{M}^{a} \qquad 1\text{-}10$$

where C is a constant, "a" is the exponent with a universal value (a=1 $\overline{M} < \overline{M}_c$ or a=3.5 $\overline{M} > \overline{M}_c$) and $\overline{M}$ is the molecular mass.

or

$$\eta = Ae^{D/RT}\left(\overline{M}_W / \overline{M}_{WO}\right)^{(C/RT+S)} \qquad 1\text{-}11$$

where A, C, D and S are constants, $\overline{M}_{WO}$ is the initial weight average molecular mass and R is the universal gas constant. However, it is difficult to establish a connection between molecular and rheological characteristics while the resin is curing due to the formation of complex branching that is taking place. Because the degree of conversion

is a function of molecular mass and because $\overline{M}$ tends toward infinity, the previous equations can also be thought of as

$$\eta/\eta_o = \left(\frac{\alpha^*}{\alpha^* - \alpha}\right)^{A+B\alpha} \qquad 1\text{-}12$$

where α is the degree of conversion, α^* is the degree of cure at the gel point, and A and B are constants [7,15]. Using the Williams-Landel-Ferry equation viscosity as a function of temperature can then be connected with the kinetics of polymerization, as seen below,

$$\log\eta(T) = \log\eta(T_o) + \frac{A(T - T_o)}{B + (T - T_o)} \qquad 1\text{-}13$$

where η is the viscosity, T is the temperature, T_o is the reference temperature and A & B are constants. Since the T and T_o are a function of the degree of polymerization they are also connected to the degree of conversion [7,14,16].

In a completely new approach to modeling the viscosity, Gillham has constructed a model that attempts to explain the avalanche-like increase of viscosity near the gel point. The model uses two phenomena that take place during the reaction. The first is the increase in the glass transition temperature and the second, is the increase in molecular mass. Therefore, using the WLF equation to determine the change in the glass transition temperature, the general formula by Gillham is shown below.

$$Ln\eta = Ln\eta_{\infty} + Ln\overline{M}_W + E/RT - \frac{C_1(T - T_o)}{C_2 + T - T_o} \qquad 1\text{-}14$$

where C_1 and C_2 are constants of the WLF equation and T_o is the reference temperature. This model does give better results than the standard WLF equation, however, it is more complex due to the introduction of molecular mass [15].

Malkin et al, originally used the following equation to model viscosity,

$$\eta = \eta_{\infty} \exp\left(\frac{E}{RT} + C\alpha\right) \qquad 1\text{-}15$$

where E is the viscous activation energy, η_{∞} is the initial viscosity, C is a constant, R is the universal gas constant and T is the temperature. Since it was developed, many authors have used it, but its main drawback is that it is only valid for low degrees of cure [15,17,18].

It has been shown that heterogeneous gelation can occur in polymer-forming networks through the formation of micro gel particles. It is possible that there are actually two gel points, one that gives an apparent infinite molecular mass due to the presence of the micro gel particles, and a second that gives the actual gel point where the resin becomes one large molecule. Because of these micro gels , it becomes possible to model the resin as a filled system where the filler is equivalent to microgel particles as shown below

$$\eta/\eta_o \approx \left(1-\theta/\theta^*\right)^{-c} \qquad 1\text{-}16$$

where, θ^* is the ultimate concentration of filler and c is a constant. Assuming that θ represents time, the following relation can be obtained to model the kinetics of the viscosity, [15]

$$\eta(t)/\eta_o(t) = \left(1-t/t^*\right)^{-b_t} \qquad 1\text{-}17$$

where $\eta(t)$ is the viscosity of the reactive system, $\eta_o(t)$ is the viscosity of the dispersion medium, t^* is the gel time and b_t is a constant [15]. If the relaxation of the state of a reactive system changes, the following relationship can be used to take into account different factors on the viscosity.

$$\eta/\eta_o = \left(\frac{1+kt}{1-t/t^*}\right)^A \qquad 1\text{-}18$$

where k is the rate constant of the reaction and A is a constant. During the reaction, if the reactive oligomers are followed by a phase segregation, the previous reaction becomes

$$\log \eta/\eta_m = \pm A \log t/t^* + B \log \frac{1}{1-t/t^*} \qquad 1\text{-}19$$

where A and B are constants [15].

According to Malkin and Zhirkov, the degree of conversion would seem to be an appropriate choice to use while modeling a liquid. A model that combines the Arrhenius formula and consideration for the gel point is shown below.

$$\eta = \eta_o \left(1 - \frac{\alpha}{\alpha^*}\right)^{-b_c} \qquad 1\text{-}20$$

where η is the viscosity, η_o is the initial viscosity, α is the degree of cure, α^* is the degree of cure at the gel point and b_c is a empirical constant related to the real properties of the resin. Equation 1-20 appears to be the well-suited for modeling epoxy resin since it is a temperature-based model that uses basic concepts [15].

1.4 Determining the gel time

The gel point can be characterized by the point where the viscosity rises very rapidly. At the gel point, the covalent bonds that are being formed connect across the sample to form an infinite network. Beyond the gel point the reaction can still continue, however, it is slowed down due to the low diffusion rates that are caused by the high viscosity. Shown in figure 1-4 are the seven distinct phases of a thermoset resin. Isothermal heating of a sample can be illustrated on the figure by a horizontal line. As time passes the sample will enter all the phases that are intersected by the line. The degree of cure is greatly affected depending on the isothermal temperature that is selected. For example, if gelation is reached before vitrification, the resin will attain a

higher degree of cure since the molecules can more easily orient themselves to form an infinite network. If the resin reaches vitrification before gelation, the molecules will be frozen in place and it will become difficult for the molecules to orient themselves, thus, it will have a lower degree of cure [4].

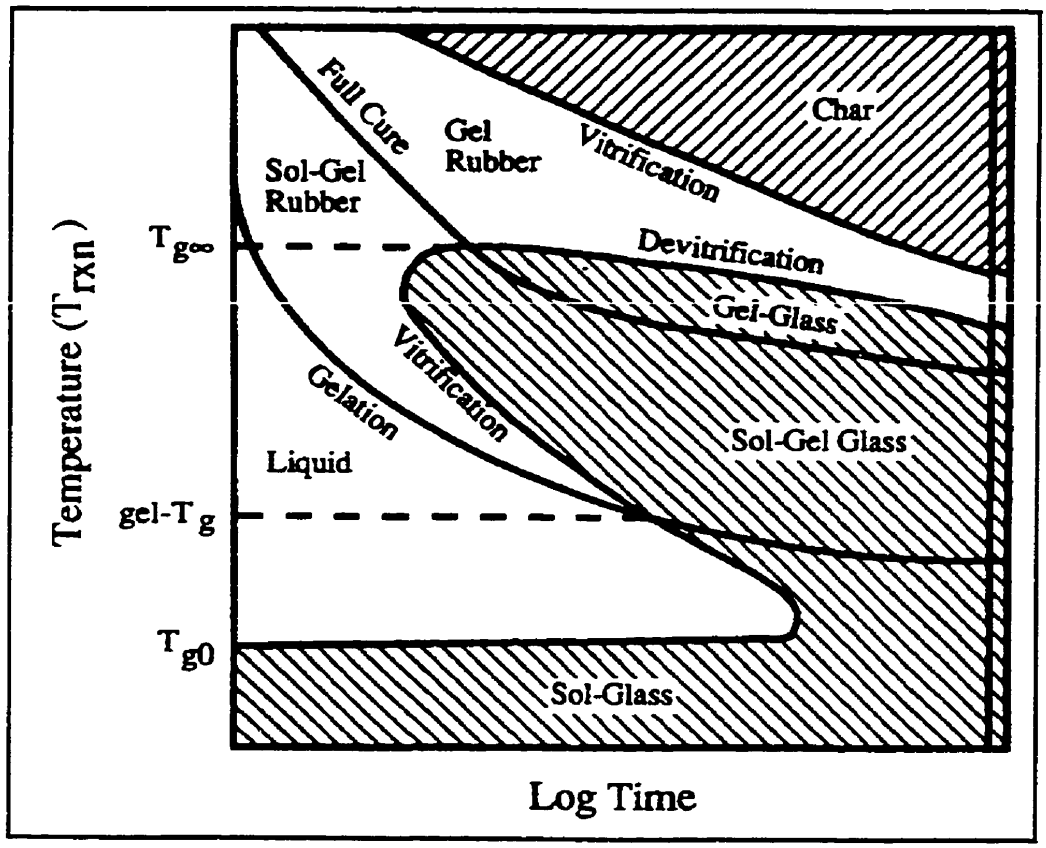

Figure 1-4: Time temperature transformation (TTT) diagram [4].

The gel point is an important characteristic of a resin since it marks the end of the first half of the process and marks the beginning of the second half. The classical definition of the gel point is where the molecular mass tends toward infinity, thus the

viscosity also becomes infinite. To determine the gel point, there are many different techniques that can be used and there is a definition that is associated with each technique. The majority of these use isothermal tests and dynamic temperature ramps. Some authors have said that the gel time can be determined through rheological measurement where the tan $\delta = 1$, (where δ is the loss factor), however, this is only valid for stoichiometrically balanced systems. Malkin and Kulichikhin have determined that the most general determination of the gel time is when the tan δ reaches its maximum [15]. Roller decided that the gel time occurred when the viscosity of resin reached 100000 cP [7]. The gelation point can also be determined when the viscosity tends toward infinity and where the loss tangent becomes independent of frequency. The effect of fillers on the gelation point has not been extensively studied, however it has been found that an increase in filler decreased the gel time [4,19].

To determine the degree of cure at the gel point, there are many techniques and models that can be used. Many of these models require a significant analysis of polymer chemistry. However, there is one model that does not require extensive analysis and it is Flory's classical approach [20,21]. To determine the degree of cure at the gel point experimentally, there are many techniques that use a wide range of equipment that varies from simple to complex.

1.4.1 Modeling the gel time

The degree of cure at the gel point can be determined using Flory's classic approach. This approach is a theoretical method that is based on the ratio of the reactive groups and the functionality of the branching unit. This equation is seen below

$$\alpha_{gel} = \sqrt{\lambda / (f-1)} \qquad 1\text{-}21$$

where λ is the ratio of the reactive groups, α_{gel} is the degree of cure at the gel point and f is the functionality of the branching unit. This theory can be used in conjunction with a kinematic model to determine the gel time [20].

For the gel to occur, a unique degree of cure must be formed that is independent of temperature. If it is supposed that the increase in cure is kinetically controlled, it can be expressed by the following relationship.

$$dx/dt = Af(\alpha)\exp\left(\frac{-E}{RT}\right) \qquad 1\text{-}22$$

Where α is the degree of cure, T is the absolute temperature, E is the kinetic activation energy, t is time, R is the gas constant and A is constant. Integrating equation 1-22 at constant temperature yields the following relationship.

$$Ln\left(\int_0^x \frac{d\alpha}{f(\alpha)}\right) = Ln(A) - E/RT + Ln(t) \qquad 1\text{-}23$$

If it is assumed that the gel point always occurs at a constant degree of cure, equation 1-23 can be rearranged to yield the following relationship.

$$Ln(t_{gel}) = Ln\left(\int_0^{\alpha^*} \frac{d\alpha}{f(\alpha)}\right) - Ln(A) + E/RT \qquad 1\text{-}24$$

Which reduces to,

$$Ln(t_{gel}) = E/RT + K \qquad 1\text{-}25$$

Therefore, plotting Ln gel time versus the reciprocal of the absolute temperature gives a linear function where its slope is E/R and the y-intercept is the constant *K*. Thus, the gel time for any temperature can be extrapolated from this line [21,22].

1.5 Volumetric changes of the resin

The volumetric changes of the resin can be positive (expansion) or negative (shrinkage) during curing. In the early stages of polymerization, the resin will expand due to thermal heating. As the resin's temperature increases, the individual molecules begin to vibrate with a greater amplitude. This motion is referred to as Brownian motion. Therefore, as the amplitude of the vibrations increases, the free volume within the resin increases. The fractional free volume of a liquid, f_v, is in equation 1-26

$$f_v = \frac{V_f}{V_T} \qquad 1\text{-}26$$

where V_f is the free volume, and V_T is the total volume occupied by the liquid. Thus, as the free volume increases, the molecular mobility and the self-diffusion rate increases and the viscosity will decreases [23].

Studies that have been performed to date indicate that the volumetric shrinkage that occurs during the polymerization process increases, as the cure temperature increases, and decreases as the concentration of filler increases [24]. The temperature increases the shrinkage because the higher temperature facilitates the molecular interaction. This leads to a higher degree of cure, thus, making the molecular structure more compact. The filler decreases the shrinkage because the filler is typically inert, therefore, chemically it does not change. Thus, it reduces the fraction of resin in the solution.

The instrumentation that has been used by many researchers to measure the volumetric expansion is typically built in-house. Even though most of the dilatometers have been designed at different research facilities around the world, they all use mainly the same principle. The theory is to maintain a constant pressure on the resin, while allowing it to expand or contract freely. Typically, a secondary fluid is used to measure the displacement of the resin during cure. Because of this condition, trends between the different studies can be compared, however, the exact numerical values may differ. The reason why the numerical values cannot be compared is that each design will have its

own inherited errors. Some designs are better than others, therefore the amount of error will vary from design to design [24-31].

1.5.1 Effect of ingredients on the volumetric changes

The main ingredient having an effect on the dilatation of a epoxy resin system during cure is the hardener. If the concentrations are not stoichiometric, there will be excess of one ingredient in the solution. Therefore, it will act as a plastifying agent and prevent the formation of bonds between all of the molecules. Thus, the cured resin will be less compact which results in less cure shrinkage [10].

The effect that additives have on the dilatation of the resin is theoretically very little. As seen in equation 1-34, section 1.5.3., there are two constants that are needed, one for the volumetric expansion of the unreacted resin and one for the volumetric expansion of the cured resin. Therefore, additions in the order of 1% should have very little effect on the volumetric expansion of the unreacted resin [24].

1.5.2 Design of a dilatometer

To date, virtually every dilatometer that has been used in a study was designed and built by the researchers themselves [24-31]. Among these designs, there are two

main types, capillary and plungers. The capillary design uses a secondary fluid that engulfs the resin. When the resin changes its volume the fluid is displaced inside the capillary. The plunger type of design is a more complex system that is similar to the capillary type with the following exception. Rather than allowing the fluid to flow freely inside the capillary, the plunger type replaces the capillary with a plunger. With the plunger in place, a force or pressure can be applied to the plunger to create a pressure on the resin. The advantage of this type of design is that it allows the user to perform dilatometric measurements at high pressure [29].

1.5.3 Modeling the volumetric changes

At the present time, there has been little information found in the literature on the modeling of the volumetric changes in a curing resin. Hill et al. [24] have developed the most complete models to do so. They noticed that the shrinkage is a function of the radical concentration, which can be expressed as

$$\left[\frac{\Delta V}{V_o}\right]_{\substack{Polymerization\\Shrinkage}} = S_f\left(\frac{c\ddot{\ddot{R}}^n}{1+c\ddot{\ddot{R}}^n}\right) \qquad 1\text{-}27$$

and

$$\ddot{\ddot{R}} = \frac{r}{r_f - r} \qquad 1\text{-}28$$

where ΔV is the change in volume, V_o is the initial volume, S_f is the final (or maximum) polymerization shrinkage, r is the radical concentration (mol/L), r_f is the final radical

concentration (mol/L) and c is a parameter obtained by plotting the percent polymerization shrinkage versus radical concentration [24]. The volumetric expansion caused by the thermal changes can be represented by

$$\left(\frac{1}{V_o}\frac{dV}{dt}\right)_{\substack{Thermal\\contribution}} = \beta\frac{dT}{dt} \qquad 1\text{-}29$$

and $$\beta = \beta_m(1-\alpha)+\beta_p\alpha \qquad 1\text{-}30$$

where β_m is the volumetric thermal expansion coefficient of monomer (or uncured resin), β_p is the volumetric expansion coefficient of polymer (or cured resin), α is the degree of cure, T is the absolute temperature and t is time. To facilitate the determining of the constant β_p , a sample of the cured resin can be measured using a ThermoMechanical Analysis (TMA). Once the linear coefficient of thermal expansion (CTE) is known, the volumetric CTE can be calculated using the following expression

$$\frac{\Delta V}{V_o} = \left(1+\Delta l/l_o\right)^3 - 1 \qquad 1\text{-}31$$

where $\Delta V/V_o$ is the volumetric CTE and $\Delta l/l_o$ is the linear CTE [26]. Therefore, combining equation 1-27 and 1-29, the overall dilatation of the system can be described as

$$\left(\frac{1}{V_o}\frac{dV}{dt}\right)_{Overall} = \left[\beta_m(1-\alpha)+\beta_p\alpha\right]\frac{dT}{dt} - S_f\frac{d\left(\frac{c\ddot{R}^n}{1+c\ddot{R}^n}\right)}{dt} \qquad 1\text{-}32$$

Hill et al. have developed a second model that is based on the conversion of the reaction. This model assumes a linear relationship between the degree of cure and shrinkage, which is seen below

$$\left(\frac{1}{V_o}\frac{dT}{dt}\right)_{\substack{Polymerization\\shrinkage}} = B\frac{d\alpha}{dt} \qquad 1\text{-}33$$

where B is a constant determined from the plot of polymerization shrinkage versus conversion and α is the degree of cure. This equation can be combined with equation 1-29 in the same fashion as above to give the over-all dilatation of the resin which is seen below.

$$\left(\frac{1}{V_o}\frac{dV}{dt}\right)_{Overall} = \left[\beta_m(1-\alpha)+\beta_p\alpha\right]\frac{dT}{dt} - B\frac{d\alpha}{dt} \qquad 1\text{-}34$$

This relationship is relatively simple to use and B is the only parameter that needs to be determined. The drawback to this model is that it tends to deviate in the later stage of curing [24].

1.6 Pressure development during cure

The pressure rise inside the die is an essential part of the pultrusion process. It is this pressure that helps consolidate the fibers and assures good fiber wetting. The pressure that develops inside the pultrusion die is directly related to two phenomenons. The first is the geometry of the die entrance and the second is directly related to the

volumetric changes in the resin. The geometry of the die entrance can be linear, circular or parabolic. The entrance length also influences the pressure within the die. This increase in pressure can be simulated by a constant that is dependent on the entrance diameter [32].

A second effect that the pressure has on the system is it causes a lag in the polymerization. As mentioned in the previous section, as the resin is heated, the heat causes a thermal agitation of the molecules and it is this agitation that causes an increase in volume. As this free volume between the molecules increases, it facilitates the interaction of the reactive species. Because of this, the reaction can propagate faster. Once a pressure is applied, the free volume decreases which makes the molecular interaction more difficult, thus slowing down the reaction rate [29,33].

1.6.1 Effect of ingredients on the pressure development

The volume fraction of fiber and/or filler in the system plays the greatest role in the pressure profile inside the die. As seen in equation 1-41, the fiber and/or filler fraction, V_f, plays a large part in determining the pressure profile within the die. As this fraction is increased, there is a greater resistance to the back flow that is caused by the volumetric expansion.

1.6.2 Measuring the pressure profile inside the die

To date, there are three techniques to measure the pressure inside a pultrusion die. The first is to use flush mounting pressure transducers mounted on the outside of the die. This technique provides accurate pressure measurements, however, they give a point measurements and their life is very limited due to the harsh abrasion that take place inside the die. The second technique is the Force Sensing Resistor (FSR). It is a thin sensor that can detect changes in pressure. This device is inserted inside the die and continuously measures the pressure as the resin cures. The limitations of this technique are that sensor remains imbedded in the material and that its physical size causes a rise in pressure thus falsifying the data [34,35]. The final technique used to measure the pressure inside the die, is with a fiber optic device. A fiber optic wire is inserted inside the die and the changes in the transmittability of the light are converted into a force value. The problem with this technique is that the system is very delicate, complex and very expensive [35].

1.6.3 Modeling the pressure profile inside the die

To date, there is very limited information on the development of the pressure inside the pultrusion die. At the fundamental level of research, there is a model described by Lee and Pae [36]. Pressure that is generated within a chemical reaction can

be attributer to a change in volume. The pressure on a chemical reaction can be described as

$$\frac{dLnk}{dP} = -\frac{\Delta V'}{RT} \qquad 1\text{-}35$$

where k is the rate constant, P is the pressure, $\Delta V'$ is the activation volume, R is the gas constant and T is the absolute temperature. The activation volume is defined by the difference between the transient state and the reactant state (V'-V_R).

To predict the pressure distribution within the die, Moschiar [37] has presented a model which is composed of two parts. The first section calculates the pressure rise due to the tapered section at the die entrance. The pressure at the entrance can be described by

$$\frac{dP}{dz} = V\left(\frac{\phi_g(\varsigma)}{\phi_g(1)} - 1\right)\frac{\eta\phi_g(\varsigma)^2}{(1-\phi_g(\varsigma))^3}\frac{16K}{D_f^2} \qquad 1\text{-}36$$

where ζ is the dimensionless length (ζ=z/L_t), L_t is the taper length, D_f is the fiber diameter, (1-ϕ) is the system porosity, V is the pulling speed, η is the viscosity and K is the Blake-Kozeny constant. The porosity at a given length is given by

$$\phi_g(\varsigma) = \phi_g(1)^{D(1)/D(\varsigma)} \qquad 1\text{-}37$$

and

$$D(\varsigma)/D(1) = Cr - (Cr-1)\left[1-(1-\varsigma)^2\right]^{0.5} \qquad 1\text{-}38$$

where Cr is the compression ratio. To predict the pressure profile for the second section, which consists the remainder of the die, can be described as [38]

$$P = \frac{\alpha_L}{\beta}\left(\overline{T} - T_o\right) - \frac{\gamma}{\beta}\overline{x} + P_o \qquad 1\text{-}39$$

where α_L is the thermal expansion coefficient, γ is the shrinkage, β is the compressibility constant, $\overline{T}$ is the average temperature and $\overline{\chi}$ is the average degree of cure [37]. The model that was developed by Moschiar was further improved by Kim [38]. The pressure profile was divided up into 3 parts: the inlet, the liquid, and the solid portions inside the die. The inlet pressure is determined by

$$\frac{dP}{dz} = V\eta \frac{16K}{D_f^2} \frac{\nu_f^2(z)}{\left[1-\nu_f(z)\right]^3}\left[1-\nu_f(z) - \left(1-\Delta\nu/\nu\right)\left(\frac{\nu_f(z)}{\nu_f(L_t)} - \nu_f(z)\right)\right] \qquad 1\text{-}40$$

where V is the speed of the system, η is the viscosity of the resin, K is the Kozeny constant, D_f is the fiber diameter, ν_f is the fiber volume, ν is the volume of the composite and L_t is the taper length. To determine the pressure profile between the taper and the gel point, the following relationship can be used.

$$\frac{dP}{dz} = V\eta \frac{16K}{D_f^2} \frac{\nu_f^2(z)}{\left[1-\nu_f(z)\right]^3}\left(\Delta\nu/\nu\right)\left[1-\nu_f(L_t)\right] \qquad 1\text{-}41$$

The final section in the die is the solid region. The pressure profile for this section can be determined by [38]

$$\frac{dP}{dz} = \frac{1}{K_b}\left[a_v \frac{dT}{dz} - \gamma \frac{d\alpha}{dz}\right] \qquad 1\text{-}42$$

where K_b is the compressibility of the resin, a_v is the thermal expansion coefficient, and γ is the volumetric shrinkage of the resin due to the chemical reaction.

As seen in equations 1-40 to 1-42, all of the previous sections are needed to model the pressure profile inside the pultrusion die. The viscosity of the resin is needed to predict pressure caused by the resin back flow. The gel time is needed to divide the die into the appropriate zones so that the pressure models can be applied correctly. The volumetric expansion is needed to determine the amount or resin back flow as well as the cure shrinkage in the solid state [38,39].

Kim claims that the actual pressure exerted on the material is less than the value that is calculated. The theory behind this is that there is a layer of resin that solidifies against the die before the majority of the resin. A description of Kim's [38] boundary layer theory can be seen in figure 1-5.

The cause of this solidification is explained using boundary layer theory where there is a velocity profile that ranges from 0 to V. Therefore, the layer of resin that is closest to the die has a longer residence time in the die. It is this outer ring of solidified resin that shields the inner material from a greater pressure. Therefore, to compensate for this effect, there is a shield correction factor that can be applied to the above equation by

$$P_S = (1 - k_{shield}\alpha_S)P(z) \qquad 1\text{-}43$$

where α_s and P_s are the degree of cure and the pressure on the materials surface [38]. The model shown above by Kim appears to be the most complete that is found in the literature to date. It uses conservation of mass to account for the back flow that occurs in the die. Darcy's law for porous media, in conjunction with the Kozeny-Carman equation is used to simulate the resin flow through the fibers. The change in density is related to the volumetric expansion and process intricacies are also included.

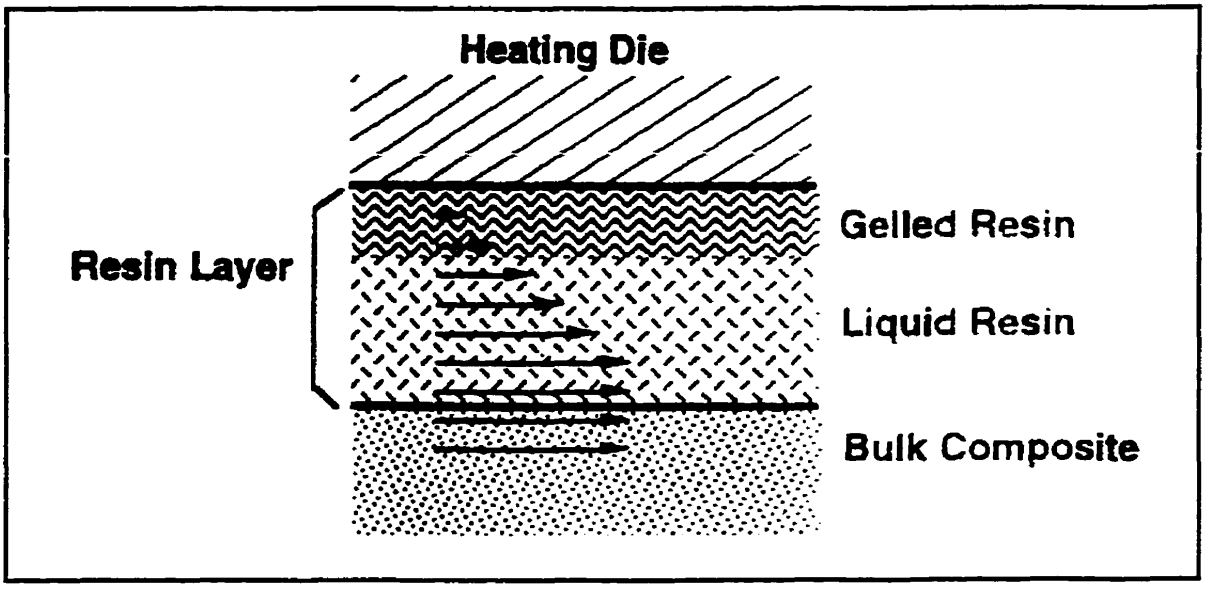

Figure 1-5: Description of the boundary layer [38].

1.7 Pull force on the profile

The pull force has been quoted as the *pulse of pultrusion*. Measuring this parameter is a very useful tool to monitor the *health* of the process. While monitoring

the pull force, if it remains constant for a given speed, the operator does not need to worry about the process. If it is noticed that it is beginning to increase while remaining at constant speed, there is cause for alarm [35].

1.7.1 Contributions to the pull force

The pull force that is observed while pultruding is a combination of many different factors. As mentioned earlier, there are three phases that the material passes through while being processed. Each of these zones gives a special contribution to the pull force. Sumerak [35] has discussed six factors which contribute to the pull force. These factors are collimation, bulk compaction, viscous drag, thermal expansion, gel adhesive debonding and shrinkage drag. Collimation is the alignment of the fibers in the racks and pre-formers. The bulk compaction, viscous drag and thermal expansion are all associated with the liquid phase of the material. The gel adhesive debonding is associated with the gelatinous phase. The shrinkage drag is associated with the solid phase.

1.7.2 Techniques to measure the pull force

There are many different techniques to measure the pull force. Because the pull force is in direct relation to the pressure inside the die, any of the pressure monitoring

technique that are mentioned above can be used [35]. To monitor the pull force directly, there are two options that can be employed. The first is to install a force transducer between the die and the die table. This is an accurate method, however, a temperature correction factor must be used to compensate for the elevated temperatures that are subjected to the transducer. The second technique is to monitor the power that the puller is consuming. To obtain a measure in force, knowledge of the gear train and motor characteristics are needed.

1.7.3 Modeling the pull force

To date, there is only one pull force model that has been found. This model is used by Moschiar [39] and Kim [38] to determine the pull force while pultruding. The shearing of the resin in the liquid phase that is close to the die wall can be modeled as a Couette flow using the following equation

$$\tau_{shear} = \eta \frac{V}{\delta} \qquad 1\text{-}44$$

and

$$\delta = D_f \left[\sqrt{\frac{\pi}{2v_f\sqrt{3}}} - 1 \right] \qquad 1\text{-}45$$

where τ_{shear} is the shear stress on the die wall, η is the resin viscosity, V is the speed of the system, δ is the thickness of the resin layer, D_f is the fiber diameter and v_f is the

volume fraction of fiber. The pull force in the solid region can be modeled using Coulomb friction, while using the following relationship,

$$\tau_r = \lambda f P_S(z) \qquad 1\text{-}46$$

where λ is the volume fraction of resin which has reached the gel point, f is the coefficient of friction and P_s is the pressure at that given point. The model that is presented above in equation 1-40 to 1-42, incorporates almost all of the factors which affect the pull force. Equation 1-40 models the effect of inlet geometry which contributes to the bulk compaction of the resin. This initial bulk compaction is associated with the initial pressure rise at the inlet. Equation 1-41 incorporates the bulk compaction, viscous drag and thermal expansion, to model the development of the pressure profile inside the die. Equation 1-42 models the effect of the shrinkage drag which continues the pressure profile from the previous section.

The total pulling force is described as

$$F = \int_0^{L_t} T_{shear}\, dz + \int_{L_t}^{L} \tau_r\, dz \qquad 1\text{-}47$$

where L_t is the length of the liquid region and L is the length of the die. The model presented here includes five of the six factors which contribute to the pull force. The factor that is missing is the gel adhesive debonding. As mentioned earlier, there are three zones inside a pultrusion die, liquid, gelatinous, and solid [31]. The model that was just presented includes only the liquid and solid forces.

Kim [38] uses boundary layer theory (seen in figure 1-5) to help predict the beginning of the solid phase. The residence time of the resin near the die wall can be calculated by

$$t = \frac{\delta}{V}\frac{z}{y^+} \qquad 1\text{-}48$$

where δ is the resin layer, z is the distance in the die, V is the speed of the system and y^+ is the distance from the die wall.

1.8 An application of pultruded composite in civil engineering

The pultrusion process is the most cost-effective way to produce high performance composite materials. This fact makes pultruded composites a cost-effective replacement for steel rebars in concrete. Since carbon, glass, aramid and other fibers have competitive properties with steel, they make a natural choice to use when replacing steel. Following are some of the applications where pultruded composites (PC) can be used with concrete. PC can be used to replace steel rebars inside concrete structures. It can be bonded to the tension side of concrete structural members to either reinforce or repair the existing structure. It can also be used as the forms used in pouring concrete, except that the forms would not be removed once the concrete has cured.

The driving force behind the development of fiber-reinforced plastics, FRP, to reinforce concrete is emerging from all over the globe. In North America, the need is to develop corrosion-free infrastructures. In Japan, the need is to automate, prefabricate and to develop a cleaner manufacturing process. In Europe, it's partially a combination of the two, as well as, the restoration of historic landmarks [42].

In Canada, the use of FRP in concrete is currently being used in pilot projects such as, bridges, girders, barrier walls and structural networks. In Europe, FRP are being used in many bridges and their behaviour is being monitored. The monitoring of the FRP tendons is done with either fiber optic or copper sensors that have been implanted in the structure. Some structures have been monitored now for over ten years and are still behaving normally. Currently, in Japan, there are roughly 15 manufacturers of fiber reinforcement. The types of fibers that are used are carbon, aramid, glass and Vinylon (polyvinyl alcohol). The main types of resins that are used are epoxy, vinyl-ester and PPS. The idea behind using FRP reinforcement in cement in the United States dates back to the 1930's. In the 50's and 60's the interest in this domain had fallen but in the 70's, the interest in this domain grew rapidly because of the corrosion of their current concrete structures[42].

There are two different ways in which FRP can be used in conjunction with concrete. It can be used in the conventional grid system or with bonded plates. In the

conventional way, the FRP rods are used inside the concrete to replace the steel rebars. The bonded plate technique consists of bonding a FRP plate to the tension side of the structural member. This technique appears to work rather well to reinforce concrete and to prevent corrosion [42].

The main benefit of using Glass Fiber Reinforced Plastic, GFRP, to replace steel rebars, is that they are much more corrosion-resistant than steel. This results in a structure that will last much longer before needing any maintenance. Another added benefit of using GFRP in concrete is that it can be used to measure the stress state of the structure. This makes for an intelligent structure that is easily monitored.

Polyvinyl alcohol fibers, PVA, were considered as a replacement of steel rebars in concrete. The chemical resistance of the fibers were unaffected by animal, vegetable and mineral oils as well as resistance to acids, alkalis and salts. The ultimate stress in the rebars was 1.6 times that of the steel bars. Another added benefit of PVA rods is that they can be shaped on the spot by simply applying heat to the rod [43].

This application of using pultruded composite as a reinforcement method for concrete is just one example to demonstrate the momentum that pultrusion is gaining in replacing conventional materials. These advancements are due to the material's resistance to corrosion, light weight, insulating properties and excellent mechanical properties. The increase in speed at which new applications of pultruded composites can

be used is dependant on the time required to perfect the process. Modeling the process will enable new ideas to be investigated easily and cost effectively.

Chapter 2 Project Description

2.1 Scope of the project

This project presents a method to model the pull forces developed while pultruding epoxy / glass and polyester / glass systems. To date, there has been much research that has focused on modeling the primary aspects which occur during the pultrusion process. However, there are few studies that present a complete and accurate description of all the factors which affect the material during processing.

The importance in modeling the pultrusion process is that it will save the operator valuable time and energy in determining the ideal settings for the process. The correct settings offer increased line speed, reduced chance of blockage and the best mechanical properties. Presently every time a new material system or profile is used, the operator has to go through a trial and error period to determine the correct settings for the process.

In the past, the pultrusion industry has seen an increase in growth of 12-15%. In addition to this, there have been major mergers between the leading materials producers and the manufacturers which typically tends to accelerate the pace of determining new applications for pultruded profiles [40]. This pace will continue to increase as better computer models of the pultrusion process are developed.

2.2 Objectives

This project is part of a research study aimed at modelling the pull force while pultruding composite profiles. The specific objective of this project is the identification of the different elements required by a pull force model and the eventual presentation of a preliminary model.

2.3 Methodology

2.3.1 General approach

The theory and instrumentation that exists for determining the degree of cure is well developed and very accurate. In addition, the degree of cure is an excellent means of following the development of the polymerisation in the resin. The degree of cure can be used to model the viscosity, gel point, volumetric changes, and pressure of the resin inside the pultrusion die. It is this characteristic of the degree of cure which make it a good choice while modelling the pultrusion process. Seen in figure 2-1, are the degree of cure profiles which run the length of the die. Therefore, the behaviour of the viscosity, gel time, volumetric changes, pressure development and pull force can be determined from these cure profiles. Equation 1-20 is used, to obtain the viscosity profile and the length of the liquid zone in figure 2-1, and is delimited with the gel time.

Equation 1-34 is applied to calculate the volumetric changes of the resin while it is being transformed. Equations 1-40 to 1-42 are used to obtain the pressure profile in the die. Finally, equation 1-47 is used to determine the pull force. The degree of cure, viscosity, gel time and volumetric changes are directly needed to calculate the pressure profile. The pressure profile is then directly connected to the pull force which is required to pull the profile through the die. As shown above, the pull force needed for a particular profile is dependent on all the properties of the resin.

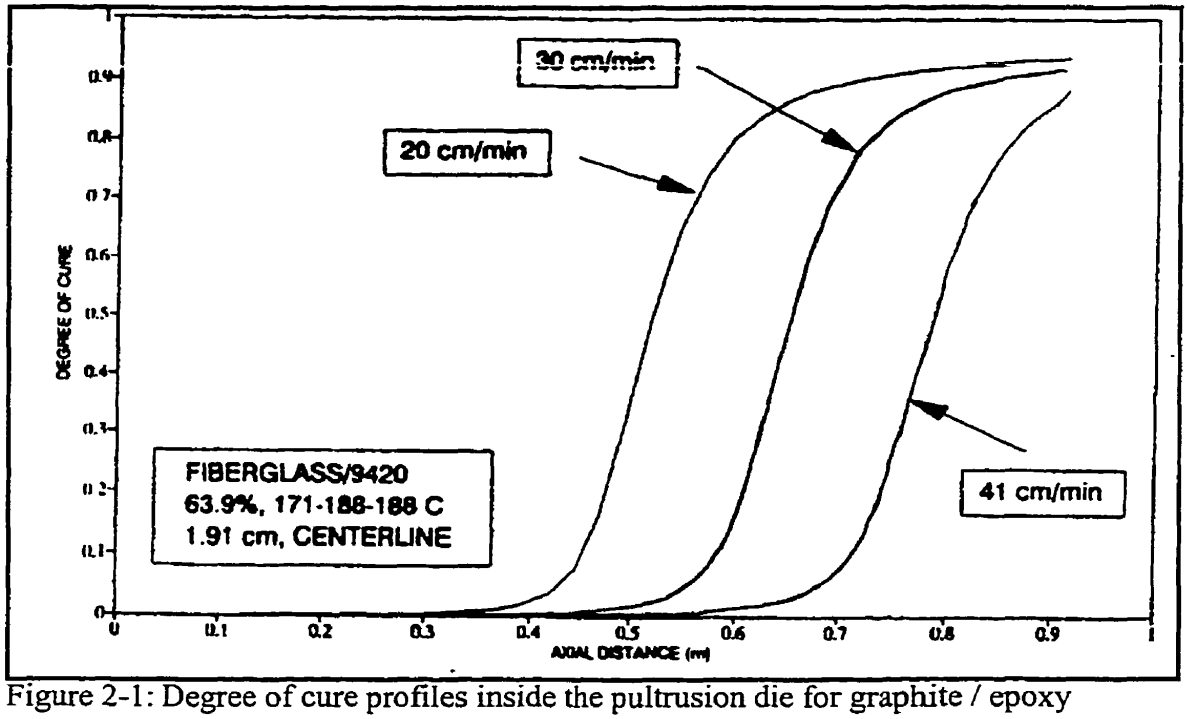

Figure 2-1: Degree of cure profiles inside the pultrusion die for graphite / epoxy composite.[41]

2.3.2 Principal steps

In order to model the pull force, five sub-models are needed to accomplish this task. These sub-models simulate the cure kinetics, viscosity, gel time, volumetric changes and pressure in or on the resin while it is being transformed in the pultrusion die. The cure kinetics have already been modeled by Atarsia and Boukhili [6] for the epoxy resin.

1. To obtain the degree of cure profiles for the polyester resin, a differential scanning calorimeter is needed to measure the cure profiles for various heating rates and temperatures. To perform isothermal tests, the sample is subjected to a constant temperature for the duration of the test, and following this, the sample is then subjected to a dynamic temperature scan to determine the residual heat in the sample. The isothermal tests are followed by a dynamic scan due to the following phenomenon. As the resin cures isothermally, after the gel point, the resin begins to vitrify. This vitrification prevents the resin from curing completely, thus preventing the resin from releasing all of its potential heat. The dynamic scan is then used to force the reaction to continue and all of the potential heat is then released.

2. Viscosity measurements are needed to validate the models that have been found in the literature. Equation 1-20 is used to model the viscosity, and predicts the viscosity using the temperature and the degree of cure. Initially, when the degree of cure

is low, it is principally the thermal stimulation which affects the viscosity. As the degree of cure increases, the molecules in the solution become larger, thus increasing the viscosity, which counter-effects the changes caused by the temperature. When the resin approaches the gel point, the model forces the viscosity to an infinite value. This is the principal advantage that sets this model apart from the others in the literature.

3. The degree of cure at the gel point is a very useful parameter to obtain while modeling a thermosetting process. Inside the pultrusion die, the continuum can be divided into three sections. In each section, the resin is in a different phase. It is this parameter that helps us to determine the location of each section within the die. The gel time experiments are required for two fundamental problems that are encountered while modeling the pultrusion process. The first is the need to determine the length of the liquid zone in the die. Since the gel time was already needed to determine the length of the liquid zone, it could easily be employed in a second application to model the resin viscosity. Many of the models that have been developed thus far do not utilise the gel time. The reason for this is that it requires another series of experiments and that there are models which can predict the viscosity without it. However, these models begin to deviate as the viscosity increases toward the gel point.

The model that will be used to predict the degree of cure at the gel point for the epoxy resin is Flory's Classical approach, equation 1-21. This model constitutes a good choice in this case because the functionality of the epoxy resin is constant, and it is

always used in stoichiometric quantities. Since both of these parameters are unchanged for all of the experiments, the degree of cure at the gel point is also constant.

4. The volumetric change in the resin is the fundamental aspect which causes the rise and fall in the pressure inside the pultrusion die. Initially, the resin expands due to thermal heating and then begins to shrink as the degree of cure progresses in the resin. It is this expansion and contraction that becomes a major factor in controlling the pressure inside the die.

The model that was chosen to predict the volumetric expansion is seen in equation 1-34. This model appears to be the best suited for the resins used because they employ coefficient for the monomer, cured resin and cure shrinkage.

5. To measure the pressure profile inside the pultrusion die is a very difficult task. Due to the complications and limitations that have been mentioned in the chapter 1, the pressure inside the pultrusion die was not measured. However equations 1-40 to 1-42 are used to model the pressure profile in the die.

6. The pull force on the profile was determined quantitatively by measuring the power supplied to the motor and the line speed of the process. Using these parameters in conjunction with a calibration chart, the pull force for various speeds can be determined.

Chapter 3 Experimental Procedures

This chapter presents the materials that have been used, details on the preparation of the samples, and the procedures used to perform the experiments in this study.

3.1 Material and resin formulation

The two material that have been used in this study are the Shell Epon 9310 epoxy resin system and the Reichhold 31-0-31 polyester resin. These systems are comprised of the ingredients found in tables 3-1 and 3-2 , respectively.

Table 3-1A: Ingredients that were used in the epoxy formulation.

Ingredient	Product name	Concentration			
Mixture number		1	2	3	4
Base resin	Shell Epon 9310	100%	100%	100%	100%
Hardener	Shell Epon 9360	33%	33%	33%	33%
Accelerator	Shell 537	0.67%	1%	1.35%	1.80%
Degassing agent	BYK-515	0.40%	0.40%	0.40%	0.40%
Degassing agent	BYK-555	XXXX	XXXX	XXXX	XXXX
Release agent	Axel plast INT-1846	XXXX	XXXX	XXXX	XXXX
External lubricant	Vybar 825	0.40%	0.40%	0.40%	0.40%
Glass filler	Microbeads 2024	XXXX	XXXX	XXXX	XXXX

Table 3-1B: Ingredients that were used in the epoxy formulation.

Ingredient	Product name	Concentration			
Mixture number		5	6	7	8
Base resin	Shell Epon 9310	100%	100%	100%	100%
Hardener	Shell Epon 9360	33%	33%	33%	33%
Accelerator	Shell 537	1.0%	0.67%	0.67%	1.0%
Degassing agent	BYK-515	0.27%	0.40%	0.40%	0.27%
Degassing agent	BYK-555	0.40%	XXXX	XXXX	XXXX
Release agent	Axel plast INT-1846	1.50%	XXXX	XXXX	1.50%
External lubricant	Vybar 825	0.4%	0.40%	0.40%	0.4%
Glass filler	Microbeads 2024	XXXX	33%	50%	XXXX

Table 3-1C: Ingredients that were used in the epoxy formulation.

Ingredient	Product name	Concentration		
Mixture number		9	10	11
Base resin	Shell Epon 9310	100%	100%	100%
Hardener	Shell Epon 9360	33%	33%	33%
Accelerator	Shell 537	0.67%	0.67%	0.67%
Degassing agent	BYK-515	XXXX	XXXX	XXXX
Degassing agent	BYK-555	XXXX	XXXX	0.4%
Release agent	Axel plast INT-1846	XXXX	1.5%	1.5%
External lubricant	Vybar 825	XXXX	XXXX	XXXX
Glass filler	Microbeads 2024	XXXX	XXXX	XXXX

The base resin, the hardener and the accelerator are part of the Epon system. The remaining ingredients improve the processability of the system and come from a variety of sources. The BYK-515 and BYK-555 were generously supplied by the BYK company. The release agent, INT-1846, was generously supplied by the Axel Plast company. The external lubricant, Vybar 825, was generously supplied by the Petrolite corporation company. The glass filler, microbeads 2024, was supplied from the Potters industries company.

Table 3-2: Ingredients used in the polyester formulation.

Ingredient	Product name	Concentration	
		Characterisation	Pultrusion
Base resin	Reichhold 31-0-31-00	100%	100%
Catalyst 1	Norax Pulcat A	1%	1%
Catalyst 2	Norax TVBV	0.5%	0.5%
Release agent	Tech lube 250-CP	1.5%	1.5%
Filler	Calcium carbonate, 300 mesh	XXXX	15%

The polyester resin 31-0-31-00 was graciously supply the by the Reichhold chemical company. The Norox Pulcat A and TVBV were generously supplied by the Norac company. The Release agent Tech Lube 250-CP was generously supplied by the Alliance International Group. It is manufactured by Technick Products. In addition to these materials, the Interplastic corporation donated resin to initiate the pultrusion program.

3.2.1 Mixing the epoxy resin

The following is the procedure that was used to mix the ingredients.

1. Place the mixing container on the scale, then zero the scale. Pour the required amount of base resin into the mixing container. Note the weight of resin that is used. This weight is needed to calculate the amounts of the other ingredients.

2. Calculate the amounts of the ingredients that are needed for the mixture.

3. Add ingredients in the following order: hardener, degassing agents, lubricants, accelerator and, finally, the filler.

4. Attach a mixer to an air drill with 50 psi of inlet pressure. Mix the system for 5 minutes to assure that the solution is completely mixed. A diagram of the mixer can be seen in figure 3-1.

3.2.2 Mixing the polyester resin

The procedure for mixing the polyester resin is the same as for the epoxy with the following exception to Step number 3. The order in which the ingredients are mixed

is the following: base resin, release agent, Pulcat A, TBPB, and the filler.

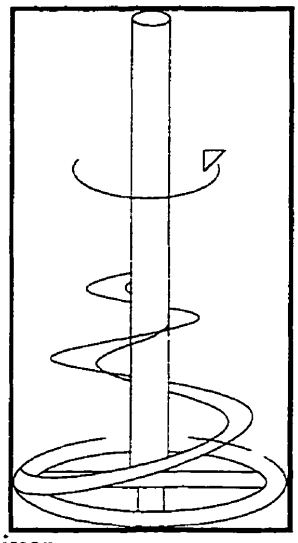

Figure 3-1: Diagram of the mixer.

3.3 Sample preparation

3.3.1 Preparation for the differential scanning calorimeter

The experiments were done using a Dupont 910, Differential Scanning Calorimeter. Place 5-20 mg of resin in a hermetically sealed capsule and place it in the calorimeter with the reference capsule. Enter the specimen information and the desired heating program into the computer. Once that the test is complete, the heat flow curves are integrated to obtain the degree of cure profiles.

3.3.2 Preparation for the viscometer

The experiments were done using a Brookfield rotary viscometer, model DV II+, in conjunction with a temperature bath, model TC200. Set the temperature bath to the desired temperature. Once that the bath has attained the operating condition, pour approximately 110 ml of resin into a disposable, quasi-cylindrical container that is 8 cm in height and has an opening of 6 cm. Since the specific gravity of the resin is close to that of the bath fluid, a jig was designed and built to hold the container in the bath. A sketch of the jig can be seen below in figure 3-2. The jig served two purposes, firstly to

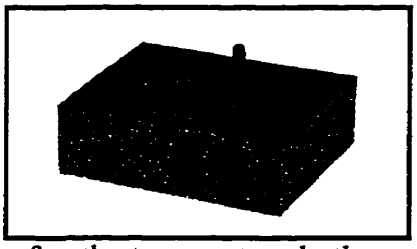

Figure 3-2: Jig assembly for the temperature bath.

hold the container in a specific position for the duration of the test and secondly, as method to control the container's depth in the bath. Connect a #3, RV spindle to the viscometer. A diagram of the spindle can be seen in figure 3-3. Place the sample in the bath and secure it in the jig. After securing the container, lower the spindle into the resin while assuring that it is well-centred in the container and that there are not any air bubbles trapped under the disk on the spindle. Begin with a spindle speed of 10 rpm,

and as the resin liquefies, increase the speed to 50 rpm. Following this, insert the thermocouple into the resin so that it does not interfere with the rotation of the spindle, but is as close to the centre as possible. Once the viscosity begins to rise rapidly, stop the viscometer and quickly remove the spindle from the resin. Immediately clean the spindle with a brass scraper and acetone.

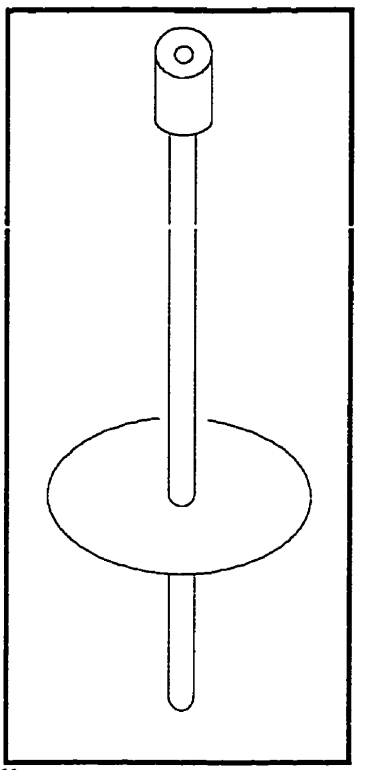

Figure 3-3: Diagram of a spindle.

3.3.3 Gel time preparation

Two techniques were used to determine the gel time of the resin. The first

technique used the viscometer and the second used a hot plate.

3.3.3.1 Low temperature gel point

The low temperature technique is based on ASTM D-3056, Standard test method for gel time of solventless varnishes [44]. This method was modified slightly by using the same equipment and sample size which was used for the viscosity measurements. This technique is used to determine the gel point of the resin for relatively low temperatures that go up to 90°C for the epoxy and 70°C for the polyester. There are two problems with this technique. The first is that the resin has a significant thermal inertia. Therefore as the temperature is increased, the time needed for the resin to reach the bath temperature becomes excessive. The second drawback with this technique is that for most resins, there is an important *mass effect*. The rate that the heat is generated inside the resin is greater than the rate at which it can be released. Therefore this phenomenon causes the core of the sample to become hotter than the bath temperature. The definition of the gel point that is used for this technique is the point at which the viscosity tends toward infinity.

3.3.3.2 High temperature hot plate technique

To overcome the problems associated with the low temperature technique, ASTM D-4217, Standard test method for gel time of thermosetting coating powder, can be used for higher temperatures. This test method was modified slightly by using resins,

rather than powder. The procedure to use this method is as follows. Turn on the heater cartridges and allow the plate to attain a steady state condition. Measure and record the temperature on the plate at the exact location where the resin is to be smeared. Using a stick with dimensions that are approximately 1 mm X 8 mm X 100 mm, dip the stick into the resin. With a fresh coating of resin on the stick, smear the resin onto the exact location that was measured with the thermocouple. Immediately after smearing the resin on the hot plate, start a timer. Using a similar stick to that described above, begin mixing the resin in a circular motion. Stop the timer when a resin build up begins in front of the stick. Once this occurs the gel point has been reached.

The advantage that this technique has over the previous one, is that the thermal lag within the resin is kept to a minimum since the film of resin is very thin. A very fast response time is needed since the gel times can be as short as 10 seconds [45].

There are many definitions that can be used to define the gel point. In this work three definitions are used. For the viscometer, it is the point at which the viscosity tends toward infinity. The second definition of the gel point that was used while using the hot plate is defined by the point where it forms a gel that builds up in front of the stirrer while mixing the resin in a circular pattern. The third definition was defined at the point where the resin could be easily sliced but still flowed under pressure.

3.3.4 Volumetric expansion

The preparation of the dilatation experiments is as follows. Add 45 g of mixed epoxy resin or 40 g of polyester resin to a quasi-cylindrical plastic container with a total volume of 120 ml, with a top diameter of approximately 6cm, and with a height of 8 cm. The secondary fluid that was used in this series of tests was Dow Corning 200 fluid, 1000 cSt., silicon oil. Slowly pour silicon oil on top of the resin, being careful not to mix the two fluids. Continue to pour the oil until its level is approximately 2 cm from the top. Plug the container with a number 11, one hole, rubber stopper. Cut a hole in the lid of the container so that a Serological 5 ml pipette can easily pass through, and screw the lid completely on to the container. After the lid is completely screwed on, some oil should flow out of the hole. With the lid and stopper in place, the air trapped under the stopper must be removed. To remove the trapped air, a tilting and rotating motion can be used to gather the trapped air near the hole so that it can escape. Once all the air is removed, the pipette can then be inserted into the stopper. The pipette should stop about 0.75 cm above the top of the resin. The sample is now ready to be inserted into the temperature bath. A bath temperature of 80 °C was used for the epoxy resin and 50°C for the polyester resin. A diagram of the dilatometer can be seen below in figure 3-4.

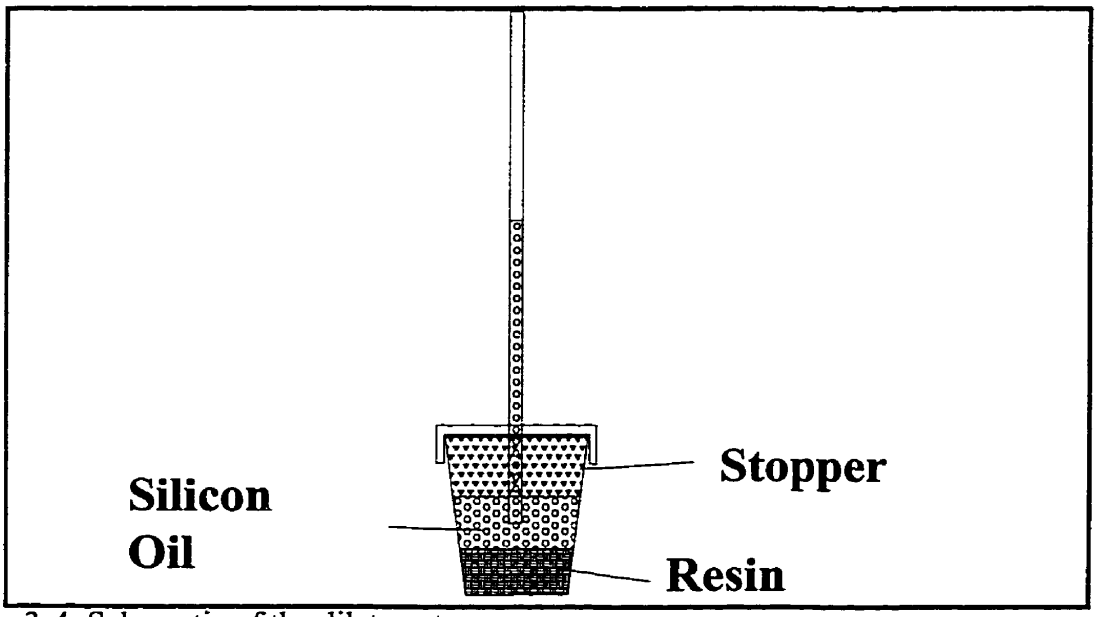

Figure 3-4: Schematic of the dilatometer.

3.3.4 Pull force on the profile

The pull force on the profile during production was determined by measuring the power that the puller motor consumed and the line speed.

3.3.4.1 Calibration of the pull force

To determine the exact pull force on the profile, the machine was calibrated using the following technique. A pulley was placed over the end of the die table. Using a nylon strap, a weight was lifted at a constant speed. The power consumption was measured for various weights and line speeds. From these results, calibration curves

were obtained for constant speeds. Therefore, during production, the pull force on the profile was determined by plotting the power consumption and the line speed on the calibration curves.

3.3.4.2 Measuring the collimation and viscous drag contributions to the pull force.

The collimating force contribution is measured by simply pulling dry fibers through the die at a constant speed. For this series of experiments, the line speed is set at 0.5 m/min and the pull force is determined using the technique described previously.

The contribution from the viscous drag is measured while pulling wet fibers that are covered with Dow corning 200 fluid, 200 Cst., silicon oil. This test was conducted by adding the silicon oil to the resin bath and setting the line speed to 0.5 m/min. The temperature of the die was kept at 25°C and the pull force was measured.

Chapter 4 : Results and Discussion

4.1 Viscosity

4.1.1 Effect of the filler on the viscosity of the epoxy-based formulations

The effect of glass filler on the viscosity of an epoxy pultrusion resin can be seen in figure 4-1 below. The two mixtures were identical with the exception that one had 33% by mass of glass filler. The filler had the following effect on the viscosity. The filler increased the viscosity at 25°C by 2000 cP and increased the minimum viscosity of the resin at 70°C by approximately 90 cP. In addition to changing the viscosity, the cure kinetics were also affected.

As seen in figure 4-1, both the filled and unfilled samples maintained a similar temperature profile, however, the rate of polymerisation in the unfilled sample was much greater. The cause of this discrepancy in the two sets is the following. The chemical reaction that is taking place within the resin is very exothermic. Therefore, in the unfilled sample, the resin is heated from the inside (due to the polymerisation) and from the outside (due to the temperature bath). Thus, the unfilled sample has two heat sources. Because of the thermal lag that exists in the resin, it is possible for the temperature in the core to become greater than the temperature near the thermocouple.

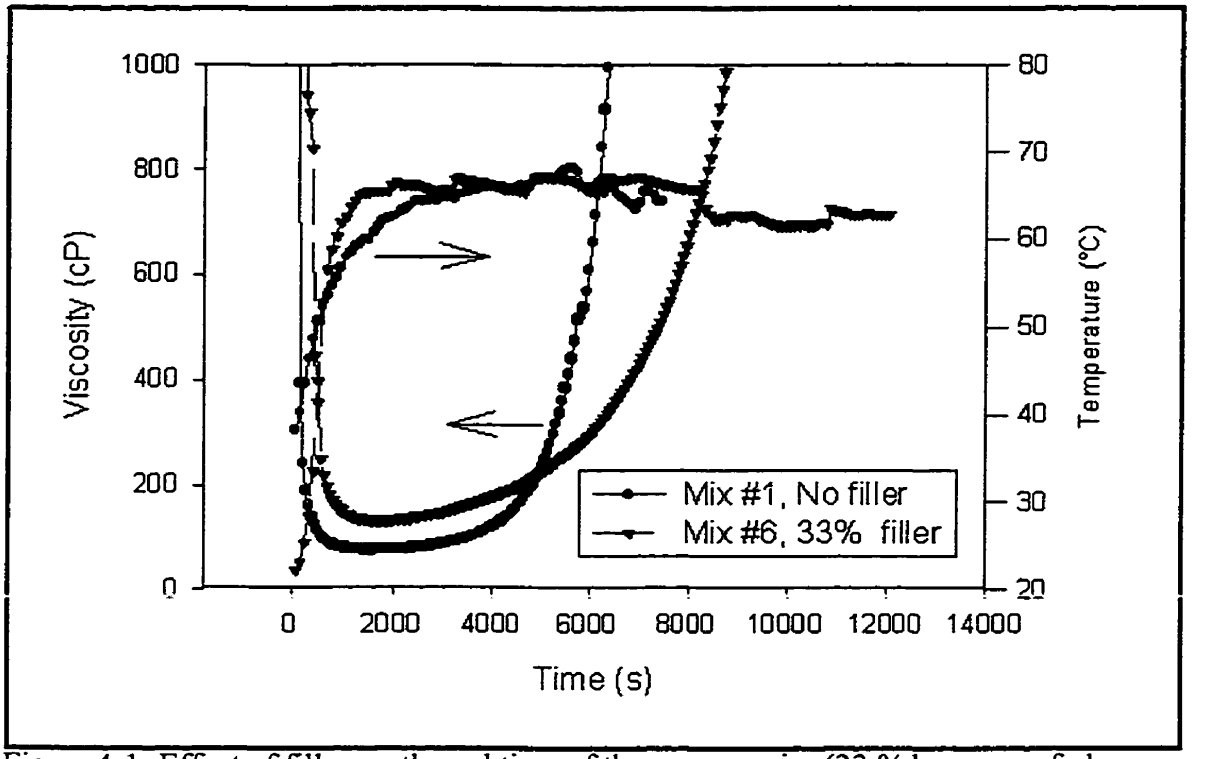

Figure 4-1: Effect of filler on the gel time of the epoxy resin. (33 % by mass of glass filler at 70°C.)

The reason why the filled sample polymerises more slowly, is twofold. Firstly, 33% of the mass of the sample is glass filler thus reducing the amount of resin in the sample. Secondly, the glass beads are inert which act as a heat sink for the resin. Therefore, the combination of these two effects stabilise the sample temperature during curing, preventing the resin from over-shooting the bath temperature and prolonging the time to polymerise.

4.1.2 Effect of additives on the pot life during pultrusion

The drive behind this series of experiments was to solve some process problems that were occurring during the pultrusion experiments. Two types of problems were encountered. The first was that the resin had a very short pot life, and the second was that there was some random chalking occurring inside the die.

Examination of the behaviour of the resin in the bath can serve as a quality control technique. The condition in the bath can be an indication of the compatibility of the resin with the additives. If two ingredients are not compatible separation with the resin may occur. This separation will cause layers to form in the bath and each layer may have a different viscosity which could affect the fiber wetting.

The pot life was considered, in the theory, to be the low temperature viscosity measurements. The focus of this section is to determine how the various ingredients affect the pot life of the resin system. In the interest of practicality, the pot life should be as long as possible thus reducing the number of parameters that can affect production.

For this study, two selected ingredients are focused on to determine how they affect the pot life of the resin. These ingredients are the BYK-555 and the INT-1846. The effect that these additives have on the pot life of the Shell Epon 9310 resin system

can be seen in figure 4-2. Following is the identification of the curves found in figure 4-2:

Curve 1 consists of the standard formulation with material set #2, without adding BYK-555 and INT-1846 (mix#9).

Curve 2 consists of the standard formulation with material set #1 (mix#5).

Curve 3 consists of the standard formulation with material set #2 (mix#5).

Curve 4 consists of the standard formulation with material set #2, where the hardener was pre-heated prior to mixing and production (mix#5).

Curve 5 consists of the standard formulation with material set #2, without adding BYK-555 (mix#8).

Curve 6 consists of the standard formulation with material set #2 used in conjunction with the 537 from set #1 (mix#5).

Curve 7 consists of the standard formulation with material set #2, and with the 9360 pre-heated to 230°C (mix#5).

While comparing curves 3 and 5, it can be seen that BYK-555 reduces the viscosity of the resin in the plateau region. Furthermore, it is also shown that BYK-555 does not affect the pot life. This reduction in viscosity is in direct relation to the BYK-555. It is the reduced viscosity that helps the air bubbles migrate to the surface, thus de-gassing the resin.

Table 4-1: Ingredients that compose the *standard* mixture.

Base resin, 9310	100%
Hardener, 9360	33%
Accelerator, 537	1%
BYK-515	0.27%
BYK-555	0.4%
Vybar	0.4%
INT-1846	1.5%

The Internal Release Agent (IRA) INT-1846, has a pronounced effect on both the viscosity in the plateau region and on the pot life. This effect is seen while comparing the curves 1 and 5. The INT-1846 causes a dramatic increase in viscosity in the plateau region and it also reduces the to pot life from approximately 11.1 hours to 8.3 hours. In addition to the quantitative effects mentioned above, there is also a qualitative problem associated with INT-1846. For two formulations (curves 3 and 5), shown in figure 4-2 that included INT-1846, both of them developed into a non-homogeneous mixture during the pot life test. After about 2 hours, the resin started separating, and after roughly 5 hours it developed into a very distinctive 3 layer solution. On the top, there was an opaque yellow layer, followed by a clear orange layer, and on the bottom a yellow 'sludge'. If this condition were to occur in the resin bath, it could explain the apparent random chalking that occurs in the cavities. The two other formulations that included INT-1846 (curves 4 and 7), did not show a distinct 3

layer solution. There are two hypotheses that could explain why the separation didn't occur. The first is that the hardener was completely liquid prior to mixing, due to its pre-heating. The second is that the viscosity increased in such a rapid manner that the liquid became too thick for this phenomenon to occur. The cause of the rapid rise in viscosity is that the pre-heating temperatures of the hardener were extremely excessive.

Therefore, to optimise the process conditions in the resin bath area, the concentration of INT-1846 should be minimised, and the concentration of BYK-555 could be increased, but an upper limit has yet to be established.

Upon delivery of some supplies from an outside source (material set #2), it was noticed that the colour of the accelerator (537) supplied was a dark brown, whereas the colour of the accelerator found at the laboratory (material set #1) was a light grey. The discrepancy between the two accelerators can be seen in figure 4-2. Shown in curves 2 and 3, is the difference in pot life between the two sets of material. The pot life of set #1 is approximately 17 hours, whereas the pot life for set #2 is approximately 8.3 hours. A third experiment was done to validate the performance of the two sets of materials. This experiment involved using set #2 in combination with set #1 accelerator. The results from this experiment are shown as curve 6. Comparing curves 3 and 6, it can be seen that set #1 version of Epon 537 is the cause for the increased pot life. The discrepancies between the curves can be attributed simply to the difference in age between the two

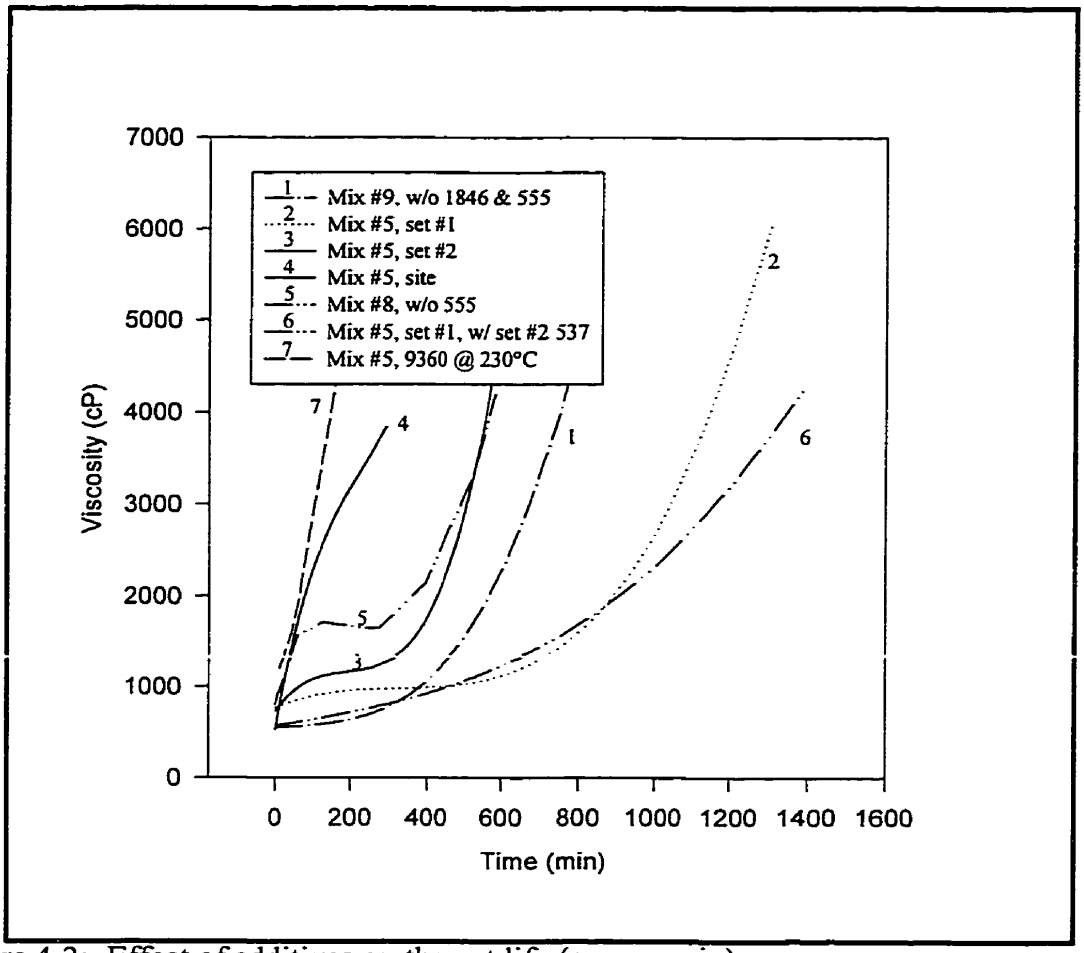

Figure 4-2: Effect of additives on the pot life (epoxy resin).

sets of material. According to the technical specifications supplied with this resin system, the pot life should be in the area of 7.5 to 8 hours. Therefore, this would indicate that the accelerator found in set #1 has aged, or been taken from a bad batch or was simply not Epon 537.

In an effort to reproduce the process conditions found in production, a batch was formulated using some hardener (Epon 9360) that was pre-heated to approximately

230°C . The reason for heating the hardener to such a high temperature was that during production, the container of hardener was constantly kept on the pultrusion die that was heated to roughly 230 °C in it's centre. Shown in figure 4-2, are the results of the experiment that was described above, in an effort to simulate the process conditions (curve 7), compared to those found during processing (curve 4). It can be seen that their advancements are relatively similar. Also, the effect of heating the hardener can have huge effect on the behaviour of the resin. A more suitable solution could be to heat the hardener prior to using it and then let it cool back to room temperature. This would eliminate the crystallisation, and would eliminate the unnecessary heating of the hardener.

The modifications that should be made to increase the pot life are to maintain or increase the concentration of BYK-555 in the system, to minimise the concentration of INT-1846, and to eliminate preheating the hardener directly before mixing.

4.1.3 Modeling the viscosity

4.1.3.1 Experimental results

Isothermal experiments have been performed at 60, 70, 75, 80, and 90 °C for the epoxy resin using mixture number 8. Experiments were also performed at 50, 60, 65, 70, 75 and 80 °C for the polyester resin using the standard formulation mentioned

previously. The results from these experiments can be seen in figure 4-3A and 4-3B. The shape that the curves follows is similar to that found in the literature. The viscosity initially drops due to the thermal heating. Following this, the viscosity maintains a constant value. It remains in the plateau region while it is at a constant temperature. Eventually, the viscosity begins to increase due to the polymerization in the resin. Figure 4-4, which represents a zooming of figure 4-3A, shows that the minimum viscosity is dependent on temperature. As the temperature is increased, the viscosity decreases.

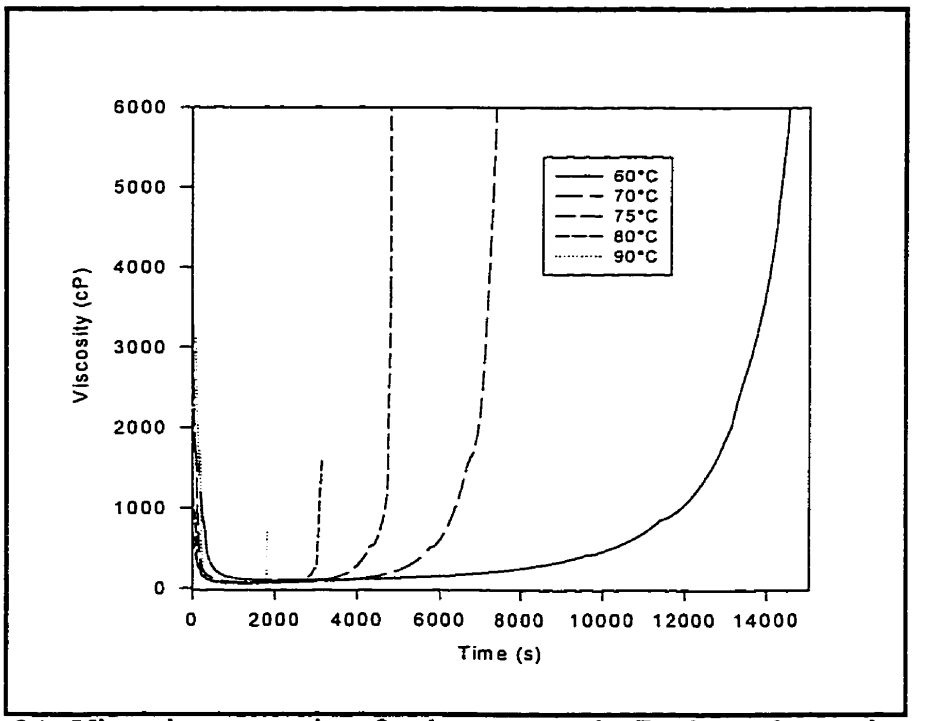

Figure 4-3A: Viscosity versus time for the epoxy resin (Isothermal experiment).

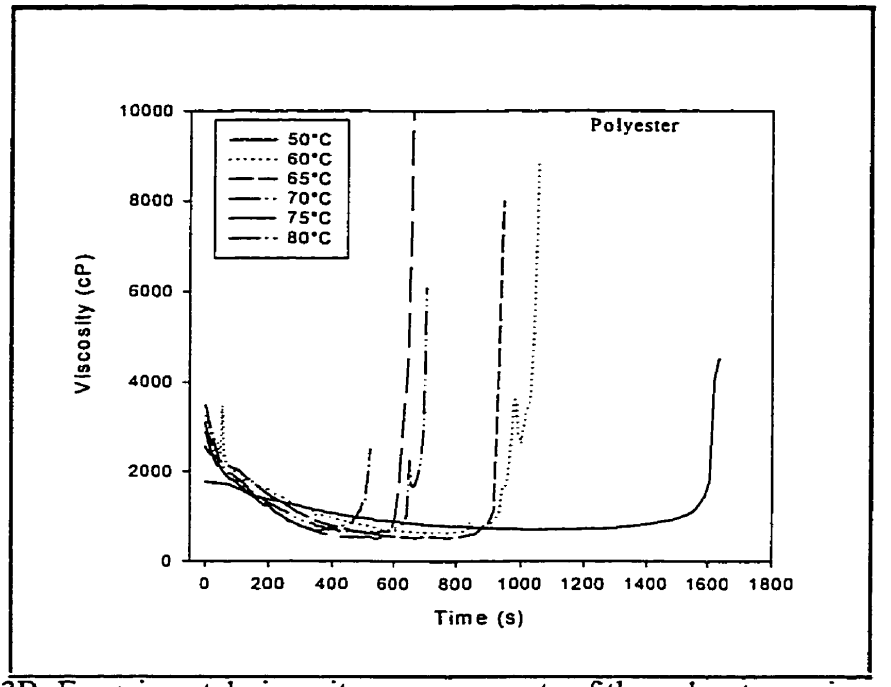

Figure 4-3B: Experimental viscosity measurements of the polyester resin.

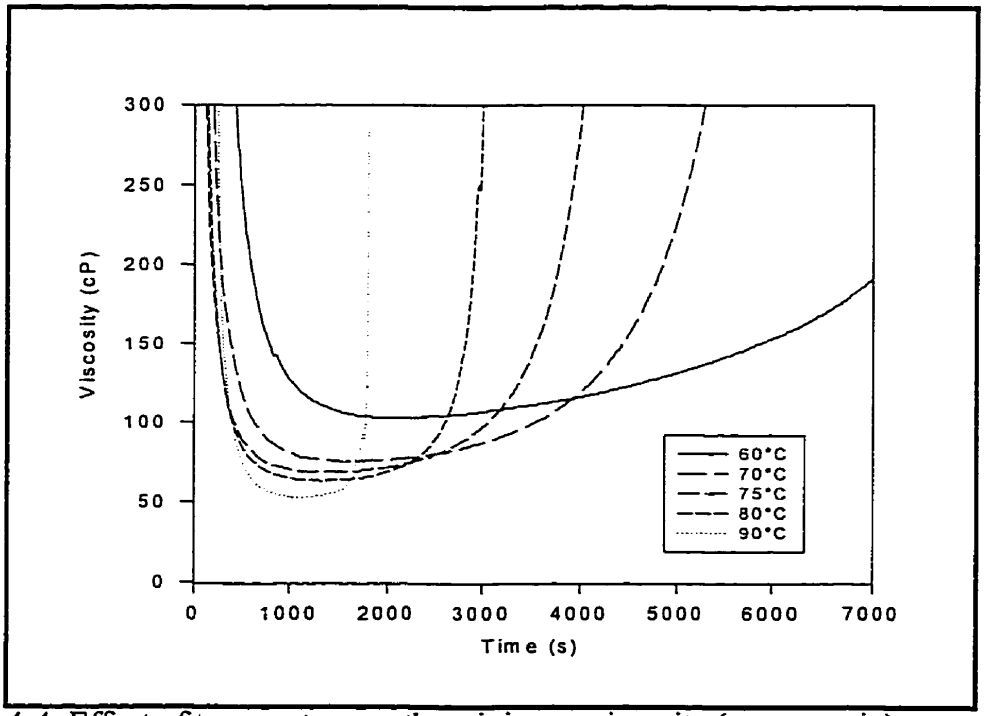

Figure 4-4: Effect of temperature on the minimum viscosity (epoxy resin).

4.1.3.2 Determining the initial Viscosity

The initial viscosity of the resin was determined by two methods. The first method is an experimental technique where the initial viscosity is simply the lowest viscosity that is obtained during the experiment. The second technique uses the following relationship to predict the initial viscosity of the resin,

$$\eta_o = A\exp(E/RT) \qquad 1\text{-}6$$

where η_o is the initial viscosity, A is the pre exponential factor, E is the viscous activation energy, R is the universal gas constant and T is the absolute temperature. The second of the two methods that was used to determine A and E is shown in figure 4-5A. Equation 1-6 has been linearized, and the intersection of the curve with the vertical axis is equal to Ln A and the slope is equal to E/R.

The cause for the deviation in the experimental points, (figure 4-5A), is the polymerization effect that increases the size of the molecules thus increasing the experimental initial viscosity. The second method that was used was a least-square curve fit. The results from the curve fit are shown in figure 4-6 ($A = 7.422\text{x}10^{-7}$ Pa·s , $E = 5.25\text{x}10^{4}$ J/g).

For the epoxy resin that was used in this study, the curve fit using the least-squares technique yielded superior results.

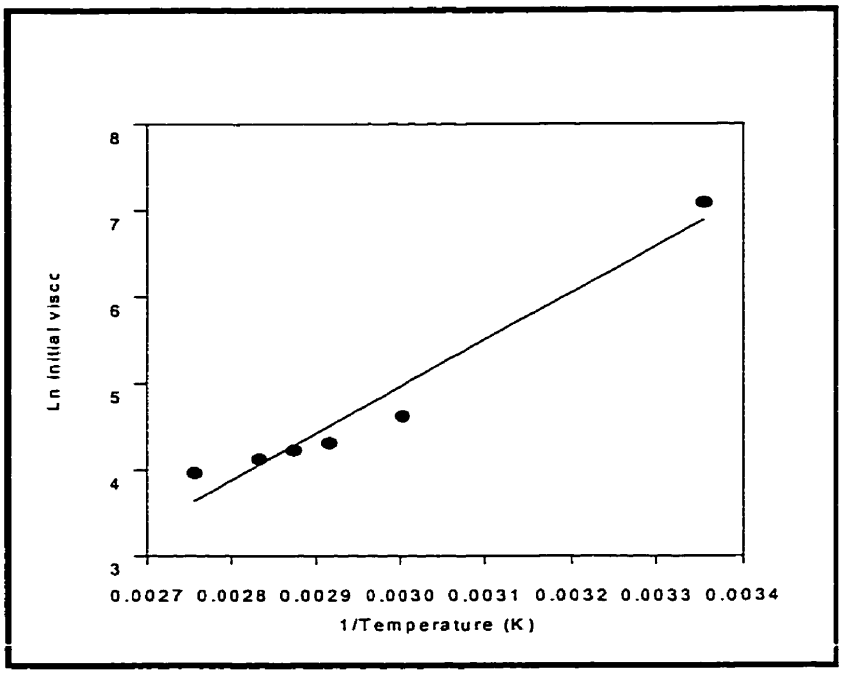

Figure 4-5A: Ln initial viscosity versus 1/temperature (epoxy resin).

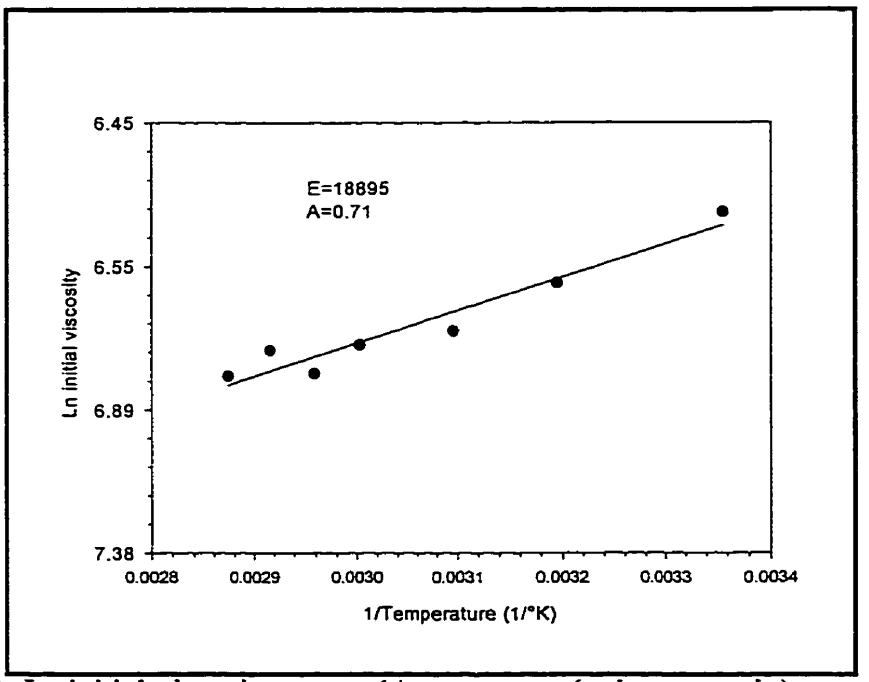

Figure 4-5B: Ln initial viscosity versus 1/temperature (polyester resin).

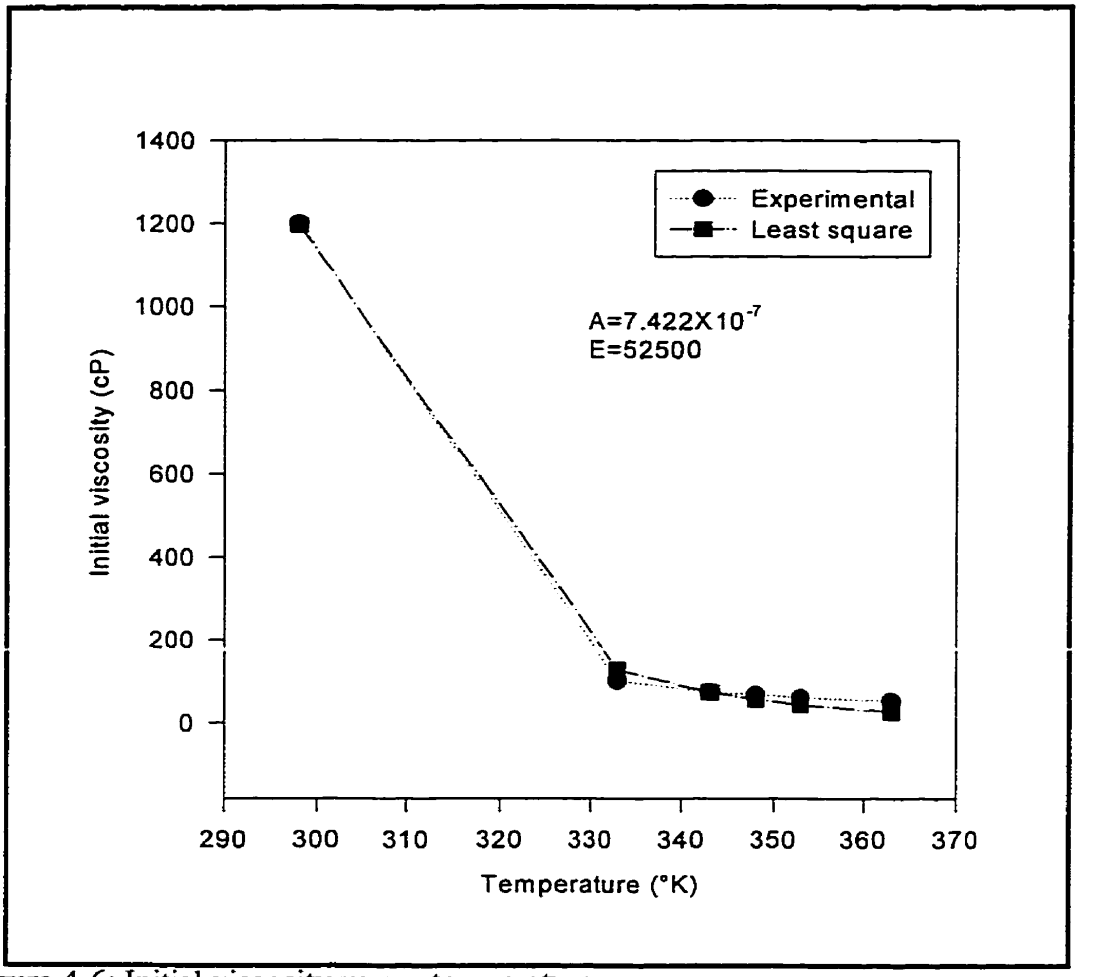

Figure 4-6: Initial viscosity versus temperature.

4.1.3.3 Time based model

The initial viscosity is needed to further model the viscosity. To model the viscosity as function of time (time-based model), the following relation was used,

$$\eta/\eta_o=(1-t/t^*)^{-b_t} \qquad 1\text{-}17$$

where t is the time, t* is the gel time, and 'b_t' is a constant. Before that the model can be used, the gel time and constant 'b_t' must be determined. The value of 'b_t' is equal to the

average of the slopes shown in figure 4-7, where Ln (η/η_o) is plotted against Ln(1-t/t*). Also illustrated in figure 4-7 by the slopes of the curves is that only the experiments at 60 and 70 degrees Celsius were truly isothermal. These two are the only curves that were parallel. All the other experiments that were conducted were affected by the exothermic reaction within the resin. For example, while the sample of resin was being heated to the desired isothermal temperature, the heat released internally caused the resin to over-shoot the desired temperature. In figure 4-8, are the temperature profiles of the epoxy resin while the viscosity profiles were taken. Shown in the graph are some of the fluctuations in temperature that are due to the temperature gradients that exists in the sample. In addition to this, only the samples at 70°C or below showed complete isothermal behaviour. At temperatures greater than 70°C, the exothermic energy begins to influence the sample.

Since the majority of the isothermal experiments were plagued by the exothermic reaction in the resin, it was very difficult to maintain a constant temperature. For all of the experiments that were conducted above 70 °C, the resin temperature exceeded the temperature of the bath. Therefore, when applying the previous method for determining the constant "b", the equation 1-6 was used in conjunction with the experimental temperatures to determine the initial viscosity. It is this step that presents the term "semi-dynamic", meaning that the results are from an isothermal experiment. However, the ever-changing experimental temperatures are used. Therefore, as seen

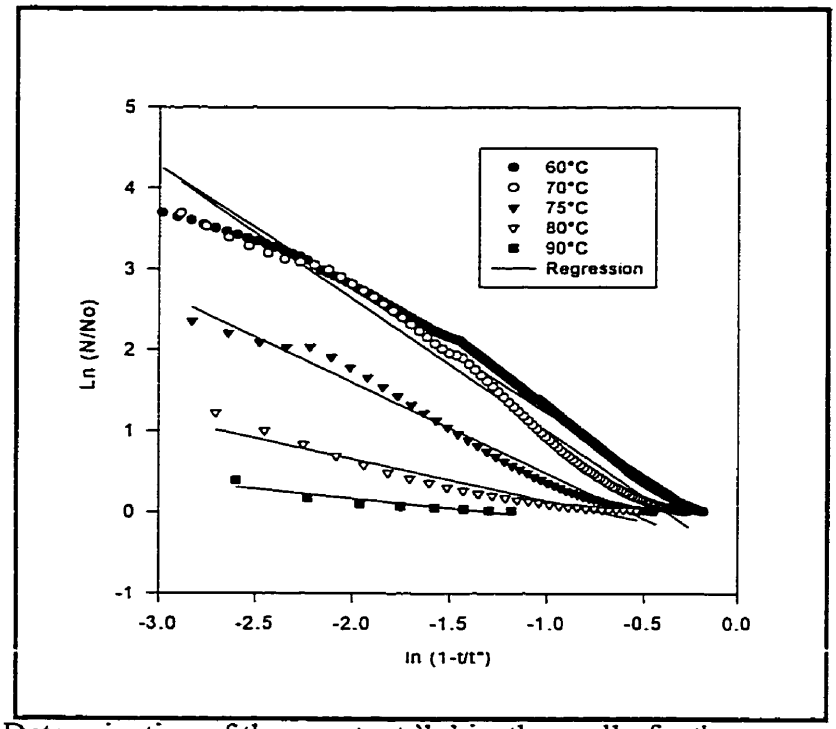

Figure 4-7: Determination of the constant 'b_t' isothermally for the epoxy.

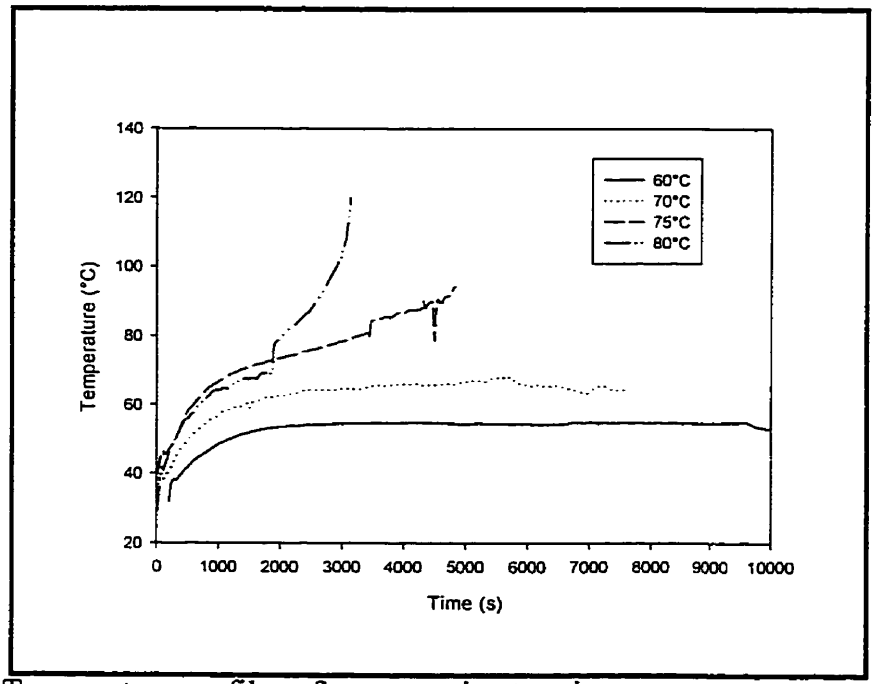

Figure 4-8: Temperature profiles of epoxy resin at various temperatures.

in figure 4-9, the slopes of the curves were much more comparable than in figure 4-7. From the average of these slopes, the constant 'b' was determined to be 1.35. The deviation that still remains between the curves could be due to the error associated with the temperature gradient inside the sample of resin.

4.1.3.4 Determining the gel time

Two methods where used to determine the gel time with the viscosimeter. The first is an experimental technique where the gel time is the time when the viscosity tends towards infinity. The second technique is based on a $1/\eta$ versus time representation shown in figure 4-10, where if the curves were extended towards the horizontal axis, the gel time would be at the point of the corresponding intersection. Also shown in figure 4-10 are some clues to determine which phases of matter that the resin followed while hardening. The curves for 60°C and 70°C show a levelling trend as the reciprocal of the viscosity approaches zero.

The curving in these plots could suggest that the resin solidified by vitrification, rather than gelation. The remainder of the experiments that were conducted above 70°C could have reached gelation before vitrification. Thus, the gel times that were determined for these experiments could be valid, while the gel times for the experiments that were conducted at 70°C or below could be invalid. The following empirical

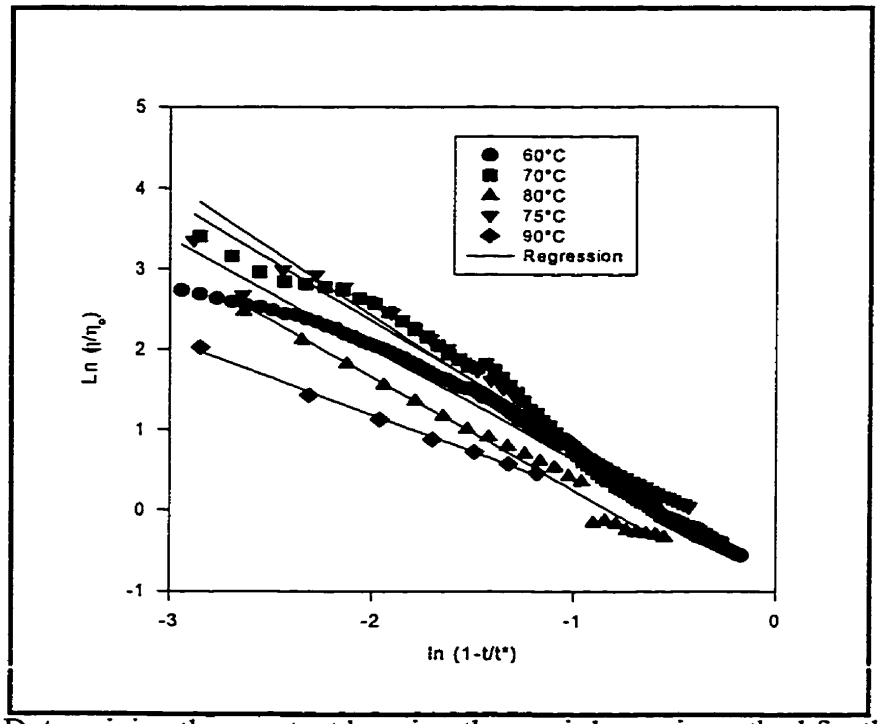

Figure 4-9: Determining the constant b, using the semi-dynamic method for the epoxy.

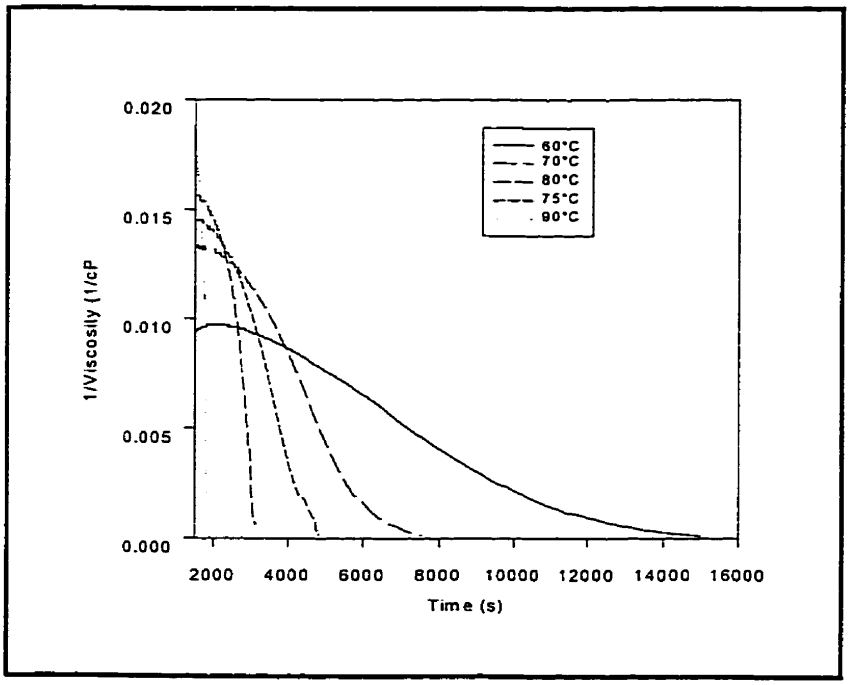

Figure 4-10: Determining the gel time.

relationship was found to predict the gel time assuming that all gel times are valid,

$$t^*=C/m^T \qquad 2\text{-}3$$

where C and m are constants, and T is the temperature in Celsius. The constants, C and m, were found using two techniques. The first was with a least-square curve fit and the second technique linearized the equation 2-3 so that the intersection point on the vertical axis was equal to Log C, and the slope was equal to Log m . ($C=1.067x10^6$ et m = 1.075) The results for these techniques are shown in figure 4-11 and figure 4-12, respectively.

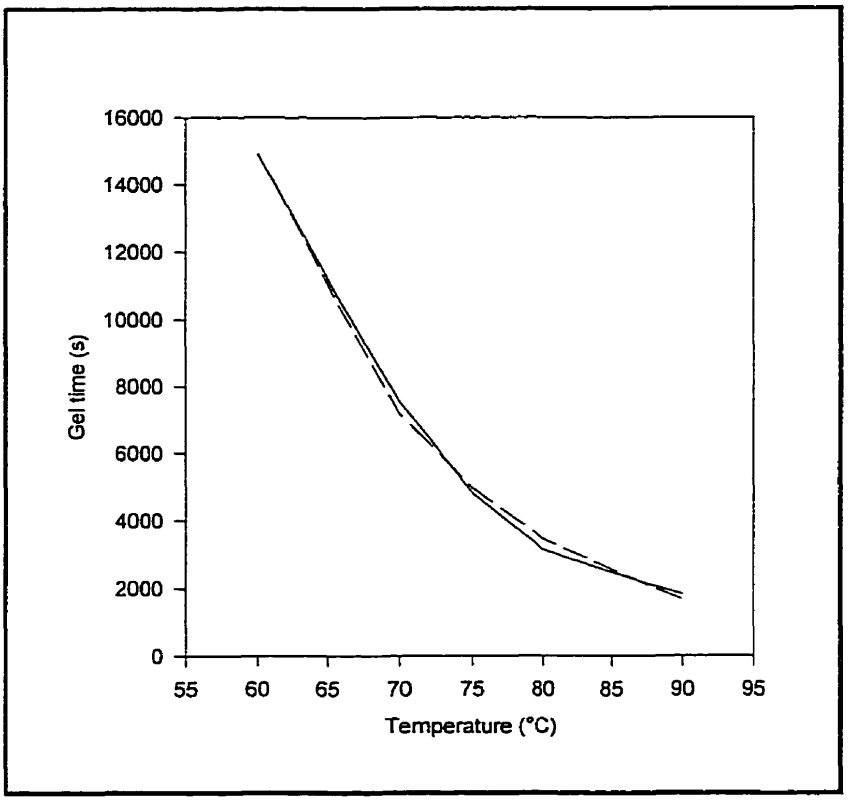

Figure 4-11: Gel time versus temperature, (empirical relationship)

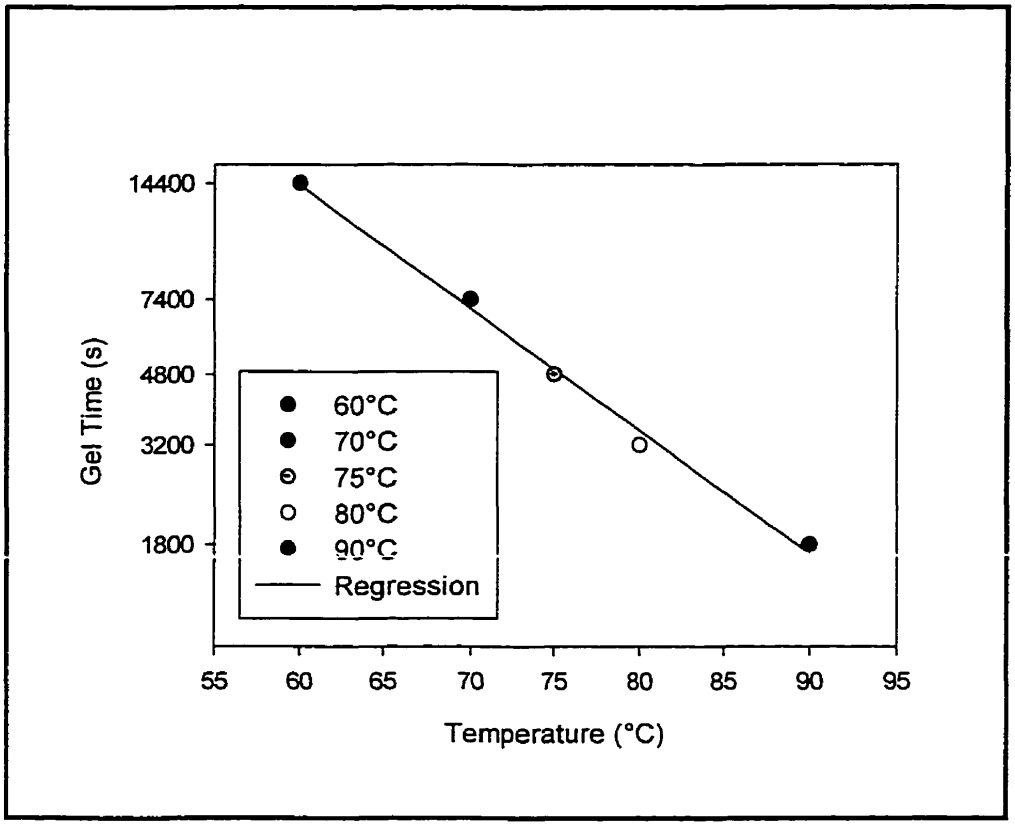

Figure 4-12: Log (gel time) versus temperature.

Very little difference was found between the two methods. Using the constants that were determined above, the results from the time-based model, equation 1-17, are shown in figure 4-13. This model was not applied to the polyester resin, for the reason that it was later discovered that the time-based model is not ideal for modeling the viscosity inside a pultrusion.

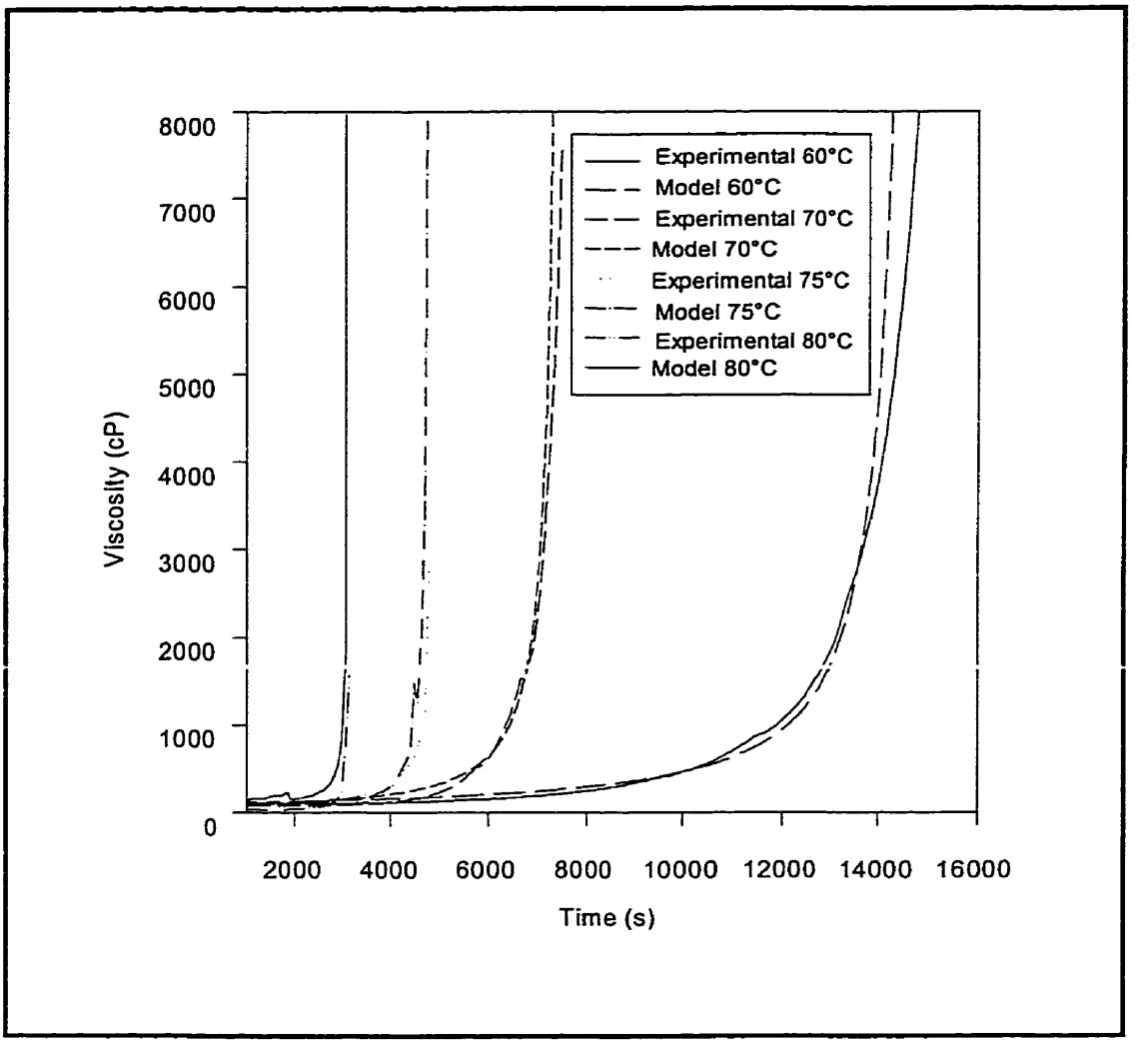

Figure 4-13: Viscosity versus time, time model.

4.1.3.5 Cure based model

The accuracy of the time-based model appears to be very good, however, it has the following limitations. A secondary empirical relationship is needed to determine the gel time as a function of temperature. The other problem associated with the model is

that it is not directly associated with the degree of cure. There is a need to associate the viscosity to the degree of cure, because the degree of cure is a well-developed method and is a base point for studying thermosetting resins. To overcome the drawbacks associated with equation 1-17, the following model is adapted.

$$\eta/\eta_o = \left(1 - \frac{\alpha}{\alpha^*}\right)^{-b_c} \qquad 1\text{-}20$$

where α is the degree of cure, α^* is the degree of cure at the gel point, η_o is the initial viscosity and "b_c" is a constant. Hereafter, this model, equation 1-20, is referred to as the cure model. In this investigation, α^* is determined from isothermal α-t curves as shown in figure 4-14. The isothermal α-t diagram is obtained from model 1-3 found in the literature for the epoxy and obtained from isothermal DSC experiments for the polyester resin. The degree of cure at the gel point should theoretically be constant, however, the results have shown that it decreases slightly with temperature. The reason for the discrepancy is due to the fact that isothermal viscosity tests were actually non-isothermal, as shown in figure 4-8. As discussed above, the temperature inside the resin increases as the reaction proceeds, therefore the viscosity's that were measured are actually for hotter semi-isothermal temperatures. Another reason for this discrepancy is that the rotating motion of the spindle promotes molecular interaction thus giving a shorter gel time. Details on the determination of the degree of cure at the gel point will be given in section 4-2.

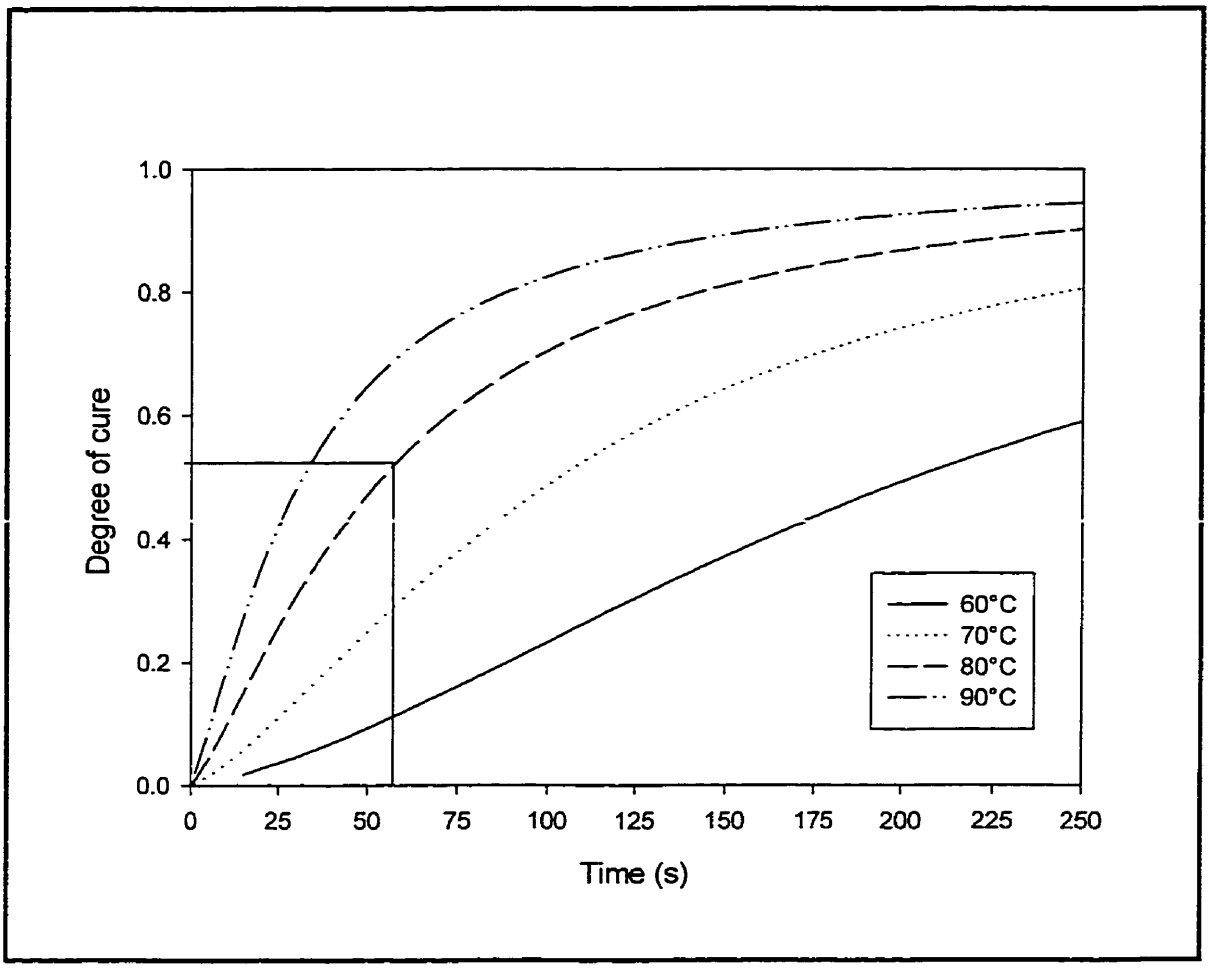

Figure 4-14: Degree of cure versus time.

The constant "b_c", from equation 1-20, was determined by calculating the average slope from the log (η/η_o) versus log$(1-\alpha/\alpha^*)$ plots in figure 4-15A using the same *semi-*

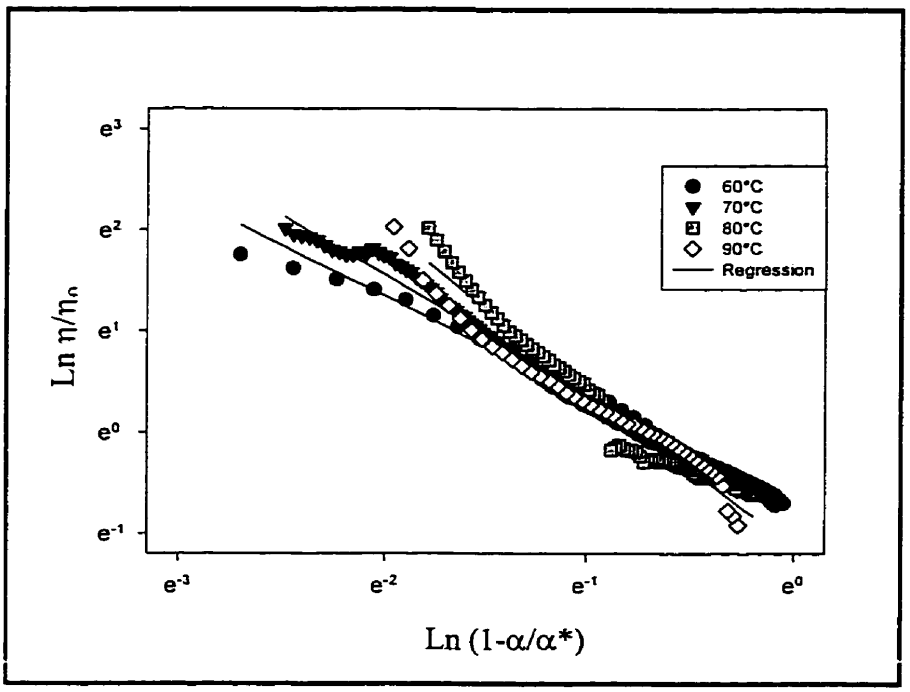

Figure 4-15A: Ln η/η_o versus Ln $(1-\alpha/\alpha^*)$, cure model (semi-dynamic, epoxy).

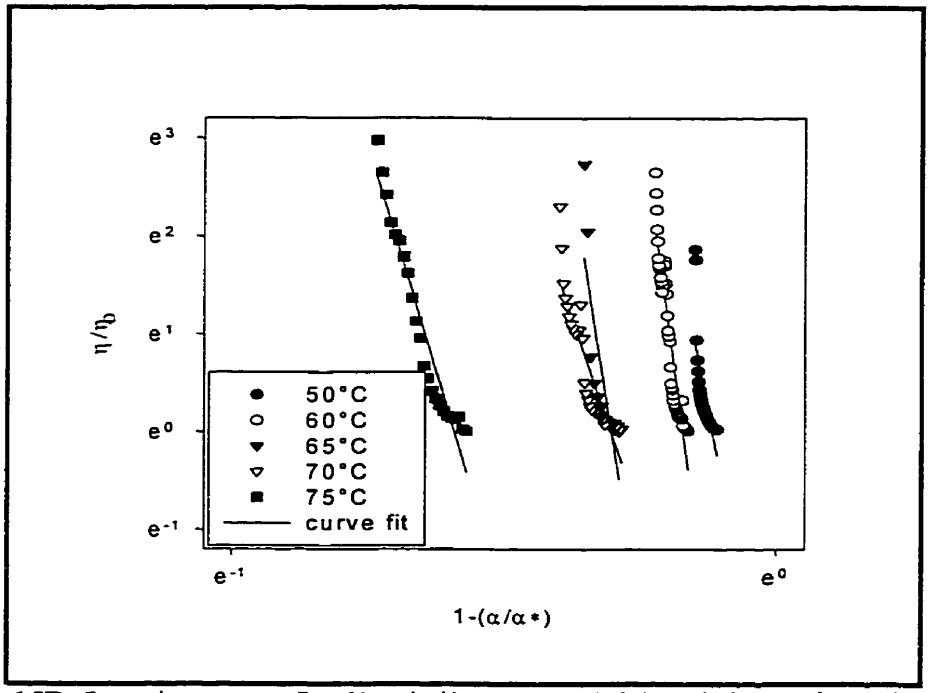

Figure 4-15B: Ln η/η_o versus Ln $(1-\alpha/\alpha^*)$, cure model (semi-dynamic, polyester).

dynamic technique that was used for the time-based model that was discussed previously. The average value for "b" using the cure model was found to be 1.27 for the epoxy resin. This technique was also applied to the polyester resin which is seen figure 4-15B. The average value for "b_c" for the polyester was found to be approximately 28. The validity of this method for the polyester resin is questionable. Shown in the following section, the degree of cure at the gel point using the viscometer was approximately 11%. It is this unusually low degree of cure at the gel point that is questionable. Therefore, since this result is carried into the method used in figure 4-15B, the confidence in this technique for the polyester is low.

Therefore, using the results that were obtained from the previous figures and equation 1-20, yields the following results which are seen in figure 4-16.

The deviation in the model for 60°C is due to the fact that the degree of cure at the gel point increased slightly as the temperature decreased. Therefore, the average degree of cure at the gel point was lower than the experimental degree of cure at the gel point for 60°C. It is this phenomenon that causes the shift in the viscosity curve. The large temperature gradient that was observed in the sample may have caused the calculated values to be slightly larger than the measured values. Since the thermocouple was placed near the surface of the resin, resulting in a significant distance between it and the core of the sample. It could be this phenomenon that causes the majority of the

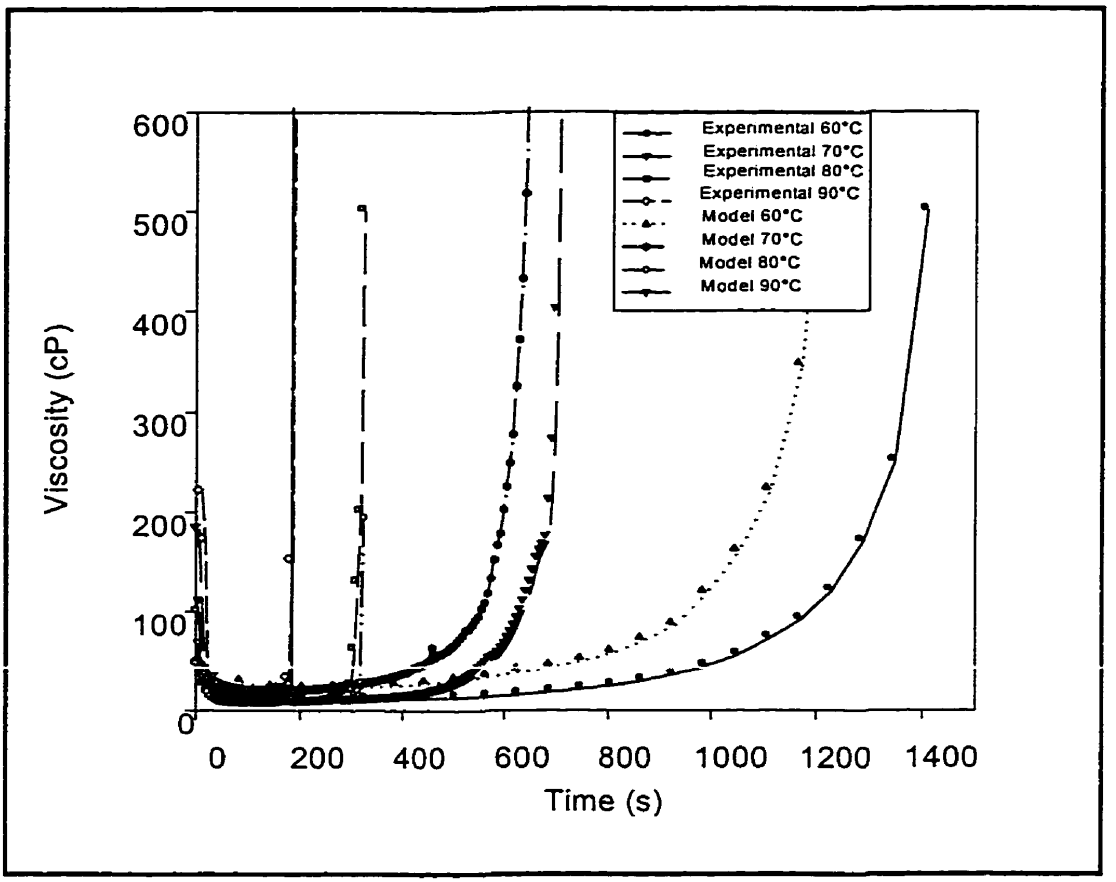

Figure 4-16: Viscosity versus time, cure model (epoxy).

discrepancy between the measured values and the calculated values. It is noticed that the model works better when the temperature is increased and typical pultrusion temperatures are high for this resin. Therefore, this model will work for epoxy pultrusion. This model was not applied to the polyester resin. A degree of cure at the gel point of 11% was not a logical value. Therefore, it is believed that the mass effect while using this technique was too large to provide valid results with the equipment used. Equation 1-20 can be taken further to model dynamic experiments where the temperature of the resin is heated at specific rates. The calculated values of viscosity for

specific heating rates are shown in figure 4-17. Experiments have not been done to validate the model dynamically, however, the results that have been found in the literature by Tajima and Crozier, can very closely match the calculated values.

As a means of determining the operating point of the resin, a viscosity versus degree of cure diagram, figure 4-18, can be used to determine minimum viscosity of the resin at different heating rates with the corresponding degree of cure. As seen in figure 4-18, the viscosity attains its minimum when the degree of cure reaches approximately 0.2. The minimum viscosity reaches this degree of cure which is independent of the heating rate.

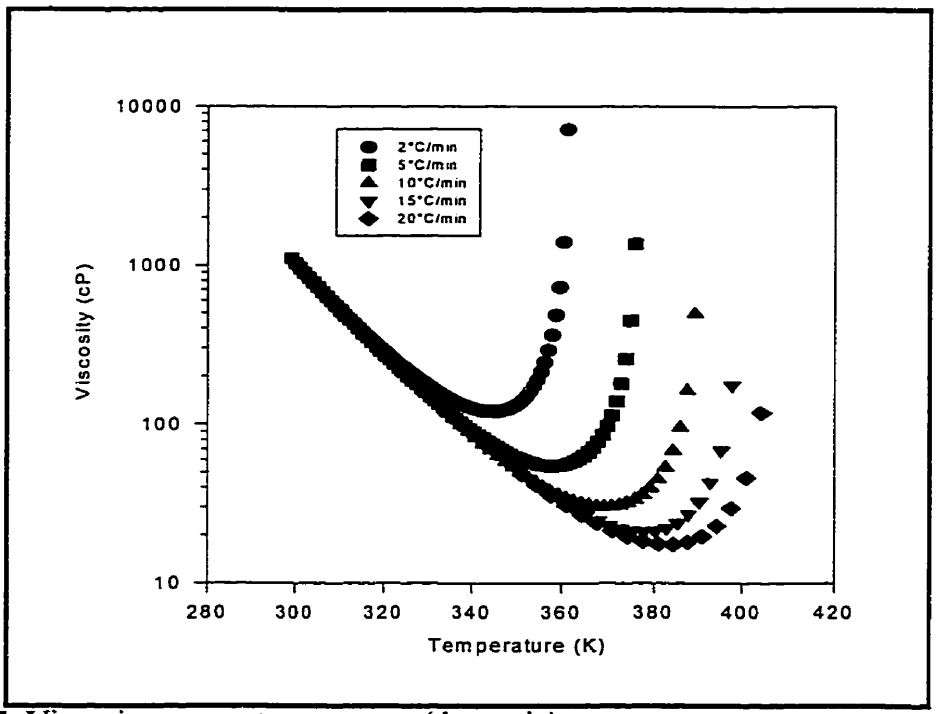

Figure 4-17: Viscosity versus temperature (dynamic).

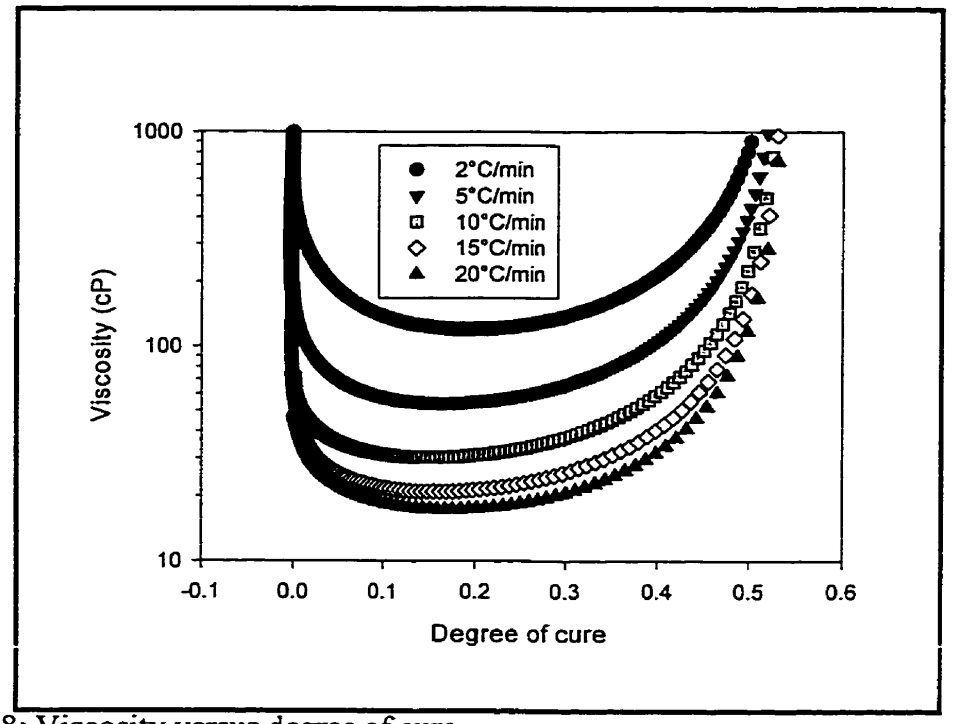

Figure 4-18: Viscosity versus degree of cure

4.2 Gel time of the resin

4.2.1 Effect of ingredients on the gel time

The effect of the accelerator on the gel time is immense. As seen in figure 4-19 below, doubling the concentration of the accelerator, can reduce the gel time by approximately 50%. Therefore, the accelerator is one of the most important ingredients to consider when discussing the gel time.

The effect of BYK-555 on the gel time can be seen in figure 4-20 below. When comparing mixtures 10 and 11, there is virtually no change in the gel time. This finding is in accordance with that found in the literature. The slight variation between the two curves could simply be that there was slightly more accelerator in one than the other. However, the release agent (INT-1846) has a greater affect on the gel point. When comparing mixture 9 to either 10 or 11, it is evident that the release agent will cause a slight increase in the gel time. Therefore, at the molecular level, the INT-1846 reduces the interaction between the hardener and the base resin.

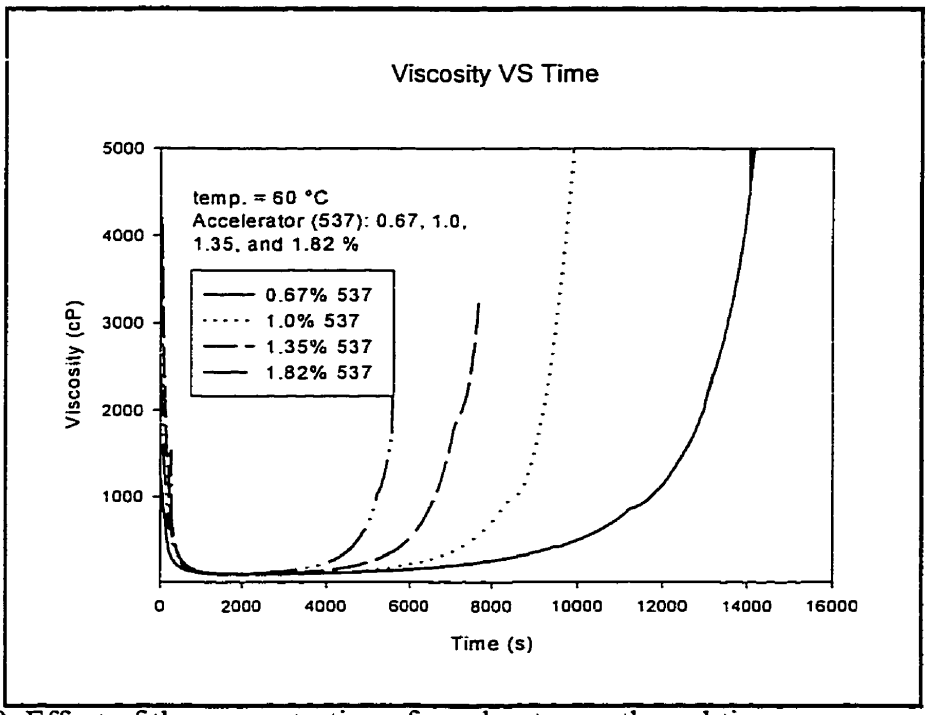

Figure 4-19: Effect of the concentration of accelerator on the gel time.

The consequence of heating the hardener is seen in figure 4-21. The particular sample that was used for this experiment was subjected to the following preparation.

The hardener was first heated and then mixed with the other ingredients. Once the mixing was complete, this sample was kept in the freezer to prevent any further polymerisation. When this sample was reheated to room temperature, it had an

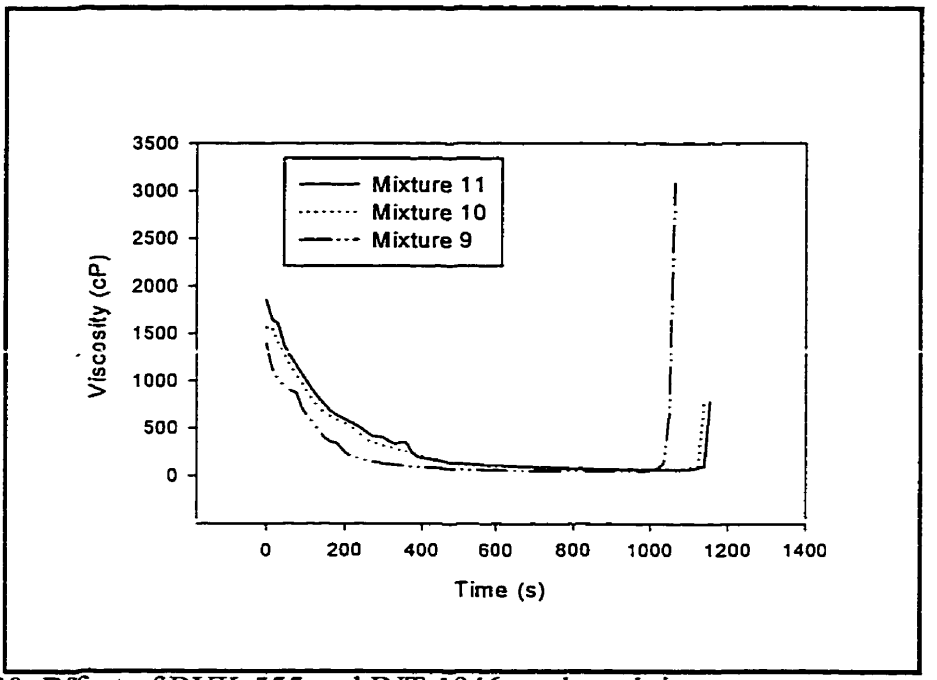

Figure 4-20: Effect of BYK-555 and INT-1846 on the gel time.

extremely high viscosity 15000 cP, which is 15 times greater than the normal viscosity at 25°C. This high viscosity is due to the fact that the resin polymerised slightly before reaching sub-zero temperatures. Because of this, when the sample was submerged in the temperature-controlled bath, its temperature did not increase at the same rate as the resin that was prepared using the standard preparation method. Therefore, the thermal conductivity of the resin is significantly reduced as the viscosity increases. This phenomenon can be easily seen in figure 4-21, when comparing the two temperature

profiles. The gel time of the resin was also influenced by excessively heating the hardener prior to mixing. The gel time was increased by roughly 30% by heating the hardener. This increase in gel time is associated with its lower thermal conductivity which subjected the resin to a lower heating rate. This delayed the influx of heat which resulted in a longer gel time.

The difference in performance between (set #1) and (set #2), can be seen in figure 4-22. The gel time of set #2 was roughly 50 % shorter than set #1. To determine the effect of what appear to be different accelerators (537), a third test was performed using the set #1 accelerator in conjunction with the material in set #2.

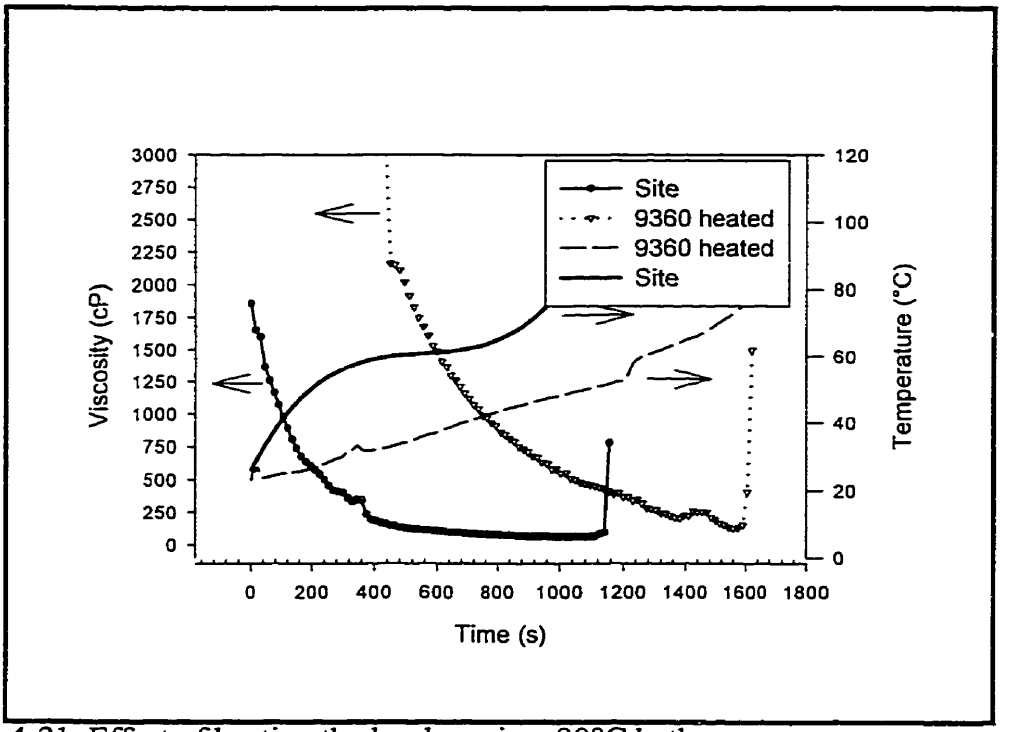

Figure 4-21: Effect of heating the hardener in a 80°C bath.

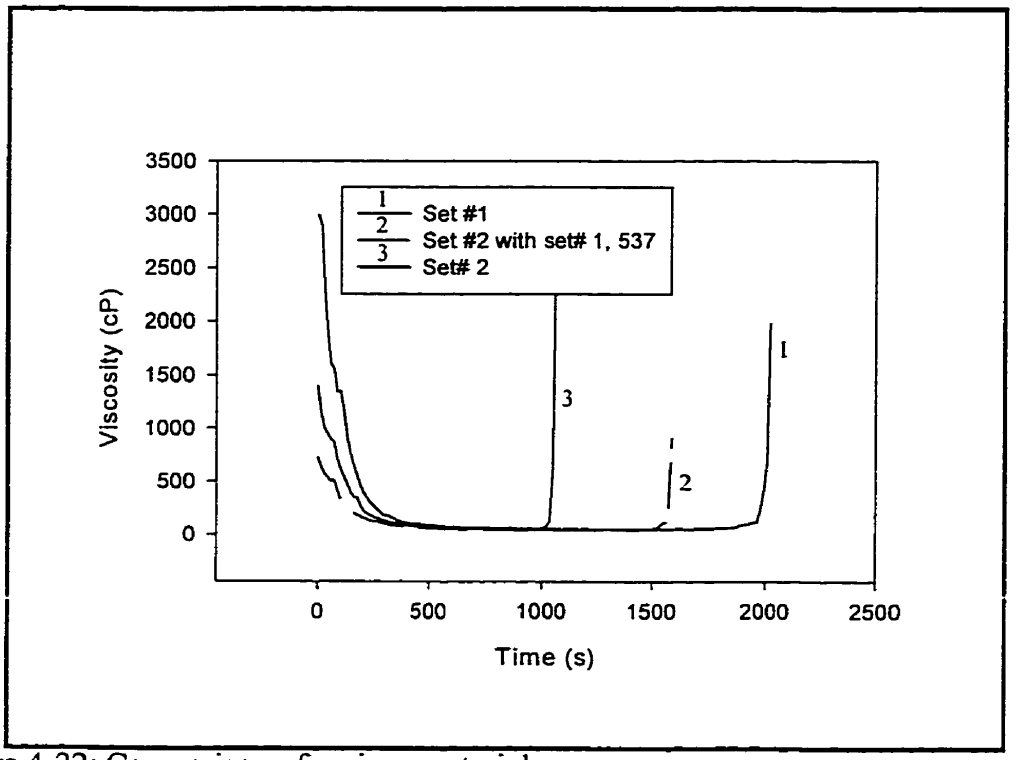

Figure 4-22: Comparison of various materials.

This test would indicate that there is not only a discrepancy between the accelerators but also with the other ingredients as well. If the only difference between the two systems was the accelerator, this test should have yielded the same result as set #1. As seen in figure 4, this test gave a response that was between set #2 and set #1. Therefore, the reactivity of some of the other ingredients found in set #1 could have aged.

4.2.2 Effect of filler on the gel time

Theoretically, the filler should not affect the gel time of the resin because it is usually an inert material. In this case, the glass filler that was used is also inert. Thus, the gel times of filled and unfilled samples should be the same. As seen in figure 4-1, the gel times are significantly lower for the unfilled sample. The cause of this difference lies in the experimental error that is associated with the resin and the test method. As mentioned previously, the resin is very exothermic, thus, during its polymerisation, heat is released. The test used 115 ml of resin during each test, therefore the heat released during the reaction also helps in heating the sample. In addition, the resin has a low coefficient of thermal conduction which helps to keep the released heat inside the resin. Therefore, when comparing the filled and unfilled samples, the filled samples not only have 33% by mass, less resin, but the glass filler also acts as a heat sink to absorb the exothermic energy. When comparing the temperature profiles of the curves below, it would appear that the temperatures were relatively the same. But because of the low thermal conductivity of the resin, the temperature on the surface is lower than in the core of the sample. Since the spindle is centred in the sample, it is not feasible to place the thermocouple in the center of sample and it would also affect the viscous measurements.

4.2.3 Modelling the gel time

The following technique was used to determine the degree of cure at the gel point. The gel times are measured by either of the techniques mentioned above. Once the gel time is known for a particular temperature, that point can be found on the degree of cure curve for that same temperature. The corresponding degree of cure for that point is the degree of cure at the gel point. This technique is demonstrated in figure 4-23. The viscosity and the degree of cure are shown on the same graph to demonstrate that the point were the viscosity tends to infinity is defined as the gel point. This point is used to determine the corresponding degree of cure, which is the degree of cure at the gel point. There is no viscosity curve for 140°C because it is physically impossible to obtain an accurate viscosity measurement at this temperature with the technique used. The reason for this is that the thermal inertia of the resin is too great. In figure 4-23, an attempt was made to determine if the degree of cure and viscosity follow a similar pattern when plotted against the normalized cure time. As seen in the figure 4-23, the curves for 60°C and 70°C have good agreement. Also, the curves for 80°C and 90°C have good agreement. These results lead to the following conclusions. Firstly, the difference between the two pairs could simply be attributed to the selection of the cure time at 100% cure. Since the degree of cure approaches a near-asymptotic value while nearing 96-97% cure, it is difficult to estimate the time to reach 100% cure. The phenomenon is caused by the vitrification of the remaining reactive sites within the macromolecule. The second hypothesis is that the resin changes its solidification mechanism somewhere

between 70°C and 80°C. For 70°C and below, the resin reaches vitrification and never enters into the gelatinous phase. For 80°C and above, the resin reaches gelation followed by vitrification. As seen in figure 4-24, trends in curves for 60°C and 70°C show a curvature when nearing the horizontal. For 80°C and 90°C curves, the reciprocal of viscosity follows a direct path toward the horizontal.

Therefore, figure 4-23 and 4-24 point to a fundamental difference in the solidification mechanism that has a transition between 70°C and 80°C. This difference in the solidification mechanism can be seen in figure 1-4, by tracing horizontal lines

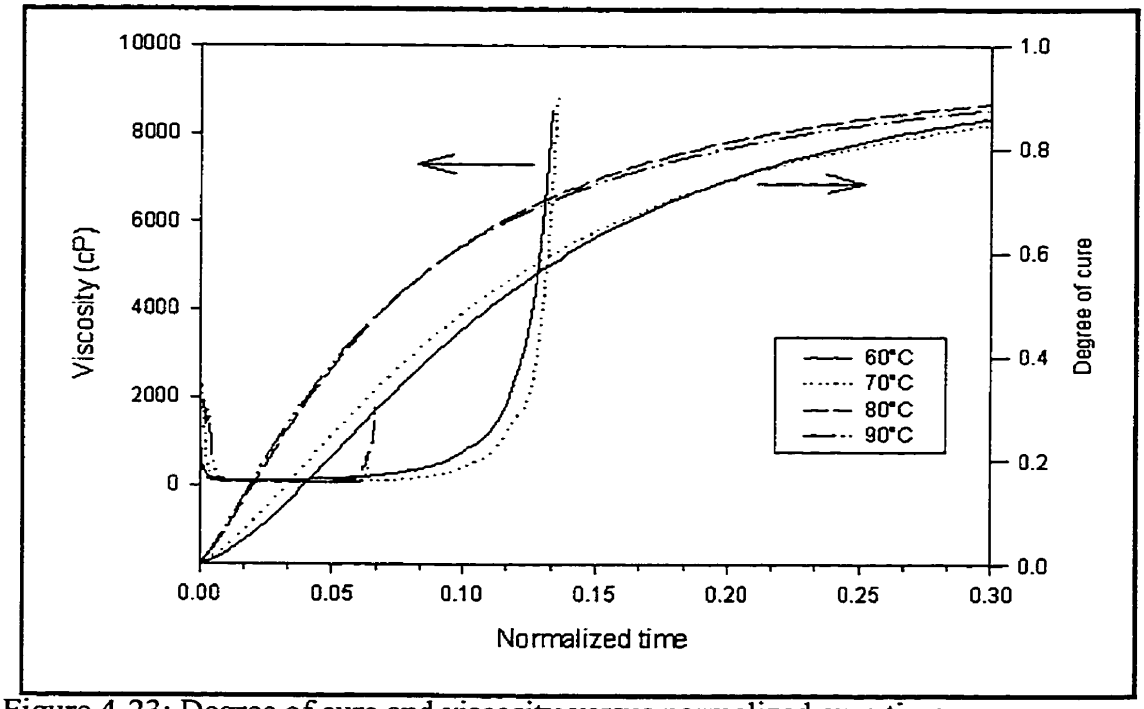

Figure 4-23: Degree of cure and viscosity versus normalized cure time.

above and below the gel T_G temperature. It could be this affect that gives the variation in normalized cure time.

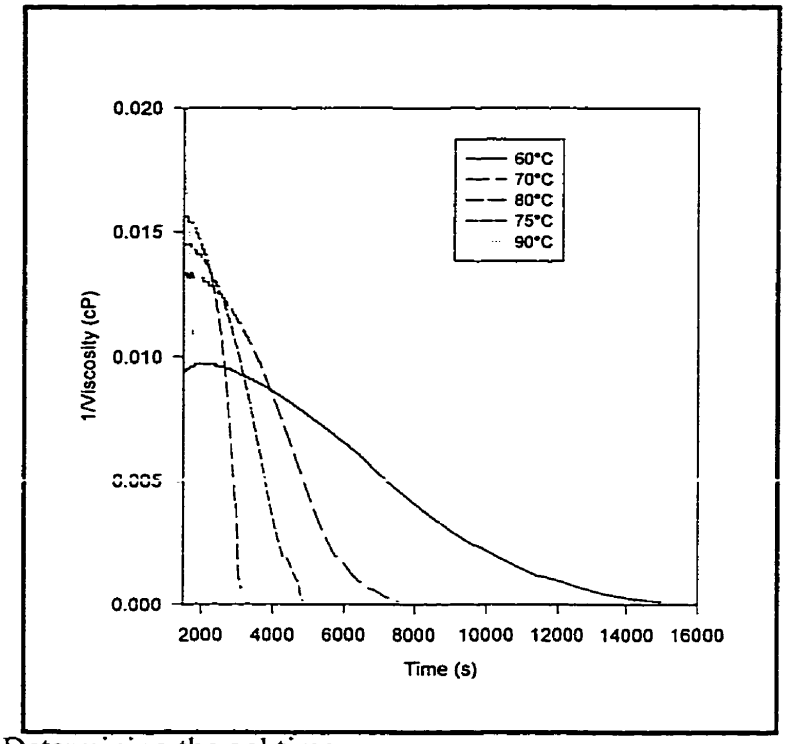

Figure 4-24: Determining the gel time.

4.2.3.1 Epoxy gel time

The experimental results obtained from both experimental techniques can be seen in the following figure 4-25. Experimental gel times were obtained for values between 60°C and 220°C for the epoxy resin. As seen in the literature, this graph of Ln gel time versus the reciprocal of the absolute temperature should yield a straight line.

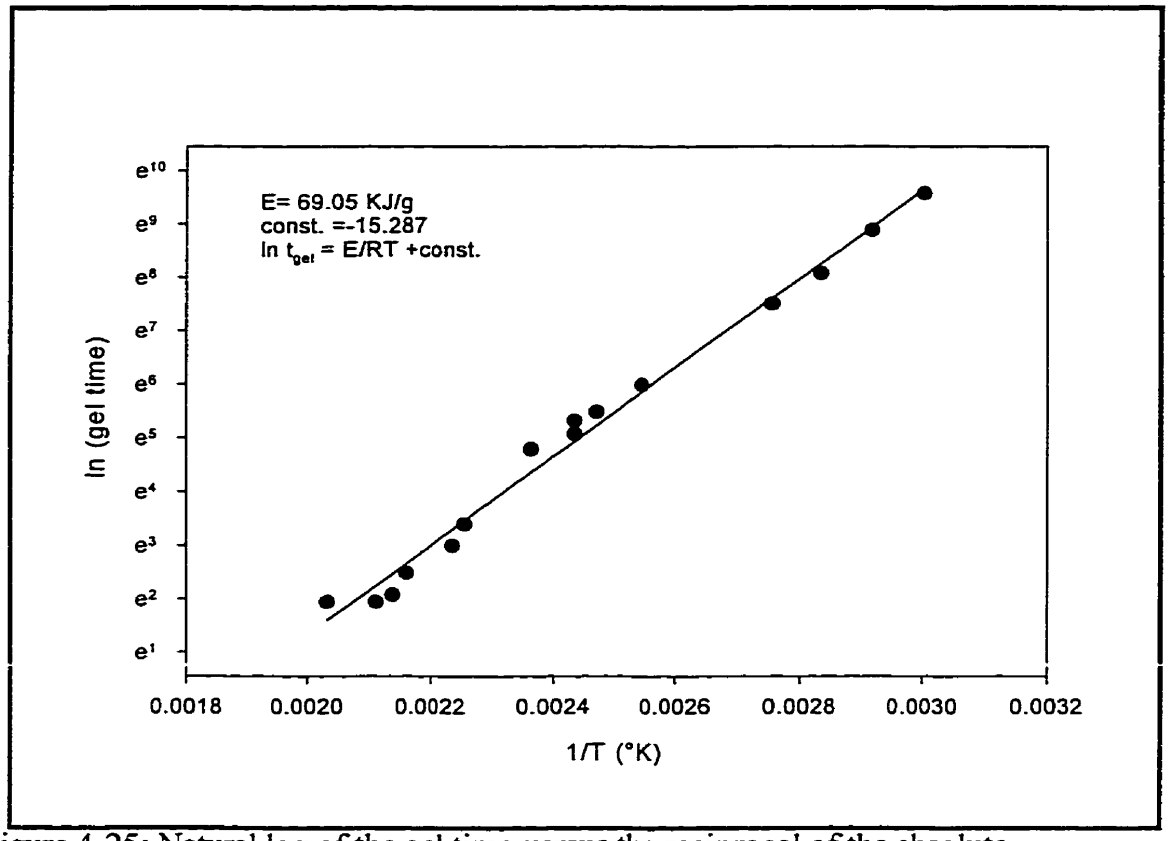

Figure 4-25: Natural log of the gel time versus the reciprocal of the absolute temperature (epoxy).

Applying the kinetic relationship shown in equation 1-25,

$$Ln(t_{gel}) = E/RT + K \qquad 1\text{-}25$$

E was found to be 69 kJ/mol, and K was –15.3. As seen in figure 4-25, the points do fall into a straight line. Therefore, it is this linearity that validates accuracy of the methodology used for these experiments.

From the experimental results that were done at 60, 70, 80, 90 and 120°C, the average degree of cure at the gel point was determined to be 54%. The reason why there are not any experimental points for 100°, 110°, 130° and 140°C is that these temperatures were simulated with the kinetic equation 1-3. Thus, while performing the gel time experiments, we were unable to obtain data for these exact temperatures. However, data was obtained for intermediate temperatures. The variation between the experimental degree of cure at the gel point (54%) and the degree of cure that was found from Flory's equation 1-21, (58%) could point to the following hypothesis. Since the experimental gel occurred before the theoretical, this would indicate that the material has aged by approximately 4%. The validity of this hypothesis is dependent upon one very important parameter, which is the functionality of the resin. It was previously sighted by Mijovic et al [7], that the functionality of the EPON 825 resin is 4. For this investigation of the EPON 9310 resin, it was also supposed that the functionality of the resin is also 4. This assumption was made because both resin systems have a very similar chemical nature. It is possible that the functionality of the 9310 resin is not exactly 4, due to the small percentage of proprietary additives in the system. However, it should be close to 4. The second possible explanation for the difference between the experimental α_{gel} and the theory is due to the exothermic nature of the resin. Due to the mass effect that takes place as the resin approaches the gel point, the resin temperature exceeds the bath temperature. This increase in temperature reduces the gel time slightly which could be attributed to the variation in α_{gel}.

In order to include all the experimental data, two curve fits were used. The first curve fit was done on a semi-log graph of the gel time versus temperature, and the second on a linear curve of the same parameters. This was done because each of these types of representations favours either the lower or higher values on the curve. Therefore, the first half of the results generated from the first fitting were used in conjunction with the results from the second half of the second fitting. The results from these curve fittings can be seen in the following figure 4-26.

As seen in the semi-logarithmic representation of figure 4-26, the linear and logarithmic curve fits are shown for comparative purposes. The linear curve fit approximates the degree of cure at the gel point rather well for temperature below 100°C, but at temperature greater than this, it begins to deviate substantially. The logarithmic curve produces the opposite affect. It gives a good approximation above 100°C, but begins to deviate below it. Therefore, a hybrid model can be obtained where the low temperature portion is from the linear curve fit, and the high temperature portion is from the logarithmic curve fit.

The degree of cure at the gel point for a temperature range between 60–140°C using the hybrid technique that is described above, can be seen in the following figure 4-27. As shown, the degree of cure at the gel point is virtually constant for this series of tests

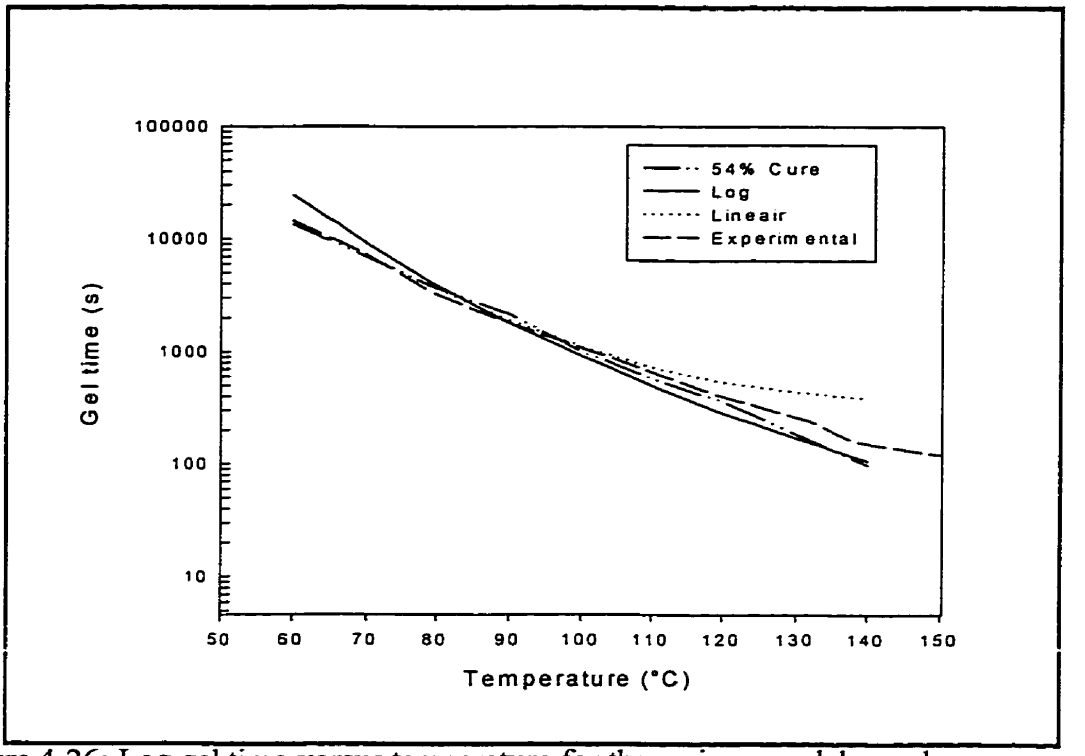

Figure 4-26: Log gel time versus temperature for the various models used.

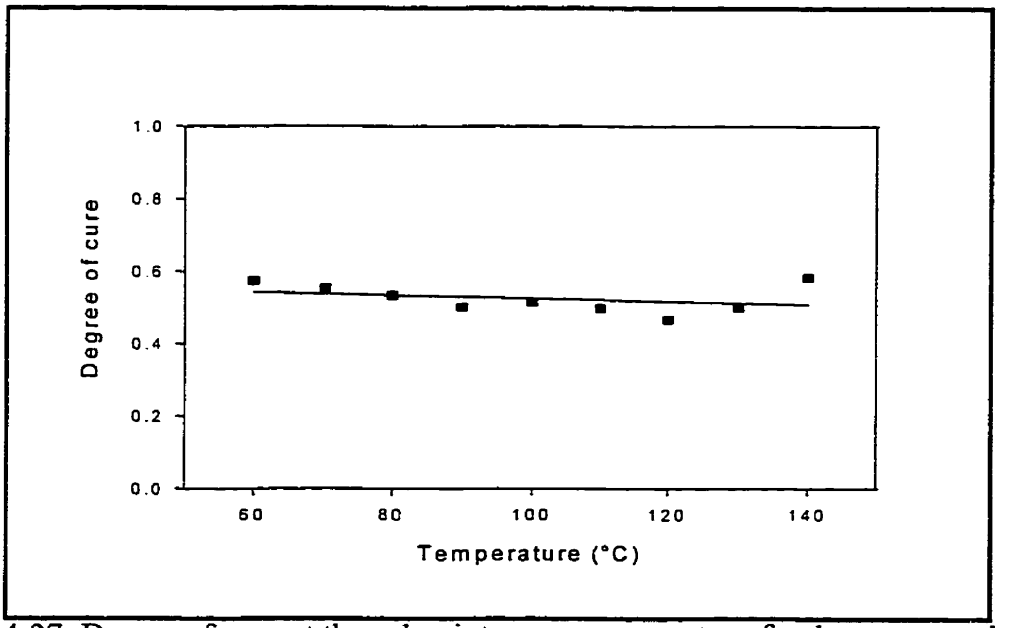

Figure 4-27: Degree of cure at the gel point versus temperature for the epoxy resin.

(hybrid curve fitting).

which is in agreement with that found in the literature. Shown in table 4-2, is the degree of cure at the gel points from the hybrid curve fitting model. Their average was found to 53%.

The degrees of cure at the gel point that are obtained from equation 1-25 can be seen in table 4-3. The values (with one exception) are close to that obtained from the hybrid technique that was used above. The results from this technique gave an average degree of cure of 57% at the gel point.

Table 4-2: Degree of cure at the gel point derived from experimental conditions (epoxy).

Temperature (°C)	Gel Time (s) experimental	α_{gel}
60	14500	0.57
70	7300	0.57
80	3200	0.49
90	1800	0.48
120	398	0.56
Average	-------	0.54
St. deviation	-------	0.045

Table 4-3: Degree of cure for isothermal conditions using the hybrid curve fitting technique, and equation 1-25.

	Hybrid curve fitting	Equation 1-25
T (°C)	α_{Gel}	α_{Gel}
60	0.57	0.61
70	0.55	0.57
80	0.53	0.55
90	0.50	0.51
100	0.51	0.56
110	0.49	0.55
120	0.47	0.52
130	0.50	0.60
140	0.58	0.72
Average	0.53	0.57
St. deviation	0.04	0.06

The results from the kinetic relationship, equation 1-25, fall between the hybrid technique and Flory's technique. Therefore, all the techniques and theory that have been used in this study yield very comparative results.

4.2.3.2 Polyester gel time

Figure 4-28, presents the gel times that were obtained for temperatures ranging from 37°C to 123°C for the polyester resin.

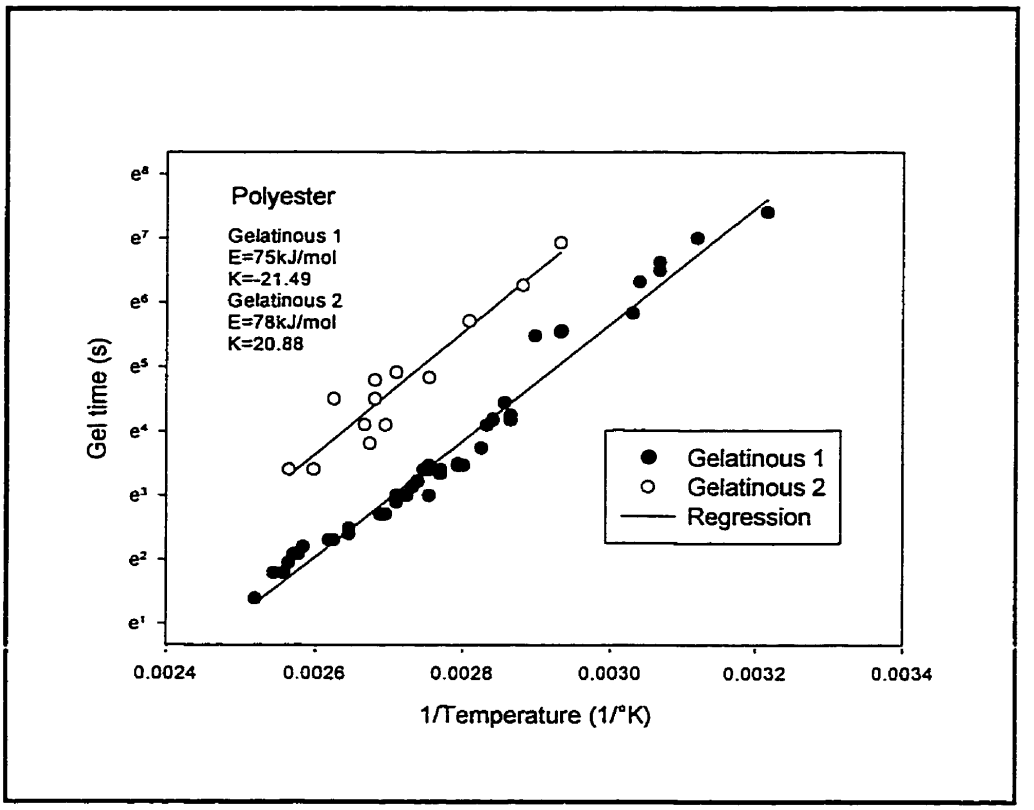

Figure 4-28: Natural log of the gel time versus the reciprocal of the absolute temperature (polyester).

Figure 4-29, shows the isothermal degree of cure profiles that were obtained for various temperatures for the polyester resin. Plotted on the figure are the average degrees of cure obtained using the two definitions of the gel point. The first is the same method used in the previous section for the epoxy resin. The second definition was specifically determined for the polyester resin used in this study. This second definition was defined as the point where the resin could be sliced, but could still flow under pressure. As seen in figure 4-28, this point was more difficult to determine, as indicated

by the scatter in the curve *gelatinous 2*. The results from both of these techniques can be seen in table 4-4 and 4-5.

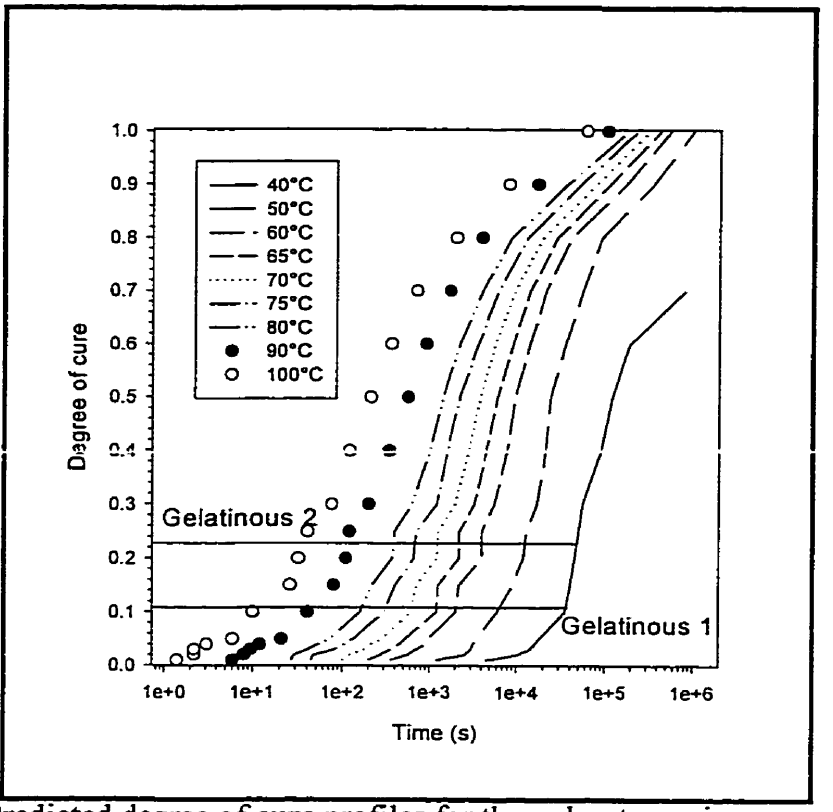

Figure 4-29: Predicted degree of cure profiles for the polyester resin.

The low degree of cure at the gel point in table 4-5 can be attributed to two factors. The first being the isothermal degree of cure curve, as in figure 4-29, could simply be a time lag in the results which would significantly lower the degree of cure for a specified time. The second cause of the low degree of cure could be that the resin's transition from liquid to solid is relatively long. Therefore, the definition used for *gelatinous 1*, the same as for the epoxy, is not adequate for this polyester resin system.

Table 4-4: Degree of cure at the gel point derived from experimental conditions (polyester).

Temperature (°C)	α_{gel} experimental
101	0.25
98	0.26
102	0.28
90	0.25
83	0.24
74	0.17
68	0.19
Average	0.23
St. deviation	0.0395

Table 4-5: Degree of cure derived from the viscosity measurements

Temperature (°C)	Gel time (s)	α_{gel} viscosimeter
40	5000	0.02
50	1650	0.02
60	1055	0.05
65	945	0.08
70	705	0.15
75	660	0.18
80	520	0.28
Average	-------	0.11
St. deviation	-------	0.0962

The degree of cure at the gel point that was obtained using *gelatinous 2* can be seen in figure 4-30 below.

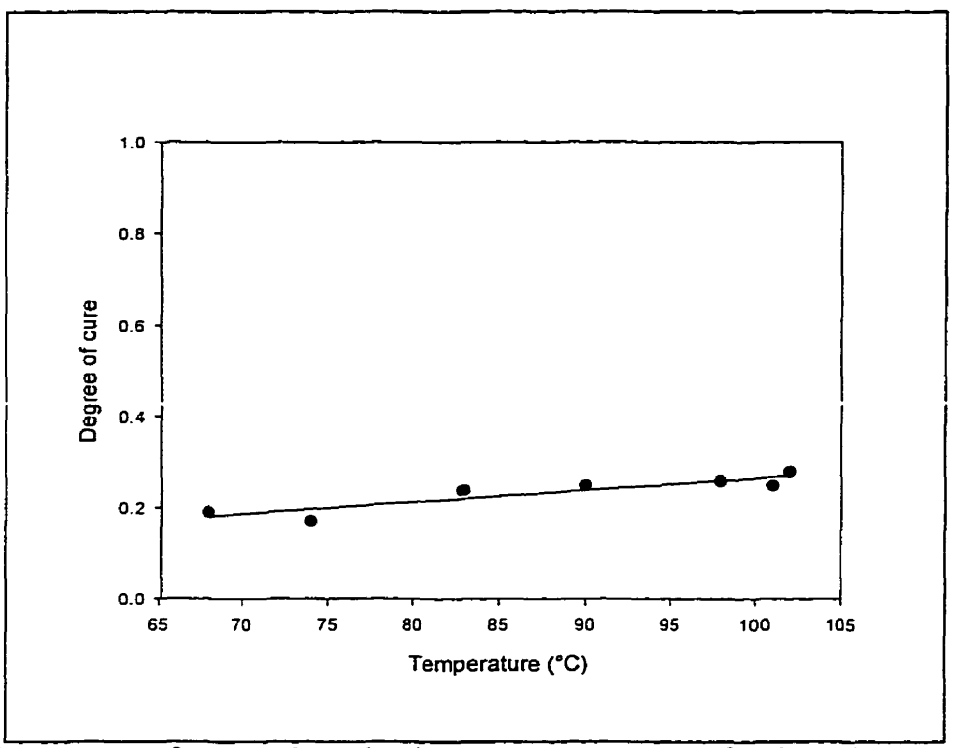

Figure 4-30: Degree of cure at the gel point versus temperature for the polyester resin (experimental).

4.3 Volumetric changes of the resin

To conduct this portion of the investigation, a dilatometer was designed and built at the laboratory. The validity and reproducibility of the design are discussed in the following section.

4.3.1 Validity of the method

To verify whether the sample had completely cured during the isothermal experiment, a post-cure was done on the sample. To post-cure the sample, it was simply subjected to a second isothermal run. The criteria that the sample had to achieve during the post-cure is the following. It had to return to the original level that it was at by the end of the first isothermal run before being cooled. As seen in figure 4-31, the cure and the post-cure curves converge at a common value. This indicates that the sample had completely cured during the first isothermal run.

A second series of tests was done to determine the repeatability of the dilatometer design. To validate the design, three identical samples of epoxy were investigated under the same experimental parameters. The results from this validation can be seen in figure 4-32. It is noted that the volumetric expansion rates showed very good agreement. The reproducibility of the peaks in the curves was also good. The design, however, was not very accurate in determining the final shrinkage of the sample. The reason is that there are small voids that form inside the polymer sample.

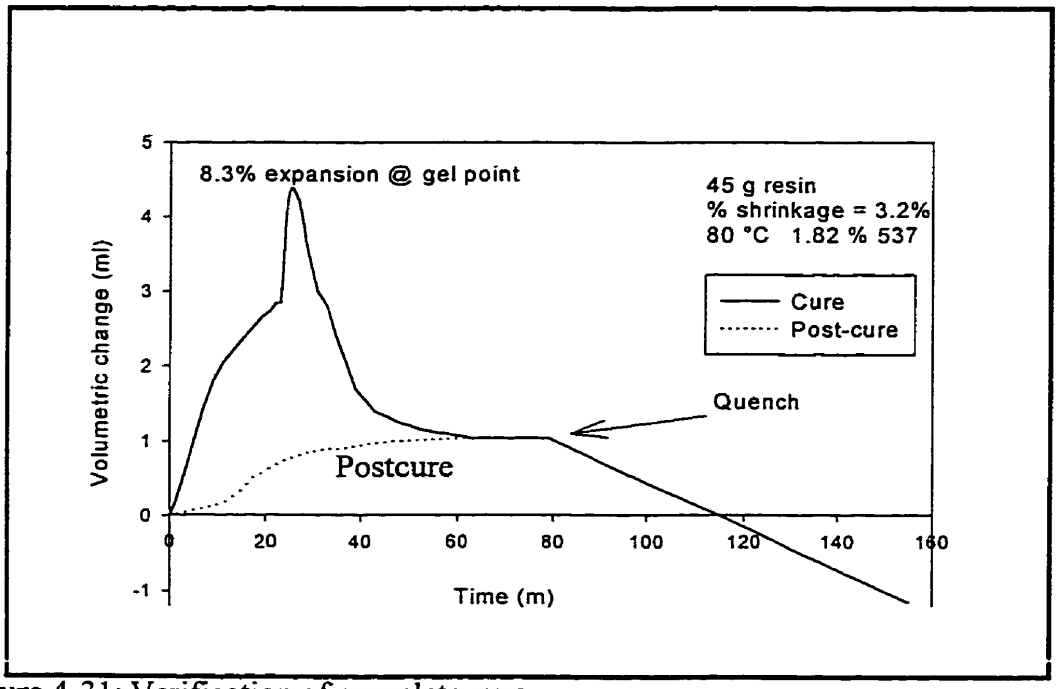

Figure 4-31: Verification of complete cure.

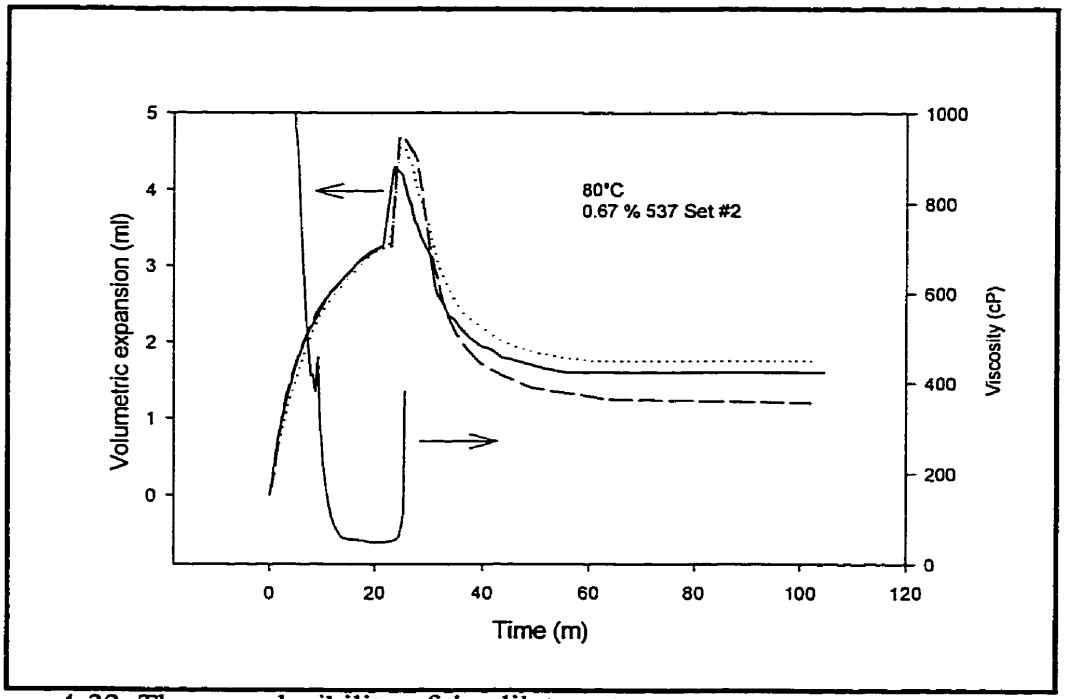

Figure 4-32: The reproducibility of the dilatometer.

Consequently, the secondary fluid is not capable of filling these voids, resulting therefore, in shrinkage values that are slightly less than the actual shrinkage.

The profile that is obtained while measuring the volumetric changes of the epoxy resin during cure can be seen in figure 4-33. This profile can be used to measure the following parameters. The maximum expansion of the resin during cure, the final shrinkage after the resin has completely cured and finally, the gel time of the epoxy resin can also be predicted. The maximum expansion during cure is found at the peak of the profile. The final cure shrinkage can be determined by subtracting the final volume with the initial volume after the sample is cooled to the initial temperature. The gel time is found to occur very close to the point where the volumetric profile reaches a maximum. Therefore, the gel time is approximately the time at the peak in the profile.

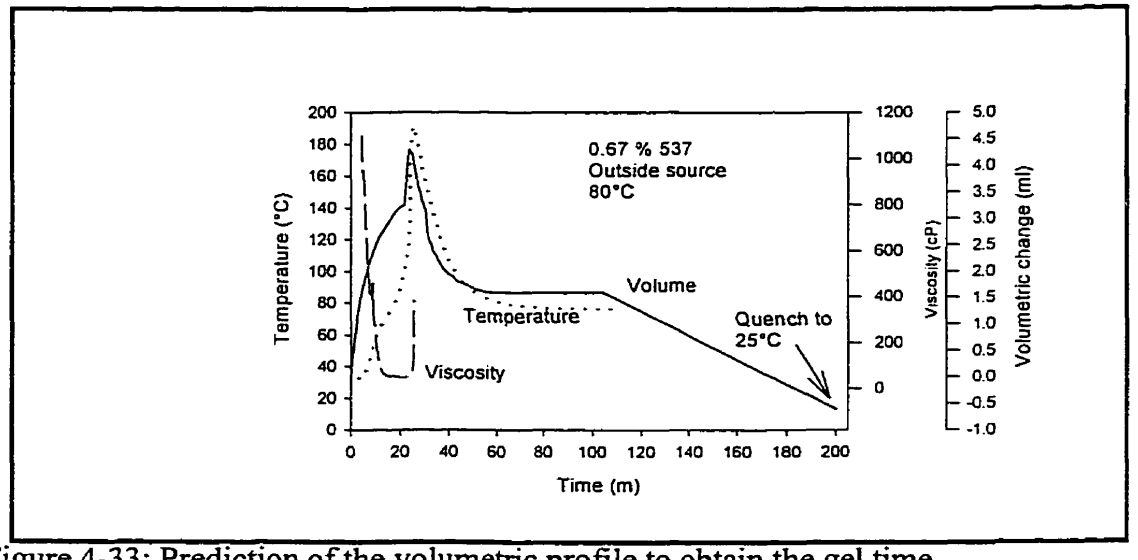

Figure 4-33: Prediction of the volumetric profile to obtain the gel time.

The ability of the volumetric expansion curve to predict the gel time is limited to only the epoxy samples that are homogeneous during the polymerisation. As seen in figure 4-33, the peak in the volumetric profile occurs very close to the point where the viscosity tends toward infinity and at the peak in the temperature profile.

4.3.2 Effect of the additives on the volumetric changes

From the results that have been obtained from this technique for determining the volumetric profile, it only appears to be valid for homogeneous mixtures. For non-homogeneous mixtures, the quantity of expansion that occurs is far too great for the current experimental set-up. The cause of this large expansion is due to the production of gas that occurs during the cure. It is this gas that causes the apparent extreme expansion and not the resin. However, it is unrealisable with the current equipment to distinguish between the two expansions that derive from the resin and the displacement caused by the production of gas.

The effect that the additives have on the volumetric expansion of the resin during cure can be seen in figure 4-34. The formulations that are represented by mixtures 9 and 10 did not produce a homogenous uniform cure. It is this non-homogeneity that causes the extremely large expansion at gelation. In both of these

samples, a multiphase cure occurred. A multiphase cure occurs when there is more than one layer of fluid in the sample and the fluids do not have the same gel time or rate of cure. Therefore, if this condition occurs inside a pultrusion die, it would cause the pressure to increase to an extremely high level and the gel zone would also be lengthened. This would result in the demand of a high pull force. This effect can be seen when comparing the time at the peaks of curves 9 and 10, to the gel times for the corresponding curves in the previous section. The time to attain the peak for curves 9 and 10 was roughly 5 minutes longer than the gel time that was obtained by the viscosimeter method. The gel times that were determined using the viscosimeter and the volumetric techniques were both in good agreement for curve 11, which was a homogenous mixture.

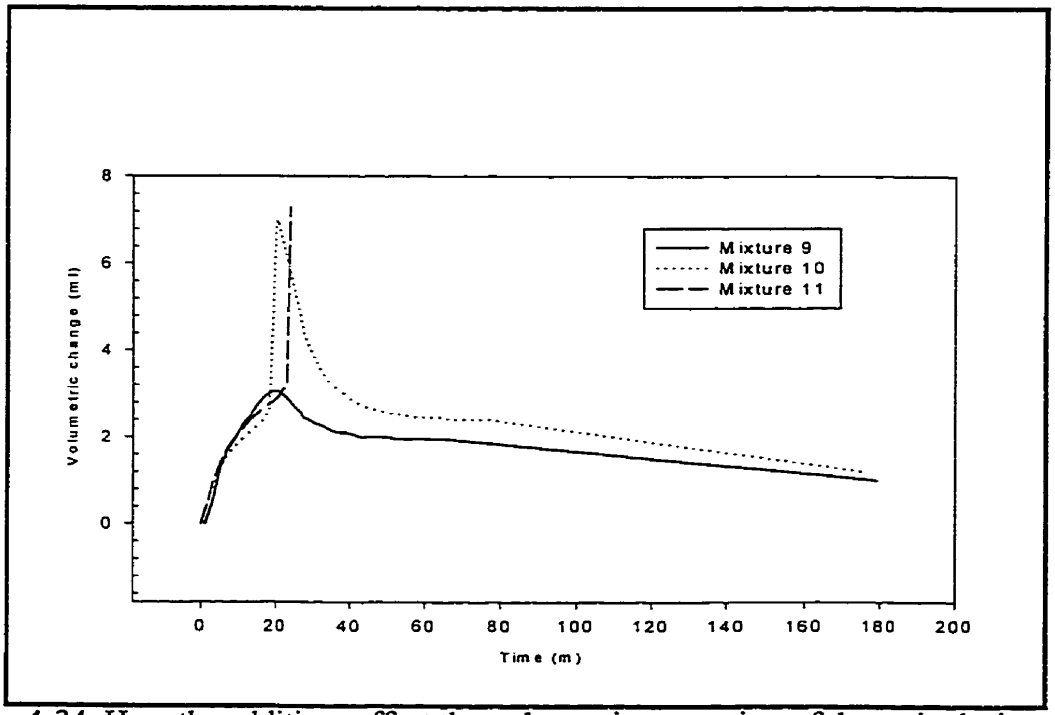

Figure 4-34: How the additives affect the volumetric expansion of the resin during cure.

The effect of pre-heating the hardener on the volumetric expansion can be seen in figure 4-35. The shape of curve 2 might initially indicate that some separation that occurred during the test, however, there was none. The same phenomenon occurred during the viscosity measurements for the same sample. This phenomenon being that there was no separation. The heating of the hardener causes an irregular cure, however there is not any separation in the sample. The pre-heating of the hardener is the factor that causes this phenomenon to occur. A gas was released which caused the volumetric profile to spike. The effect that the two different accelerators have on the volumetric profile is also seen in figure 4-35. The amount of shift in the peaks is similar to that already predicted by the viscosimeter method. The shape of the profiles is also similar

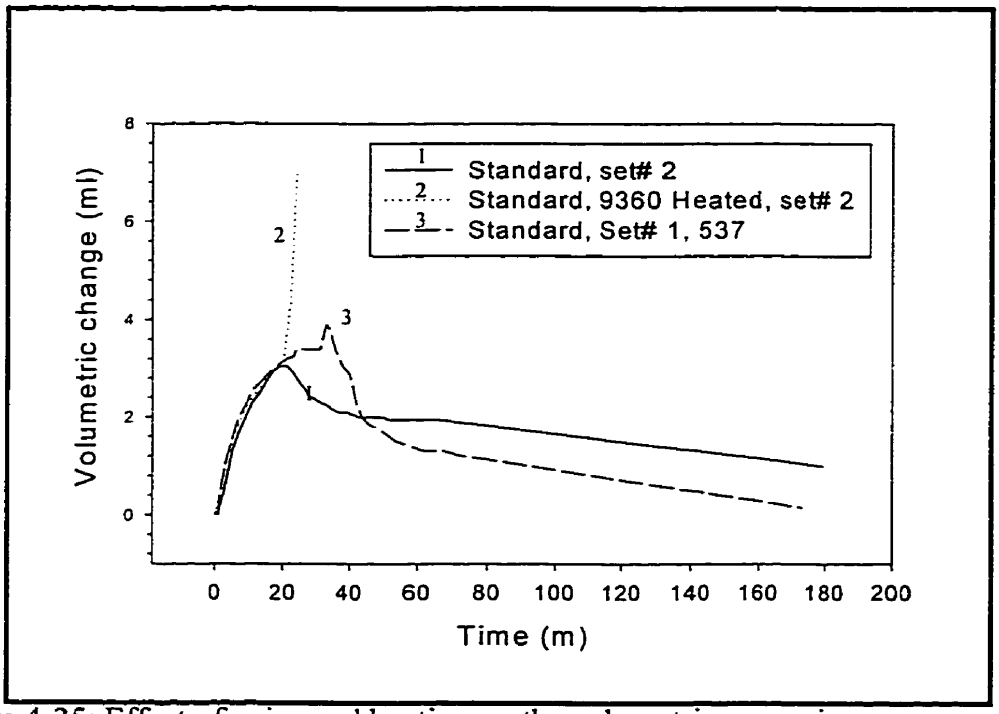

Figure 4-35: Effect of aging and heating on the volumetric expansion.

with the exception that the accelerator from set #1 produced a slightly higher peak and there was slightly more overall shrinkage.

4.3.2 Effect of the accelerator on the volumetric changes

The volumetric changes of the standard formulation have been measured for concentrations of accelerator (537) that ranged from 1 % to 1.8 %. The results from these experiments can be seen in the figures 4-36 to 4-38. The following trend was observed. As the concentration of 537 is increased, the expansion of the resin at the gel point is also increased. Once again the peaks in the volumetric profiles coincide with the gel point shown by the viscosity curves.

Due to the thermal inertia of the resin, the additives can give the perception that they have an affect on the volumetric expansion. As the reaction rate increases, the rate that the heat is released by the resin is greater than the rate at which the heat can exit from the resin. This imbalance caused the temperature within the resin to rise above the isothermal bath temperature, thus affecting the results.

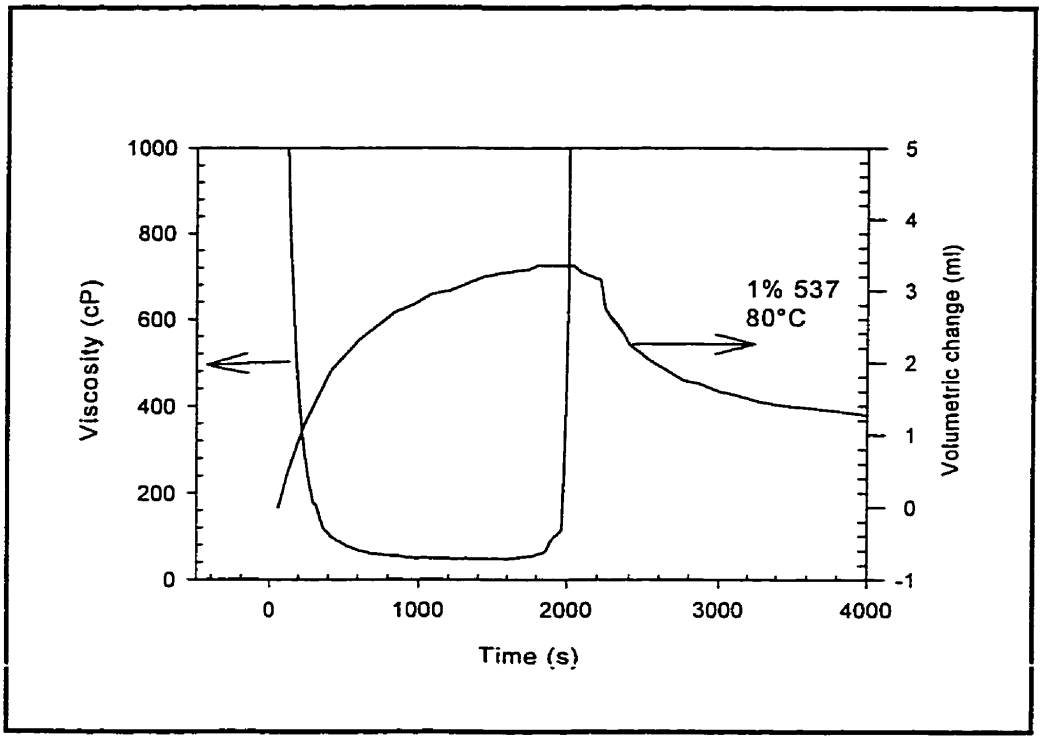

Figure 4-36: Volume change with 1 % accelerator.

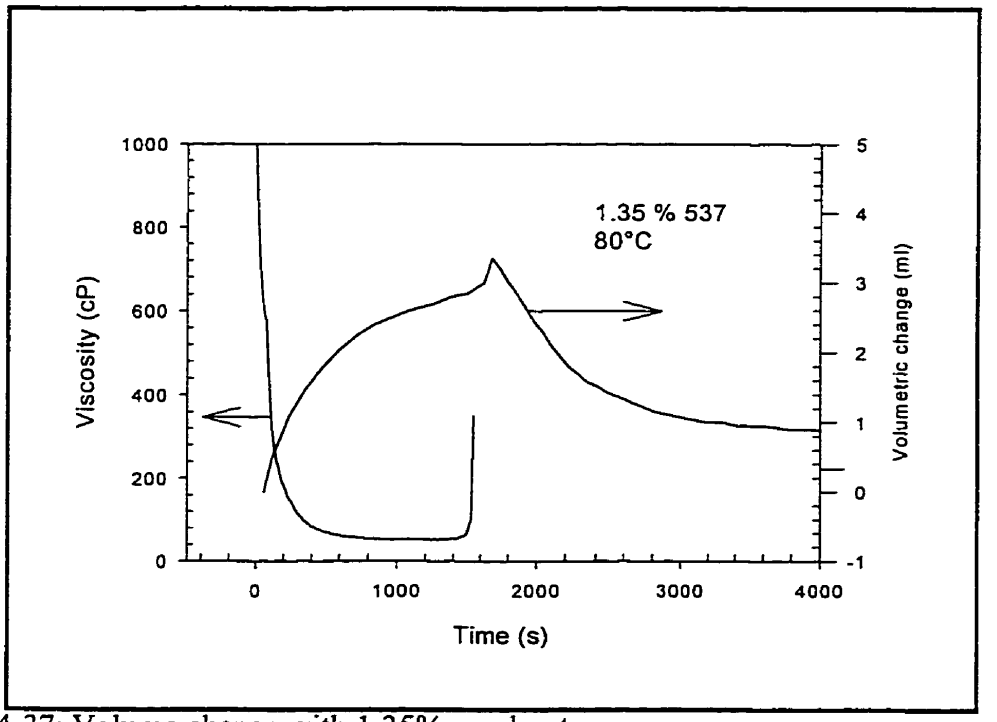

Figure 4-37: Volume change with 1.35% accelerator.

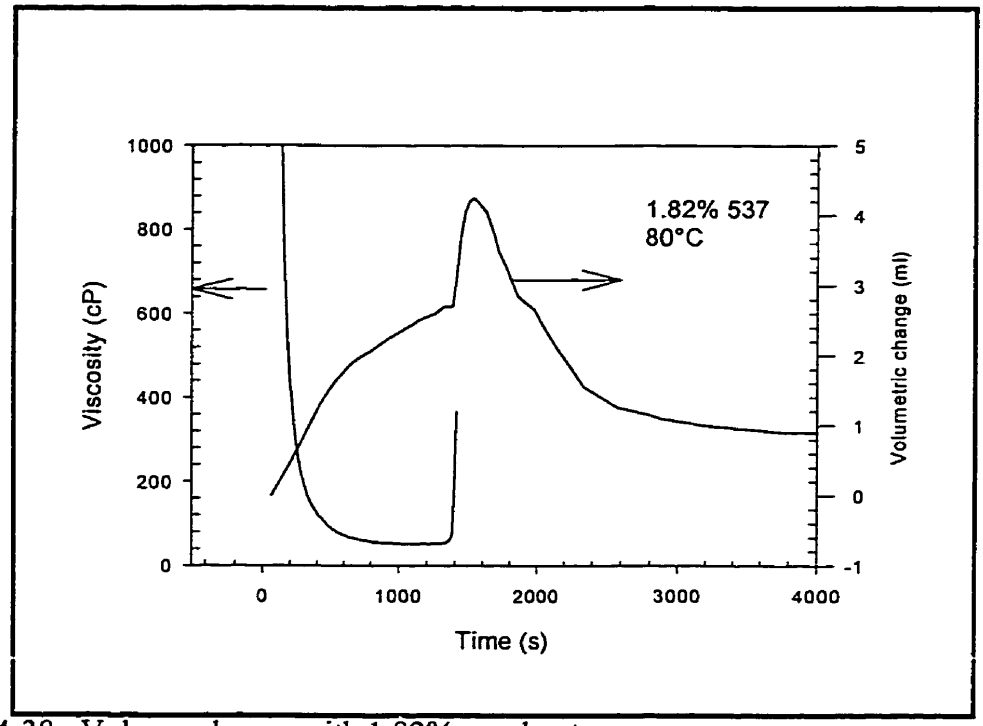

Figure 4-38: Volume change with 1.82% accelerator.

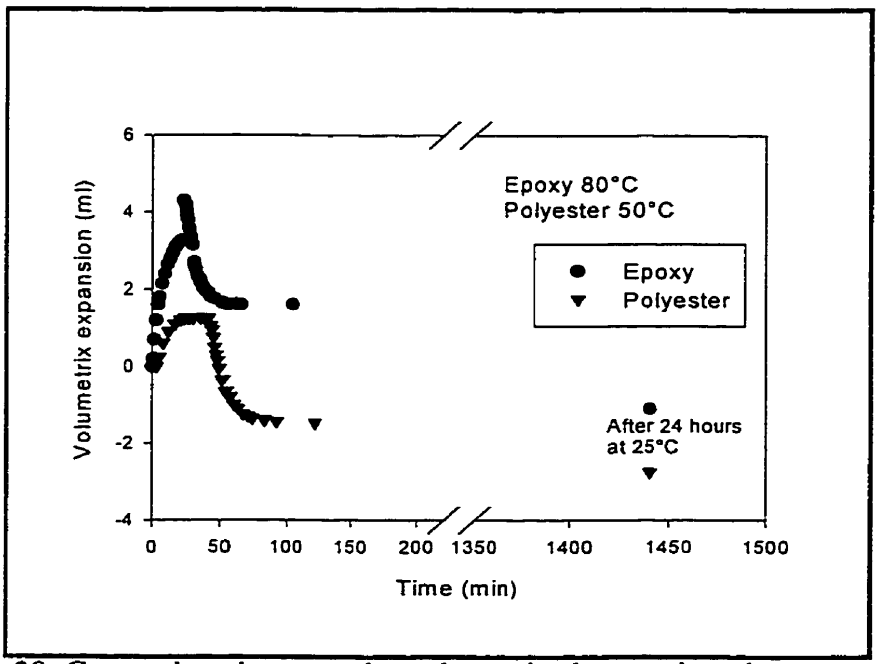

Figure 4-39: Comparison between the volumetric changes in polyester and epoxy resins.

4.3.3 Modelling the volumetric changes

The model that was chosen to simulate the volumetric changes of the resin is the following,

$$\left(\frac{1}{V_o}\frac{dV}{dt}\right)_{Overall} = \left[\beta_m(1-\alpha)+\beta_p\alpha\right]\frac{dT}{dt} - B\frac{d\alpha}{dt} \qquad 1\text{-}34$$

To simulate the volumetric changes that take place in the resin, there are three constants that need to be determined. The first constant, β_m, is the volumetric expansion coefficient of the monomer or unreacted resin. The second constant, β_p, is the volumetric expansion coefficient of the solidified resin. The final constant, B, that is needed, relates to the shrinkage due to the curing of the resin. The first constant can be obtained by dividing the thermal expansion of the resin by a change in temperature while there is a low degree of cure in the resin. This measurement can be taken from the results at the beginning of the tests described above. Assuming that within the first 4 minutes of the test at 80°C, negligible cure has taken place, the volumetric expansion coefficient of the unreacted resin, β_m, is $5.64\text{x}10^{-3}$ ml/ml °C after normalising it by the sample size for the epoxy resin. A similar measurement was taken for the polyester resin at the start of a test at 50°C. The coefficient of volumetric expansion of the unreacted polyester is $2.48\text{x}10^{-3}$ ml/ml °C. A comparison between the epoxy and polyester resin is seen in figure 4-39. The difference in peak heights could explain why the epoxy resin is more difficult to pultrude. The large expansion would increase the pressure in the die, therefore the pull force would also increase.

To determine the volumetric expansion of solidified resin, a post cure on the resin was done. The post cure consisted of performing a second volumetric test on a sample that had previously gone through a volumetric experiment. The results from this test can be seen in figure 4-31, and 4-40. To determine the coefficient of expansion of solidified resin, the following procedure was done. The post cure expansion of the resin was divided by the change in temperature. This resulted in the coefficient of thermal expansion of the solidified resin, β_p. This coefficient was found to be 0.515×10^{-3} ml/ml °C for the epoxy and $9.07 \times 10^{-4\ 3}$ ml/ml °C for the polyester resin after normalising them by their sample size.

The final constant that needs to be determined is the constant "B" which is determined by the cure shrinkage of the resin. This constant is determined by fitting the model to the experimental data. The fitting of the model can be seen in figures 4-41A and 4-41B for both the epoxy and polyester resins, respectively. The final constant B was found to be 0.025 for the epoxy resin and 0.105 for the polyester resin

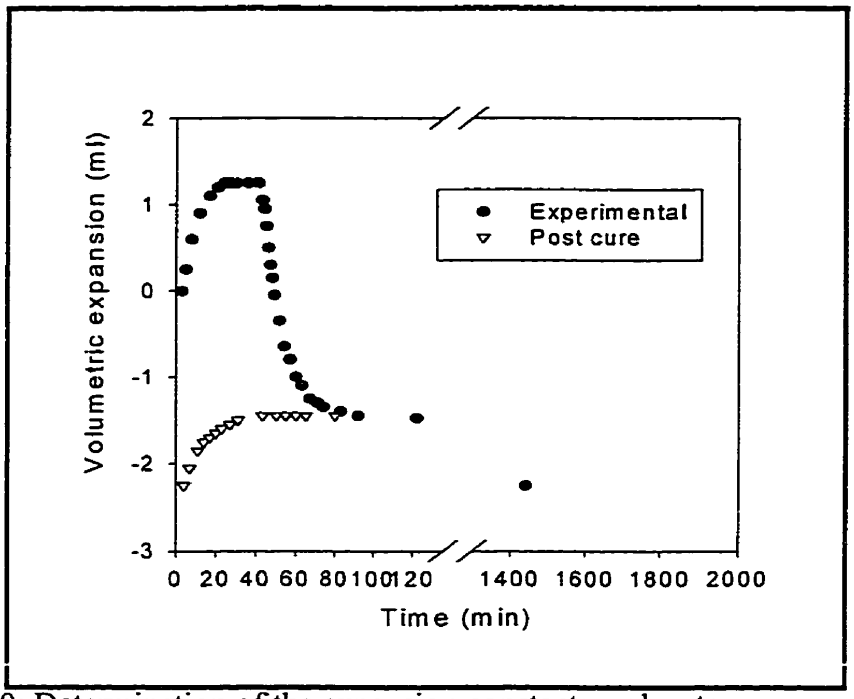

Figure 4-40: Determination of the expansion constants, polyester

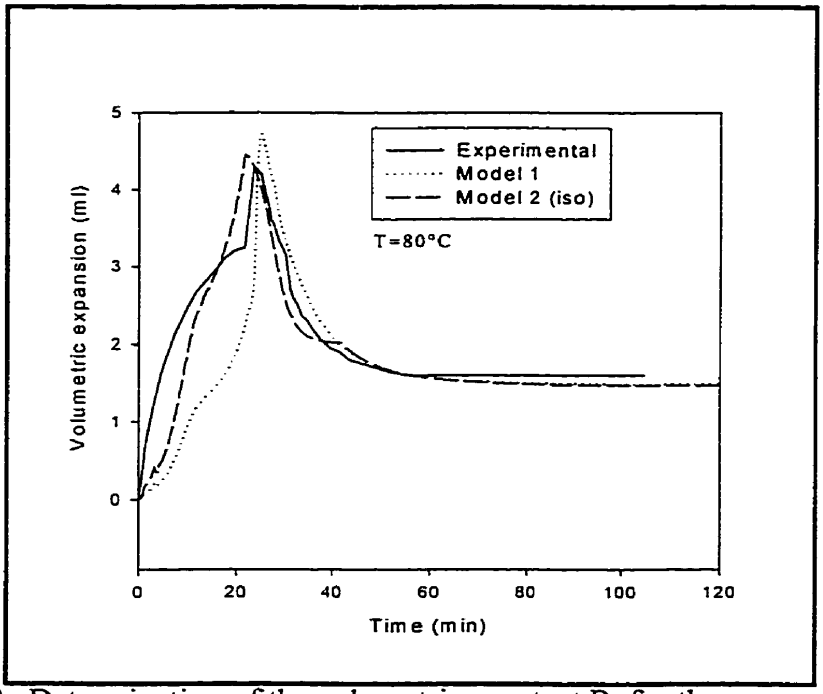

Figure 4-41A: Determination of the volumetric constant B, for the epoxy resin.

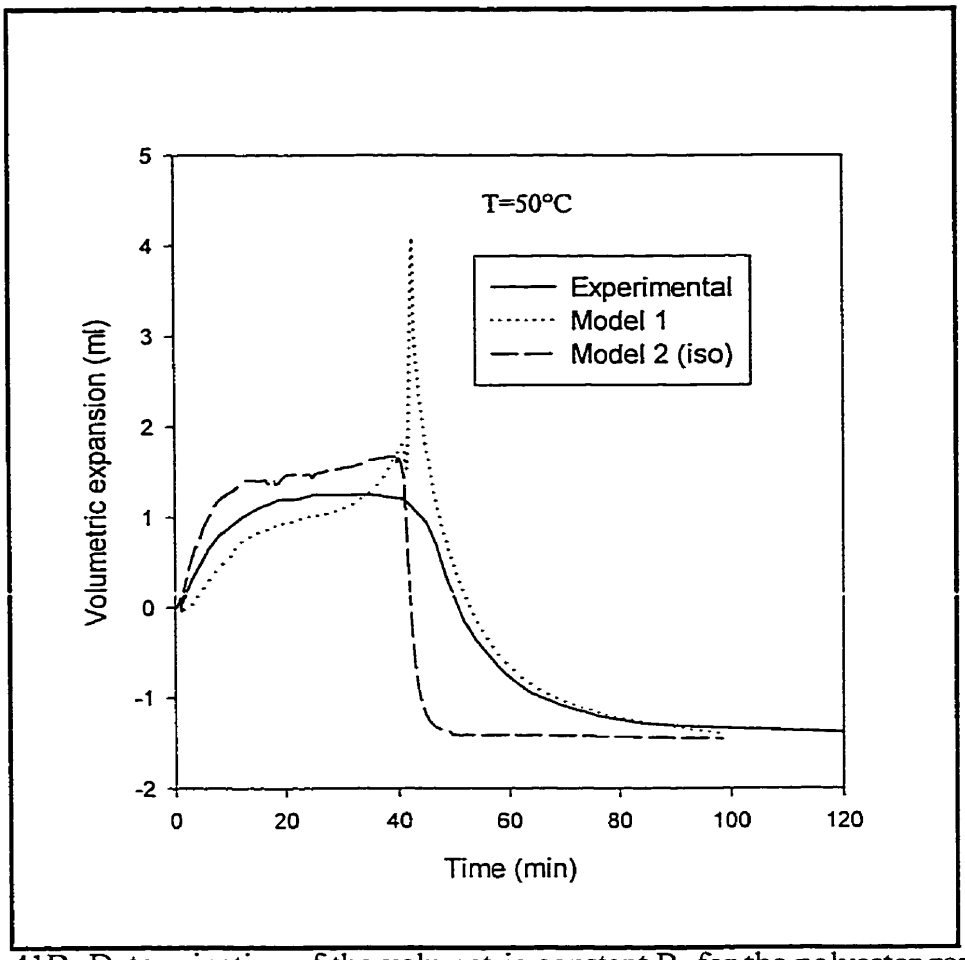

Figure 4-41B: Determination of the volumetric constant B, for the polyester resin.

4.4 Modelling the pressure profile in the die

An analogy to describe the development of the pressure profile can be seen in figure 4-42. Supposing a volume, dV, is constrained on the top and bottom by the mold, and on the right by solidified resin. The pressure P, in the volume will increase as the force F, increases. Therefore, as the volume fraction of fiber or viscosity increases, the

resins resistance to flow also increases. This increase in resistance to flow, increases F, which in turn increases the pressure on the volume dV.

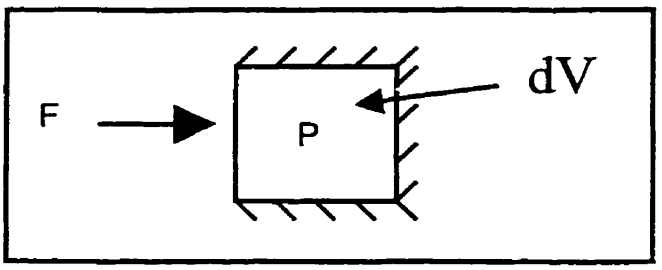

Figure 4-42: Description of the pressure build up.

Shown in figure 4-43 and 4-44 are the predicted pressure profiles that were obtained from equations 1-41 and 1-42.

$$\frac{dP}{dz} = V\eta \frac{16K}{D_f^2} \frac{\nu_f^2(z)}{\left[1-\nu_f(z)\right]^3} \left(\Delta\nu/\nu\right)\left[1-\nu_f(L_t)\right] \qquad 1\text{-}41$$

$$\frac{dP}{dz} = \frac{1}{K_b}\left[a_v \frac{dT}{dz} - \gamma \frac{d\alpha}{dz}\right] \qquad 1\text{-}42$$

4.5 Pull force on the profile

4.5.1 Calibrating the pull force

The calibration curves are shown below in figure 4-45. The calibration was performed as described in section 3.3.4. To obtain the pull force on the profile, one

simply has to plot the power consumed on the correct line speed curve and then read the corresponding pull force. The only restriction found for this method is that it is not valid at line speeds below 0.5m/min. The reason for this is that the efficiency of the motor decreases as the speed decreases below 0.5m/min.

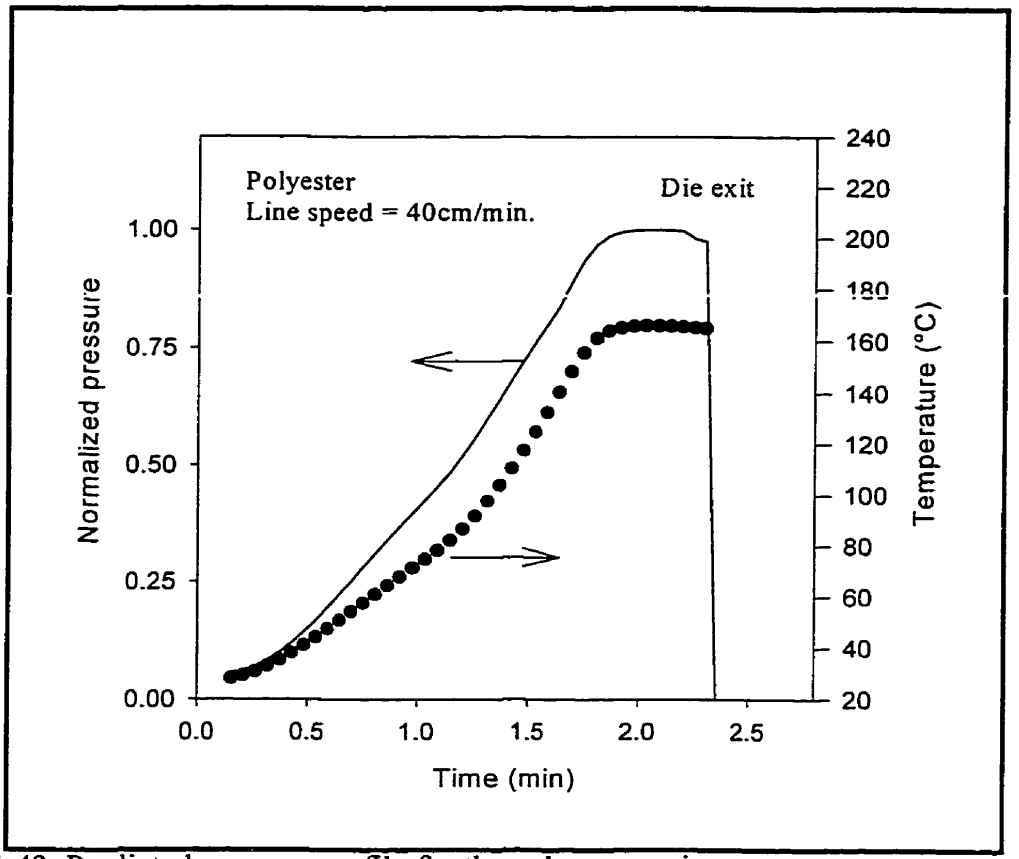

Figure 4-43: Predicted pressure profile for the polyester resin.

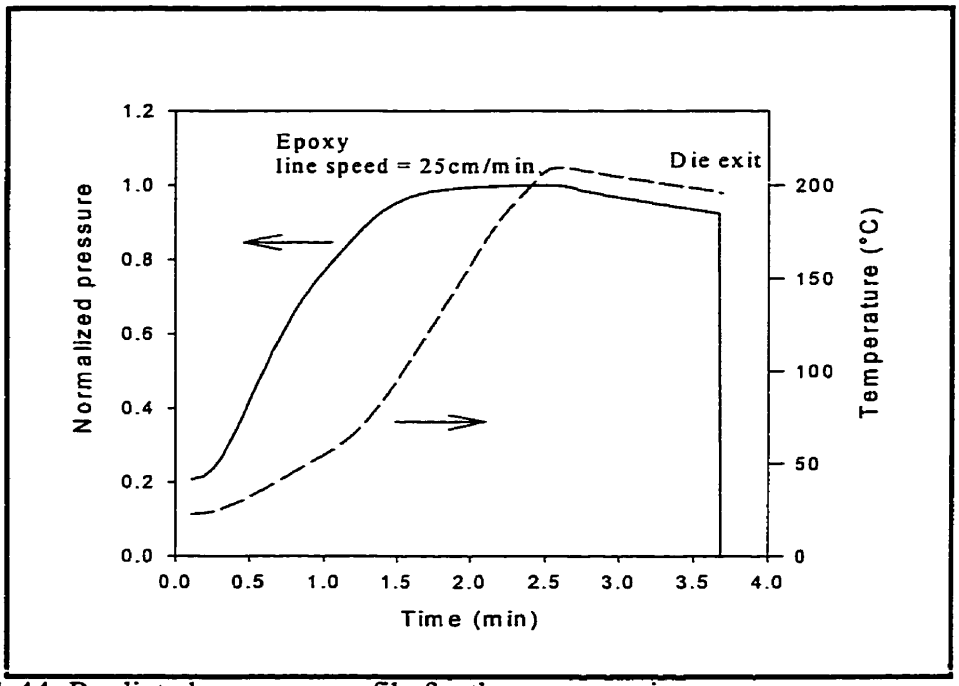

Figure 4-44: Predicted pressure profile for the epoxy resin.

4.5.2 Determining the components of the pull force

Mentioned in the literature are 6 contributions to the total pull force. In an effort to isolate the contribution of each component, the pull force was measured while pultruding dry fibers, wet fibers with silicon oil and wet fibers with polyester resin through the die. At a line speed of 0.5 m/min., the pull force was 800 N for the dry fibers, 890 N for the fibers wetted with silicon oil and 1600N while pultruding the polyester resin. From these three experiments, it can be determined that the collimating forces account for 50% of the total pull force. The viscous drag accounts for only 5.6% of the total pull force. The remaining gel adhesive bonding and shrinkage drag account

for 44% of the total pull force. This particular breakdown for the pull force was for one instance during production when an excellent profile was being produced.

Shown in figure 4-46, is the increase in pull force for a few moments before the profile jammed. Therefore, the pull force can be used as an means of monitoring problems inside the die. For example, during production at constant speed, the pull force should remain constant. However, if it slowly increases, this indicates there is a build up starting inside the die. This type of monitoring will allow the operator time to take corrective measures to prevent the profile from jamming.

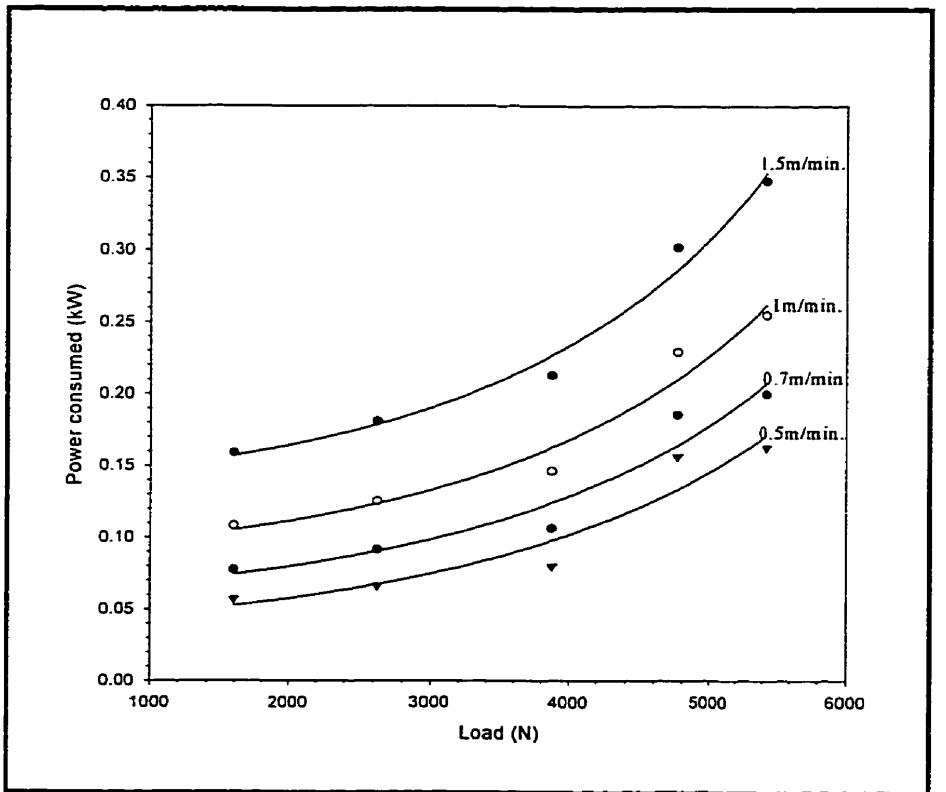

Figure 4-45: Calibration curves to determine the pull force of the profile.

4.5.3 Effect of line speed on the pull force

While varying the line speed from 0.5 m/min. to 1.5m/min., it was found that the pull force increased linearly, as seen in figure 4-47 below. This finding is contrary to that discussed in the literature. The literature claims that the pull force should increase exponentially, which it did not. From the results of the silicon oil pultrusion test, it is reasonable that the pull force increases linearly, since the viscous drag only accounted for 5% of the total pull force.

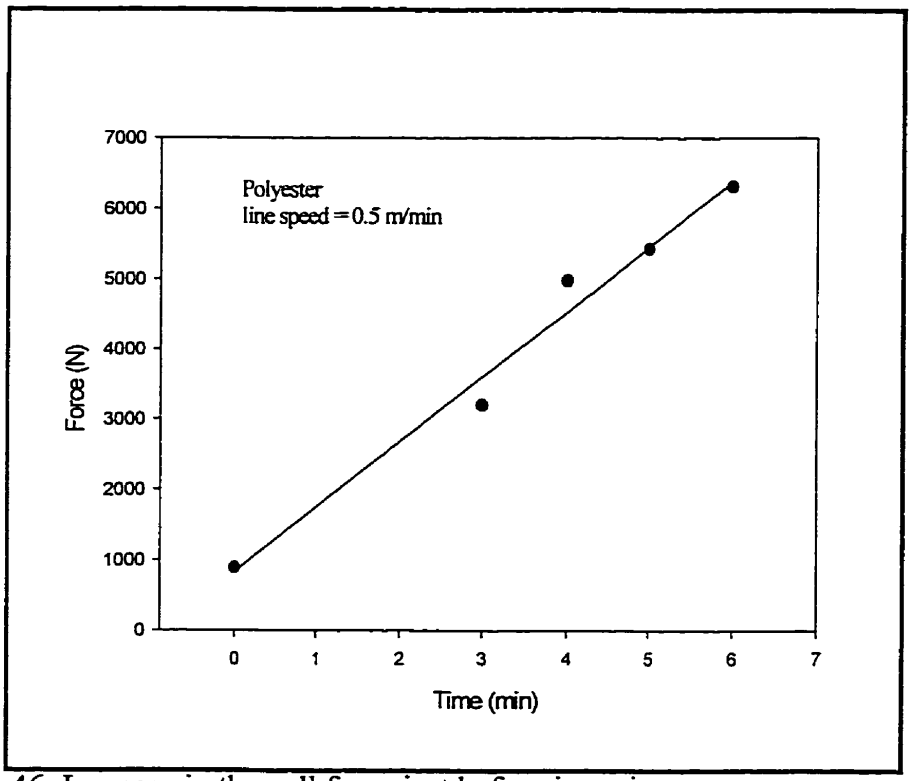

Figure 4-46: Increase in the pull force just before jamming.

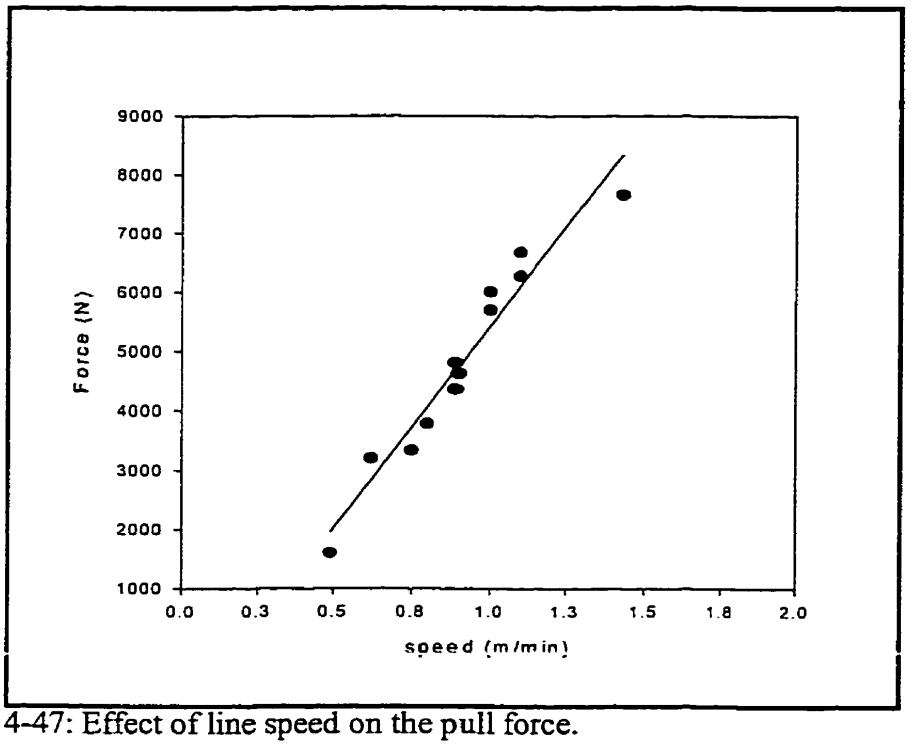

Figure 4-47: Effect of line speed on the pull force.

4.5.4 Pull force modeling

The current pull force model follows the form shown below,

$$F = \int_0^{L_l} T_{shear} dz + \int_{L_l}^{L} \tau_r dz \qquad 1\text{-}47$$

This model accounts for the viscous forces and the shrinkage drag. ie. the liquid and solid zones. As demonstrated previously in this study, the viscous forces account for only 5%. Therefore, to better model the pull force, the die forces should be divided into three sections rather than two. This additional section would incorporate the gel

adhesive forces bonding that takes place in the gelatinous zone. For low line speeds, the additional gelatinous component would be negligible, however, as the line speed increases, this zone will also increase. The three part model which is proposed is in the following form,

$$F = \int_0^{L_G} T_{shear}\,dz + \int_{L_G}^{L_S} f_G P(z)\,dz + \int_{L_S}^{L} f_S P(z)\,dz \qquad 4\text{-}1$$

where L_G is the length of the liquid zone, L_S is the length up to the end of the gel zone, L is the total length of the die, T_{shear} is the shear force on the liquid, f_G is the coefficient of friction in the gelatinous zone, f_S is the coefficient of friction in the solid zone and P(z) is the pressure distribution inside the die. This model is similar to that found in the literature with the exception of the middle term which accounts for the gelatinous zone.

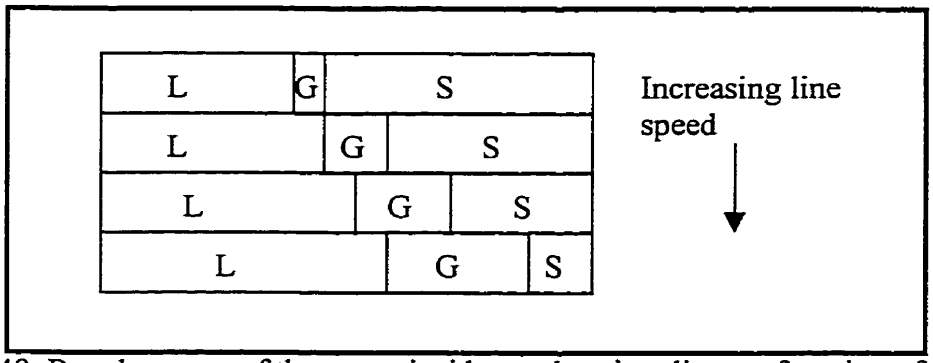

Figure 4-48: Development of the zones inside a pultrusion die as a function of speed.

In figure 4-48, assuming a constant temperature profile, the lengths of the zones in the die would take the following form as the line speed is increased. The linear increase of the gel zone is the reason for adding the middle portion to the model. The pull force model for the liquid zone gave 1900N, which did not agree with experimental work

with the silicon oil, which gave 90N. Therefore, as seen in figure 4-50 above, it is the liquid and gelatinous zones that increase as the line speed increases. Thus the experimental increase in pull force was due to the increase in the gelatinous zone.

The constants for the pull force model were not determined, because this research was beyond the intent of the project. The task of determining the constants for the pull force model will remain to be completed in the future.

Conclusion

This research project demonstrated the parameters which are used to model the pultrusion process. The degree of cure, viscosity, gel time, volumetric changes, pressure and pull force are all examined. To determine one of these properties, one needs to employ all the parameters which precede it in this given order. As shown in the report, the temperature and degree of cure are always needed to determine any of the other characteristics of the process. They are the fundamental parameters needed to model the process. The viscosity, gel time and volumetric expansion can be considered as secondary parameters. The pressure and pull force in or on the profile are considered as a third generation of parameters. This project used the first generation parameters to model the viscosity, gel time and volumetric changes of the resin. The models and techniques presented are generally in good agreement with the experimental results. The one main drawback with this portion of the study is that the *mass effect* plagued all the tests with the exception of the hot plate. Due to the exothermic nature of the resin, all tests that use more than a few grams of resin will be affected by the internal release of heat.

This study also included preliminary work to model the pressure and pull force on the profile. Experimental work has been done to determine the pull force and the contribution from some of its components on the profile. Models have been proposed to

model the pressure and the pull force on the profile. However, these parameters are not modeled in this study.

In addition to modelling the parameters mentioned above, the effect of ingredients on the viscosity, gel time and volumetric expansion was investigated for the epoxy resin. The contribution of the collimation and viscous forces to the total pull force was also investigated. A process monitoring technique was used to determine the stability of the process.

Research can be continued on all aspects discussed in this study. The database can be enlarged to model the viscosity, gel time, and volumetric changes for other pultrusion resins. The pressure development inside the die is predicted, however, very little work exists in the literature that accurately measures the pressure profile inside the die. This is one area of research that has a tremendous potential for development in the future. A better understanding of the pressure inside the die would lead to a more accurate prediction of the pull force on the profile and of the forces that compose it.

Bibliography

1. Meyer, R. W. (1985). Handbook of pultrusion technology. Chapman and Hall. London.

2. Mallick, P. K. (1993). Fiber-reinforced composites; Materials, manufacturing, and design. Second edition. Marcel Dekker, Inc. New York.

3. Champoux, L. (November 1995). Effet de l'humidité sur le comportement sous chocs répétés des stratifies. École Polytechnique de Montréal. Mémoire do maîtrise.

4. Halley, P. J. and Mackey, M. E. (Mid-March 1996). Chemorheology of thermosets-An overview. Polymer engineering and science, Vol. 36, No. 5, 593-609.

5. Haddad, D. K., and May, C. A. (1988) Physical, chemical, and thermal analysis of thermoset resins. Engineering Plastics, Engineered materials handbook, Vol. 2. ASM International, Metals Park.

6. Atarsia, A., and Boukhili, R. (June 1998) Relationship between isothermal and dynamic cure of thermoset via the isoconversion representation. Submitted to: Polymer engineering and science

7. Roller, M. B. (March 1986).Rheology of curing thermosets: A Review. Polymer engineering and science, Vol. 26, No. 6, 432-440.

8. Trivisano, A., Maffezzoli, A., Kenny, J. M. and Nicholas, L. (1900). Mathematical modeling of the pultrusion of epoxy based composites. Advances in polymer technology, Vol. 10, No. 2, 251-264.

9. Malkin, A. Y. and Zhirkov, P. V. (1990). "Flow of polymerising liquids. Advances in Polymer Science, 95. Springer-Verlag Berlin Heidelberg.

10. Vratsanos, M. S. and Farris, F. J. (June 1989). Network mechanical properties of amine cured epoxies. Polymer engineering and science, Vol. 29, No. 12, 806-816.

11. Axel Plastics Research Laboratories INC. Technical data, Mold Wiz INT-1846N

12. Shell Chemical Company. Data sheet SC:716-94. EPON Resin 9310 / EPI-Cure Curing agent 9360 / EPI Cure Curing agent accelerator 537, Epoxy resin system for pultrusion.

13. Ryan, M. E. (June 1984) Rheological and heat transfer considerations for processing of reactive systems. Polymer engineering and science, Vol. 24, No. 9, 698-706.

14. Tajima, Y. A. and Crozier, D. (March 1986). Chemorheology of an amine cured epoxy resin. Polymer engineering and science, Vol. 26, No. 6, 427-431.

15. Malkin, A. Y. and Kulichikhin, S. G. (1991). Rheokinetics of curing. Advances in Polymer Science,101. Springer-Verlag Berlin Heidelberg.

16. Tajima, Y. A. and Crozier, D. G. (1988 Mid-April). Chemorheology of an epoxy resin for pultrusion. Polymer Engineering and Science., Vol. 28, No. 7, 491-495.

17. Gorthala, R., Roux, J. A. and Vaughan, J. G. (1994). Resin flow, cure and heat transfer analysis for pultrusion process. Journal of composite materials, Vol. 28, No. 6, 486-506. Technomic publishing.

18. Dusi, M. R., Lee, W. I., Ciriscioli, P. R. and Springer, G. S. (March 1987). Cure kinetics and viscosity of Fiberite 976 resin. Journal of composite materials, Vol. 21, 243-261.

19. Ng, H., and Manas-Zloczower, I. (February 1993). Chemorheology of unfilled and filled epoxy resins. Polymer engineering and science, Vol. 33, No. 4, 211-216.

20. Mijovic, J., Kenny, J. M., and Nocolais, L. (1993). Comparison of kinetic and rheological evaluation of gel time for an amine-epoxy system. Polymer, V.43, No. 1, 207-209.

21. Oyanguren, P. A., and Williams, R. J. J. (1993). Cure of epoxy novolacs with aromaticdiamines. I. Vitrification, gelation, and reaction kinetics. Journal of Applied Polymer Science, Vol. 47, 1361-1371.

22. Hwang, J. G., Row, C. G., Hwang, I., and Lee, S. J. (1994). A chemorheological study on the curing of thermosetting resins. Ind. Eng. Chem. Res. Vol. 33, 2377-2383

23. Hamed, G. (January 1988). Free volume theory and the WLF equation. Elastomerics, 14-17.

24. Hill jr, R. R., Muzumdar, S. V. and Lee, L. J. (May 1995). Analysis of volumetric changes of unsaturated polyester resins during curing. Polymer engineering and science, Vol. 35, No. 10, 852-859.

25. Sandalls, P. L.,Yates, B., Baggott, R., Kanellopoulos, V. N., Wostenholm, G. H. and Stevenson, B. C. J. (1988). Influence of the cure cycle upon selected physical properties of a vinyl ester resin. Journal of material science, No. 23, 1443-1452.

26. Huang, Y. J. and Liang, C. M. (1996). Volume shrinkage characteristic in the cure of low-shrink unsaturated polyester resins. Polymer, Vol. 37, No. 3, 401-412

27. Kia, H. G. and Viscomi, P.V. (August 1994). High-pressure/High-temperature dilatometry of SMC low profile additives. Journal of reinforced plastics and composites, Vol. 13, 666-681.

28. Kinkelaar, M., Muzumdar, S. and Lee, L J. (May 1995). Dilatometry study of low profile unsaturated polyester resins. Polymer engineering and science, Vol. 35, No. 10 823-836.

29. Kinkelaar, M. and Lee, L .J. (1992). Development of a dilatometer and its application to shrink unsaturated polyester resins, Journal of applied polymer science, Vol. 24, 37-50.

30. Snow, A. W. and Armistead, P. J. (1994). A simple dilatometer for thermoset cure shrinkage and thermal expansion measurements. Journal of applied polymer science, Vol. 52, 401-411.

31. Hunter, G. A. (1988). Pultruding epoxy resin. SPI 43rd annual conference, 6-C, February 1-5.

32. Gorthala, R., Roux, J. A. and Vaughan, J. G. (1993). A model to predict resin pressure/back flow in the tapered inlet of a pultrusion die. SPI 48th annual conference, 2-D, February 8-11.

33. Huang, Y J., Lu, T. J. and Hwu, W. (January 1993). Curing of unsaturated polyester resins.- Effects of pressure. Polymer engineering and science, Vol. 33, No.1. 1-17.

34. Nolet, S. C. and Fanucci, J. P. (1990). Measurement of the presure distribution inside a pultrusion die. SPI 45th annual conference, 3-B, February 12-15.

35. Sumerak, J. E., and Martin, J. D. (1993). The pulse of pultrusion: Pull force trending for quality and productivity management. Polymer and polymer composites, Vol. 1, No. 3, 199A-210A.

36. Lee, J. K. and Pae, K D. (1993). Effects of hydrostatic pressure on curing of DGEBA-DDS system. Journal of macromol. Sci. -Phys., b32(1), 79-98.

37. Moschiar, S. M., Reboredo, M. M., Larrondo, H. and Vazquez, A. (December 1996). Pultrusion of epoxy matrix composites: Pulling force model and thermal stress analysis. Polymer composites, Vol. 17, No. 6, 850-858.

38. Kim, D. H., Han, P. G., Jin, G. H., and Lee, W. I. (1997). A model for thermosetting composite pultrusion process. Journal of composite materials, Vol. 31, No. 20, 2105-2122.

39. Moschiar, S. M., Reboredo, M. M., Kenny, J. M., and Vasquez, A. Analysis of pultrusion processing of composites of unsaturated polyester resin. Polymer composites, Vol. 17, No. 3, 478-485.

40. Wilder, R. (July 1988). Just how big is pultrusion's future in structural components. Modern Plastics, 37-39.

41. Chachad, Y. R., Roux, J. A. and Vaughan, J. G. (July 1996). Effects of pull speed on die wall temperatures for flat composites of various sizes. Journal of reinforced plastics and composites, Vol. 15, 718-738.

42. Nanni, A. (1993). Fiber-reinforced-plastic (FRP) reinforcement for concrete structures: Properties and applications. Developments in civil engineering, 42. Elsivier, New York, p.129-166.

43. Nanni, A. (1993). Fiber-reinforced-plastic (FRP) reinforcement for concrete structures: Properties and applications. Developments in civil engineering, 42. Elsivier, New York, p.189-222.

44. Standard test method for gel time of solventless varnishes. ASTM D 3056 – 96. (1997).

45. Standard test method for gel time of thermosetting coating powder. ASTM D 4217 – 91. (1997).